UNIVERSITÀ DEGLI STUDI DI MILANO

divas
DIPARTIMENTO DI MEDICINA VETERINARIA E SCIENZE ANIMALI

Università degli Studi di Milano
Department of Veterinary Medicine and Animal Sciences

GRADUATE SCHOOL OF VETERINARY AND ANIMAL SCIENCE

Academic Year: 2018-2022

Establishing *in vitro* intestinal epithelial cell models in translational animal nutrition

Tamil Selvi Sundaram
(Class XXXIV)
Ph.D. Thesis

Programme of the study:	Molecular Animal Nutrition (MANNA)
Tutor:	prof. Antonella Baldi, PhD. University of Milan
Co-tutor:	prof. MVDr. Juraj Pistl, PhD. doc. MVDr. Mangesh Ramesh Bhide, PhD. The University of Veterinary Medicine and Pharmacy in Košice (Slovakia)
Non-academic tutor:	prof. Maria Filippa Addis, PhD. Porto Conte Ricerche Srl

Acknowledgements

First and foremost, I would like to express my immense gratitude to all my supervisors, prof. Antonella Baldi, PhD., prof. MVDr. Juraj Pistl, PhD., doc. MVDr. Mangesh Ramesh Bhide, PhD., and prof. Maria Filippa Addis, PhD., for providing this great opportunity to pursue my doctoral research in the field of molecular animal nutrition. Their profound knowledge, encouragement, and continuous support have always motivated me to overcome the challenges in both my academic and as well as daily life. Besides my supervisors, I would like to thank the entire team of Animal nutrition department (UNIMI) and LBMI (UVLF), especially my collogues Dr. Raffaella Rebucci, PhD., and Dr. Carlotta Giromini, PhD., who has willingly shared their hours of precious time in mentoring and motivating throughout my academic year. I would like to acknowledge the entire MANNA consortium and the European Union's Horizon 2020 research and innovation programme H2020-MSCA- ITN-2017- EJD: Marie Skłodowska-Curie Innovative Training Networks (European Joint Doctorate) – Grant agreement no: 765423, for providing the financial and technical support for pursuing my degree. Additionally, I would like to express my gratitude to prof. Fabrizio Ceciliani, PhD., who has been a moral support at difficult times. I'm always thankful to mother (Arul), brother (Mahe), fiancée (Sunil) and the rest of my family and friends for believing in me, keeping me harmonious and help put the pieces together in the entire process. I will be grateful forever for your love.

Abstract

Immunomodulatory nutrients as the omega-3 polyunsaturated fatty acids (n-3 PUFA) and citrus pectins (CPn) are reported to beneficially affect the host intestinal immunity. However so far, the biological pathways modulated by these nutrients in intestinal inflammation at the level of intestinal epithelial layer (IEL) remains elusive.

To bridge this knowledge gap, the aim of our present study was set in the direction to delineate the effects of n-3 PUFA in porcine IPEC-J2 cell line under (LPS) stress conditions underpinning pig nutrition, combining the state-of-the-art cell-based assays and bioinformatic analysis. The second part of our study was directed towards establishing a primary intestinal epithelial cell (IEC) culture from chicken embryos for the assessment of CPn against LPS stress, underpinning poultry nutrition.

Utilizing different cell-based assays, we have successfully demonstrated the proliferative effects of n-3 PUFAs as eicosapentaenoic acid (EPA) and docosahexaenoic acid (DHA) in the IPEC-J2 cells. Besides, n-3 PUFA pre-treatment (DHA:EPA, 1:2, 10 µM, 24 h) was shown to counteract the cellular damage elicited by different stress factors as LPS, hydrogen-peroxide (H_2O_2) and dextran sulphate sodium (DSS). In addition, through system biology and multi-omics integration (transcriptomics and proteomics), we have demonstrated the cytoprotective properties of n-3 PUFA in IPEC-J2 cells against LPS-induced inflammatory and metabolic damage.

Specifically, in these cells, we have identified that n-3 PUFA regulate the biological process as, (i) Axon guidance for developmental process; (ii) Defensin and interferon-mediated antimicrobial defense response for homeostasis; (iii) Cell junction assembly under stress-related cell proliferation; (iv) Amelioration of TLR/MyD88 and cytokine signaling in innate immune response; (v) Fatty acid storage in lipid droplets for lipid homeostasis; (vi) Recovery of central carbon metabolic process from dysregulation under infection; (vii) Lipolysis of fatty acids stored in lipid droplets for prevention of cell starvation during infection. To the best of the knowledge, this is the first study to comprehensively map the bioactivity of n-3 PUFA in enterocytes using multi-omics approach. The outcome of the present study, will enable us to better understand the role of n-3 PUFA in intestinal barrier for planning nutritional or therapeutic strategies.

Further in the chicken *in vitro* study, we have preliminarily demonstrated a simplified method of cell isolation and establishment of primary IEC culture from chicken embryos using mechanical tissue disruptions method. We have also shown that the response of chicken cells is in accordance with the reference IPEC-J2 line using a dose-response study with CPn and LPS. This primary IEC culture model can further be utilized as a starting point for setting up poultry *in vitro* studies on intestinal barrier.

Keywords: omega-3 polyunsaturated fatty acids, Citrus pectin, Lipopolysaccharides, Intestinal epithelial layer, Cell-based assays, Bioinformatic analysis

Publications

- Giromini C, Lovegrove JA, Givens DI, Rebucci R, Pinotti L, Maffioli E, Tedeschi G, Sundaram TS, Baldi A. In vitro-digested milk proteins: Evaluation of angiotensin-1-converting enzyme inhibitory and antioxidant activities, peptidomic profile, and mucin gene expression in HT29-MTX cells. *J Dairy Sci.* 2019 December;102(12):10760-10771.

- Sundaram TS, Giromini C, Rebucci R, Baldi A. Omega-3 Polyunsaturated Fatty Acids Counteract Inflammatory and Oxidative Damage of Non-Transformed Porcine Enterocytes. *Animals.* 2020 May;10(6):956.

- Dell'Anno M, Giromini C, Reggi S, Cavalleri M, Moscatelli A, Onelli E, Rebucci R, Sundaram TS, Coranelli S, Spalletta A, Baldi A, Rossi L. Evaluation of Adhesive Characteristics of *L. plantarum* and *L. reuteri* Isolated from Weaned Piglets. *Microorganisms*. 2021 July;9(8):1587.

- Sundaram TS, Giromini C, Rebucci R, Pistl J, Bhide M, Baldi A. Role of omega-3 polyunsaturated fatty acids, citrus pectin, and milk-derived exosomes on intestinal barrier integrity and immunity in animals. *J Animal Sci Biotechnol*. 2022 April;13(40).

- Sundaram TS, Giromini C, Rebucci R, Baldi A, Pistl J, Bhide M. Transcriptomic profiling and functional assessment of omega-3 fatty acids in the lipopolysaccharides-induced porcine enterocytes. (Manuscript in preparation).

- Sundaram TS, Addis MF, Giromini C, Rebucci R, Pisanu S, Pagnozzi D, Baldi A. Comprehensive proteomic profiling reveals the abrogation of LPS-induced metabolic dysregulation by omega-3 fatty acids in the porcine IPEC-J2 cells. (Manuscript in preparation).

- Sundaram TS, Giromini C, Rebucci R, Baldi A, Pistl J, Bhide M. Establishment of primary intestinal cell culture from chicken embryos for the assessment of bioactive dietary compounds. (Mini article in preparation).

Oral and poster communications

- Sundaram TS, Giromini C, Rebucci R, Baldi A. Establishment of inflammatory in vitro intestinal epithelial models for translational animal nutrition. 23rd Animal Science and Production Association (ASPA) congress, 11-14th June 2019, Sorrento, Italy. (Poster presentation).
- Rebucci R, Giromini C, Sundaram TS, Comi M, Baldi A, Pinotti L, Cheli F. Effect of omega-3 fatty acids on porcine intestinal ex vivo model exposed to stress conditions. 71st Annual Meeting of the European Federation of Animal Science (EAAP), 1-4th December 2020, Virtual meet. (Co-author).
- Sundaram TS, Giromini C, Rebucci R, Baldi A, Bhide M, Pistl J. Transcriptomic profiling and functional assessment of omega-3 polyunsaturated fatty acids in porcine enterocyte model. 72rd Annual Meeting of the European Federation of Animal Science (EAAP), 30th August – 3rd September 2021, Davos, Switzerland. (Oral presentation).

- Giromini C, Baldi A, Rebucci R, Sundaram TS, Purup S. Role of Short Chain Fatty Acids to counteract inflammatory stress in mucus secreting HT29-MTX cells. Role of Short Chain Fatty Acids to counteract inflammatory stress in mucus secreting HT29-MTX cells. 72rd Annual Meeting of the European Federation of Animal Science (EAAP), 30th August – 3rd September 2021, Davos, Switzerland. (Co-author).
- Dell'Anno M, Giromini C, Reggi S, Sundaram TS, Coranelli S, Spalletta A, Rossi L. Evaluation of *Lactobacillus plantarum* and *Lactobacillus reuteri* as feed additives for swine. 24rd Animal Science and Production Association (ASPA) congress, 21-24th September 2021, Padova, Italy. (Co-author).
- Sundaram TS, Giromini C, Rebucci R, Pisanu S, Pagnozzi D, Addis MF, Bhide M, Pistl J, Baldi A. A comprehensive proteomics and transcriptomics analysis on the effects of omega-3 fatty acids in the porcine small intestinal enterocytes. 73rd Annual Meeting of the European Federation of Animal Science (EAAP), 5-8th September 2022, Porto, Portugal. (Abstract accepted for poster presentation).

Contents

List of Tables and Figures

List of abbreviations

ALA	Alpha-linolenic acid
ABHD5	1-acylglycerol-3-phosphate O-acyltransferase
ADAM	A Disintegrin and Metallopeptidase
ADSL	Adenylosuccinate lyase
AIFM1	Apoptosis Inducing Factor Mitochondria Associated 1
AJs	Adherens junctions
ALDOC	Fructose-bisphosphate aldolase C
AMPs	Antimicrobial proteins
AP-1	Activator Protein-1 complex
APPL2	Phosphotyrosine interacting with PH domain and leucine zipper 2
APRT	Adenine phosphoribosyltransferase
ARA	Arachidonic acid
ARR3	Arrestin 3
ATF6B	Atrial fibrillation, familial, 1
ATOX1	Antioxidant 1 Copper Chaperon
ATP	Adenosine triphosphate
BAX	BCL2 Associated X
BCL-2	B-cell lymphoma 2
BTG	B-cell translocation gene)
CAT	Catalase
CAV1	Caveolin 1
CCS	Copper Chaperone For Superoxide Dismutase
CD	Crohn's disease
CD28	T-Cell-Specific Surface Glycoprotein
CDC42SE1	CDC42 Small Effector 1
CDH11	Cadherin 11
CKMT1A	Mitochondrial creatine kinase-1
CLDN	Claudin(s)
CLDN1	Claudin 1
CLU	Clusterin
COX	Cyclooxygenase
COX6B	Cytochrome c oxidase

CPn	Citrus pectin
CPT1A	Carnitine O-palmitoyltransferase 1A
CSF1	Colony Stimulating Factor 1
CXCL2	C-X-C Motif Chemokine Ligand 2
DAMPs	Damage-associated molecular patterns
DAPs	Differentially abundant proteins
DBI	Acyl-CoA-binding protein
DE	Degrees of esterification
DEFB110	Beta defensin 110
DEGs	Differentially expressed genes
DHA	Docosahexaenoic acid
DHAP	Dihydroxyacetone phosphate
DLL4	Delta Like Canonical Notch Ligand 4
DM	Degrees of methyl esters
DMEM/F12	Dulbecco's modified Eagle's-Ham's F12 mixture
DMSO	Dimethyl sulfoxide
DON	Deoxynivalenol
DP	Distal proctocolitis
DPEP1	Dipeptidase 1
DSS	Dextran sulphate sodium
ECM	Cell-extracellular matrix
EGF	Epidermal growth factor
EPA	Eicosapentaenoic acid
EPCAM	Epithelial cell adhesion molecule
EPHA4	Ephrin type-A receptor 4
EPHX1	Epoxide hydrolase 1
FADS	Fatty acid desaturase
FADS1	Fatty Acid Desaturase 1
FADS2	Fatty Acid Desaturase 2
FAIM	Fas Apoptotic Inhibitory Molecule
FASP	Filter-aided sample preparation
FBS	Fetal bovine serum
FD4	Fluorescein isothiocyanate-labelled dextran 4kDa
FDPS	Farnesyl pyrophosphate synthase
FDR	False discovery rate
FO	Fish oil

FOS	Fos proto-oncogene
FOSL2	FOS like 2
G3P	Glyceraldehyde 3-phosphate
GADPH	Glyceraldehyde-3-phosphate dehydrogenase
Gal-3	Galectin-3
GCLM	Glutamate-cysteine ligase modifier subunit
GI	Gastrointestinal tract
GIT	Gastrointestinal tract
GNAI2	G Protein Subunit Alpha I2
GO	Gene Ontology
GPCR	G protein-coupled receptors
GRP94	Glucose-regulated protein-94
GSH	Glutathione
GSS	Glutathione synthetase
H2O2	Hydrogen-peroxide
HCD	Higher Energy Collisional Dissociation
HMGCS1	3-hydroxy-3-methylglutaryl coenzyme A synthase
HMOX1	Heme oxygenase 1
HO-1	Heme oxygenase-1
HRP	Horseradish peroxidase
IBD	Inflammatory bowel diseases
ICAM-1	Intercellular adhesion molecule-1
IDH1	Isocitrate dehydrogenase
IECs	intestinal epithelial cells
IEL	Intestinal epithelial layer
IFIT	Interferon-induced protein with tetratricopeptide repeats
IFN	Interferon
IFNB1	Interferon Beta 1
IFNGR1	Interferon Gamma Receptor 1
IFNL3	Interferon lambda 3
IGF-1R	Insulin-like growth factor-1 receptor
IKK	IkappaB kinase
IKK-α	NF-κB kinase subunit alpha
IKK-β	NF-κB kinase subunit beta
IKK-γ	NF-κB kinase subunit gamma
IL	Interleukin

IL10RB	IL10 receptor beta
INFγ	Interferon gamma
iNOS	Inducible nitric oxide synthase
IPEC-J2	Intestinal Porcine Epithelial Cells of Jejunum region
IRAK	Interleukin-1 receptor-associated kinase
IRF	Interferon regulatory factor
ITGAV	Integrin alpha V
ITGB3	Integrin Subunit beta 3
IκB	Inhibitor of nuclear factor kappa B
IκB	IkappaB
IκBα	NF-κB inhibitor alpha
IκBζ	NF-κB inhibitor zeta
JAM	Junctional adhesion molecules
KEGG	Kyoto Encyclopedia of Genes and Genomes
LDH	Lactate dehydrogenase
LDHA	Lactate Dehydrogenase A
Lgr5	G-protein coupled receptor-5
LO	Linseed oil
LOX	Lipoxygenase
LPS	Lipopolysaccharides
LT	Leukotriene(s)
LX	Lipoxin(s)
LY96	Lymphocyte antigen 96
MAC	Membrane attack complex
MAPK	Mitogen-activated protein kinase
MaR	Maresin(s)
MCP-1	Monocyte chemoattractant protein-1
MDE	Milk-derived exosome(s)
ME1	Malic Enzyme 1
MGLL	Monoglyceride Lipase
miRNA	MicroRNA(s)
MPO	Myeloperoxidase
MTT	3-(4,5-dimethylthiazol-2-yl)-2,5-diphenyltetrazolium bromide
MUC	Mucin
MVD	Diphosphomevalonate decarboxylase
MYD88	Myeloid differentiation factor 88

NADPH	Nicotinamide adenine dinucleotide phosphate
NCK1	Non-catalytic region of tyrosine kinase adaptor protein 1
ND1	NADH ubiquinone oxidoreductase chain 1
NDUFV3	NADH ubiquinone oxidoreductase 9 kDa subunit
NEC	Necrotising enterocolitis
NFKB1	Nuclear Factor Kappa B Subunit 1
NF-κB	Nuclear factor-κB
NKAP	NF-kappa-B-activating protein
NO	Nitric oxide
NOD	Nucleotide-binding oligomerization domain-containing protein
Nrf2	Nuclear factor erythroid 2-related factor 2
NUBPL	Nucleotide binding protein-like isoform A
OAS2	2'-5'-Oligoadenylate Synthetase 2
OASL	2'-5'-Oligoadenylate Synthetase Like
OCLN	Occludens
OD	Optical density
OPLAH	5-oxoprolinase, ATP hydrolysing
OXPHOS	Oxidative phosphorylation
PAMPs	Pathogen-associated molecular patterns
PARD6B	Partitioning defective 6 homolog beta
PBS	Phosphate-buffered saline
PCNA	Proliferating cell nuclear antigen
PDCD10	Programmed Cell Death 10
PG	Prostaglandin(s)
PGK1	Phosphoglycerate kinase 1
PHB2	Prohibitin 2
PLIN2	Perilipin 2
PLIN3	Perilipin 3
PNPLA	Patatin Like Phospholipase Domain Containing
PP	Protein phosphatase
PPARγ	Proliferator-activated receptor γ
PPP	Pentose phosphate pathway
PPP1CA	Protein phosphatase 1 catalytic subunit alpha
PRRs	Pattern-recognizing receptors
RIPK	Receptor interacting protein kinase
ROS	Reactive oxygen species

Rv	Resolvin(s)
SDS-PAGE	Sodium dodecyl sulphate-polyacrylamide gel electrophoresis
SCD	Stearoyl-CoA Desaturase
SCD5	Stearoyl-CoA Desaturase 5
SCFAs	Short-chain fatty acids
SERPINE	Serine protease inhibitor clade E
SIGIRR	Single Ig IL-1 receptor-related molecule
SOCS1	Suppressor of Cytokine Signaling 1
SOD	Superperoxide dismutase
TAK1	Transforming growth factor-β activated kinase 1
TCR	T cell receptor
TEER	Transepithelial electrical resistance
TGF	Transforming growth factor
TJs	tight junctions
TKT	Transketolase
TLR	Toll-like receptor(s)
TNBS	2,4,6-Trinitrobenzene sulfonic acid
TNF	Tumor necrosis factor
TPI1	Triosephosphate Isomerase 1
TXB	Thromboxane(s)
TYK2	Tyrosine kinase 2
UC	Ulcerative colitis
V/C	Villus height/crypt depth
VEGF	Vascular endothelial growth factor
W/L	Weight/length
$\alpha_V\beta_3$	Alpha-v beta-3
n-3/n-6 PUFAs	Omega-3/omega-6 polyunsaturated fatty acids

1 Introduction

The gastrointestinal tract of livestock and poultry is prone to challenge by foodborne antigens, pathogens, and other stress factors in the farm environment. Excessive physiological inflammation and oxidative stress that arise firstly disrupt the intestinal epithelial layer (IEL), followed by other components of the gastrointestinal tract. Apart from nutrition absorption, IEL acts as the first line of defense in the host-innate immune system (ALLAIRE et al., 2018; OKUMURA et al., 2017). Loss of IEL integrity can predispose to poor nutrition, growth deficiencies, chronic inflammatory and metabolic diseases. Therefore, the integrity of IEL is of paramount importance in the maintenance of not just the intestine but the overall health of farm animals. Traditionally antibiotics are supplemented in animal diets to enhance growth performance and ameliorate excessive physiological stress (ANADÓN et al., 2019; GUSTAFSON et al., 1997). Given that antibiotics could stimulate potential health hazards, there is a need for alternative, naturally available immunomodulatory compounds.

The European Food Safety Authority (EFSA) has categorized several such immunomodulatory compounds based on its source and properties (IRTA, 2015). The plant- or marine-derived omega-3 (n-3) polyunsaturated fatty acids (PUFA) and citrus pectin (CPn) are two such EFSA categorized immunomodulatory compounds known for its strong anti-inflammatory and anti-oxidative properties. Moreover, EFSA has described the property of these compounds to stop the local inflammation at intestinal level and prevent further damage to immune system (IRTA, 2015). Generally, PUFAs are structural constituents of phospholipid cell membranes, that maintains cell flexibility and fluidity (CALDER, 1998; RUSTAN et al., 2005). Besides, they perform immunomodulatory functions such as regulation of inflammatory process by generating lipid-based signaling mediators called eicosanoids (CALDER, 2009). It is widely reported that n-6 PUFA-derived mediators play a central role in pro-inflammation and development of inflammatory diseases (CALDER, 2009; DAS, 2006; SUGIHARA et al., 2018). However, supplementation of n-3 PUFA was identified to replace the n-6 PUFA in the immune cell membranes and give rise to low potency lipid-mediators that acts as `agonist' of pro-inflammation (LEVY et al., 2001; SCHWAB et al., 2006; SERHAN et al., 2008; SERHAN et al., 2005).

Overwhelming data supporting the beneficial effects of n-3 PUFA in controlling intestinal inflammation exist. However, till date a comprehensive picture on the biological process and pathways that regulated by n-3 PUFA at gene/protein level in the porcine

enterocytes, especially under infection remains unexplored. On the other hand, existing data describing the activity of CPn in intestinal inflammation remains elusive for harnessing its application as an immunomodulatory feed additive. Although few studies have demonstrated its immunomodulatory properties in murine models (FAN et al., 2020; MARKOV et al., 2011; PACHECO et al., 2018), and cancer enterocytes (BEUKEMA et al., 2021; DE PAULA MENEZES BARBOSA et al., 2020; VOGT et al., 2016), its activity in normal enterocytes was not well characterized.

In vitro intestinal cell models and cell-based assays are the foremost techniques applied for nutrition assessment prior to the *in vivo* trials. Presently, the intestinal cell models, specifically the enterocyte model used for nutrient assessment are either cancer-derived or virus immortalized cell lines. These transformed cell lines exhibit altered signal transduction and metabolic activity, and hence are not a realistic representative of normal cellular environment (HAKOMORI, 1996; LANGERHOLC et al., 2011; S.A. BROOKS et al., 2008). In order to characterize the bioactivity of nutrients as close to native intestinal barrier physiology, it is essential to develop or utilize non-cancer and non-transformed cell models.

Recently, the field of 'Omics' is increasingly recognized in human and animal medicine, owing to the advancement of bioinformatics technologies. Of note, the omics technologies applied in food science to study the impact of dietary nutrients on the genome, transcriptome, proteome and metabolome of cells or organism is referred to as 'Nutrigenomics' (GONZALEZ et al., 2015). It focusses on how nutrients and non-nutritive components affect the gene expression during disease and healthy status at cellular level to whole organism (GONZALEZ et al., 2015). Unlike the traditional molecular techniques, the bioinformatics technologies are able to integrate all the cellular information from mRNA, protein and metabolites to comprehensively map the biological pathways regulated by nutritional compounds (GRAW et al., 2021). Information acquired from these bioinformatic technologies, not only enumerates the molecular targets of nutritional compounds, but as well assist in monitoring the nutritional efficacy in individuals.

With this motivation as a starting point, the first part of this thesis is focused on characterizing the *in vitro* properties of n-3 PUFAs as the eicosapentaenoic acid (EPA) and docosahexaenoic acid (DHA) in the pig intestinal epithelial cells (IECs) underpinning pig nutrition. To this goal, the non-transformed porcine small intestinal epithelial cell model, IPEC-J2 was utilized to characterize the impacts of n-3 PUFA against lipopolysaccharides

(LPS) challenge by cell-based assays and high-throughput bioinformatic analysis as transcriptomics and proteomics. The second part of this study is aimed at characterizing the *in vitro* properties of CPn against LPS stress in chicken intestinal epithelial cells, underpinning poultry nutrition. Unlike pig, there are no previously established epithelial cell model available for chicken. Therefore, for this part of the study, we primary focused on establishing primary intestinal epithelial cell culture from chicken embryos as an *in vitro* model of poultry intestinal barrier. Then demonstrate the functionality of the primary cell model by comparison against a reference model (IPEC-J2) in characterizing the dietary CPn against LPS challenge by cell viability assay. Overall, the outcomes of the present study will enable us to better understand the role of naturally available immunomodulatory nutrients (n-3 PUFA and CPn) in the intestinal barrier for development of nutritional-based strategies to improve the intestinal immunity of pig and poultry.

2 Review of Literature

2.1 Intestinal epithelium – a dynamic barrier

GIT is secured by a series of protective layers collectively described as the intestinal mucosa. It mainly encompasses the mucus layer, gut microbiota, IEL, immune cells dispersed in lamina propria and lamina. The IEL physically separates the circulatory system from the external milieu. Besides, IEL is the key component that orchestrates gut homeostasis by establishing communication between the microbiota and the underlying immune cells (ALLAIRE et al., 2018; OKUMURA and TAKEDA, 2017). Further, the IEL is formed by a monolayer of intestinal epithelial cells (IECs) interconnected by different protein complexes such as tight junction (TJ) proteins, junction adherent proteins (JAM) and, desmosomes. TJ proteins such as the occludens (OCLN) and claudins (CLDN) are important structural units that strictly governs the permeability of molecules across the barrier (CHASSAING et al., 2014) (Figure 1).

Besides, the IEL comprises several specialized absorptive and secretory cell types for digestion, nutrition uptake, and host defense. Particularly, the enterocytes are the most abundant (~80%) and fast regenerating absorptive cell type (PETERSON et al., 2014; SALVO et al., 2015). Goblet cells secrete gel-like glycoproteins called mucin (MUC) that forms a mucous layer above the IEL. Further, the mucus layer is embedded with trillions of commensal bacteria called gut microbiota. Paneth cells exhibit the longest life span and produce antimicrobial proteins (AMPs) such as defensins, lysozymes, and phospholipases (CHASSAING et al., 2014; KURASHIMA et al., 2013). The microfold cells regulate the adaptive immune responses by presenting the luminal pathogens and antigens to the immune cells of lamina propria (CHASSAING et al., 2014). Enteroendocrine cells primarily secrete hormones and other AMPs for different physiological functions. The multipotent intestinal stem cells at the crypt base continuously regenerate to form other specialized cell types (SALVO et al., 2015) (Figure 1). Altogether, the IEL forms a dynamic barrier that selectively permits the nutrients while block the detrimental factors as pathogens and toxins from entering into the circulatory system.

Figure 1 Structure of intestinal epithelium

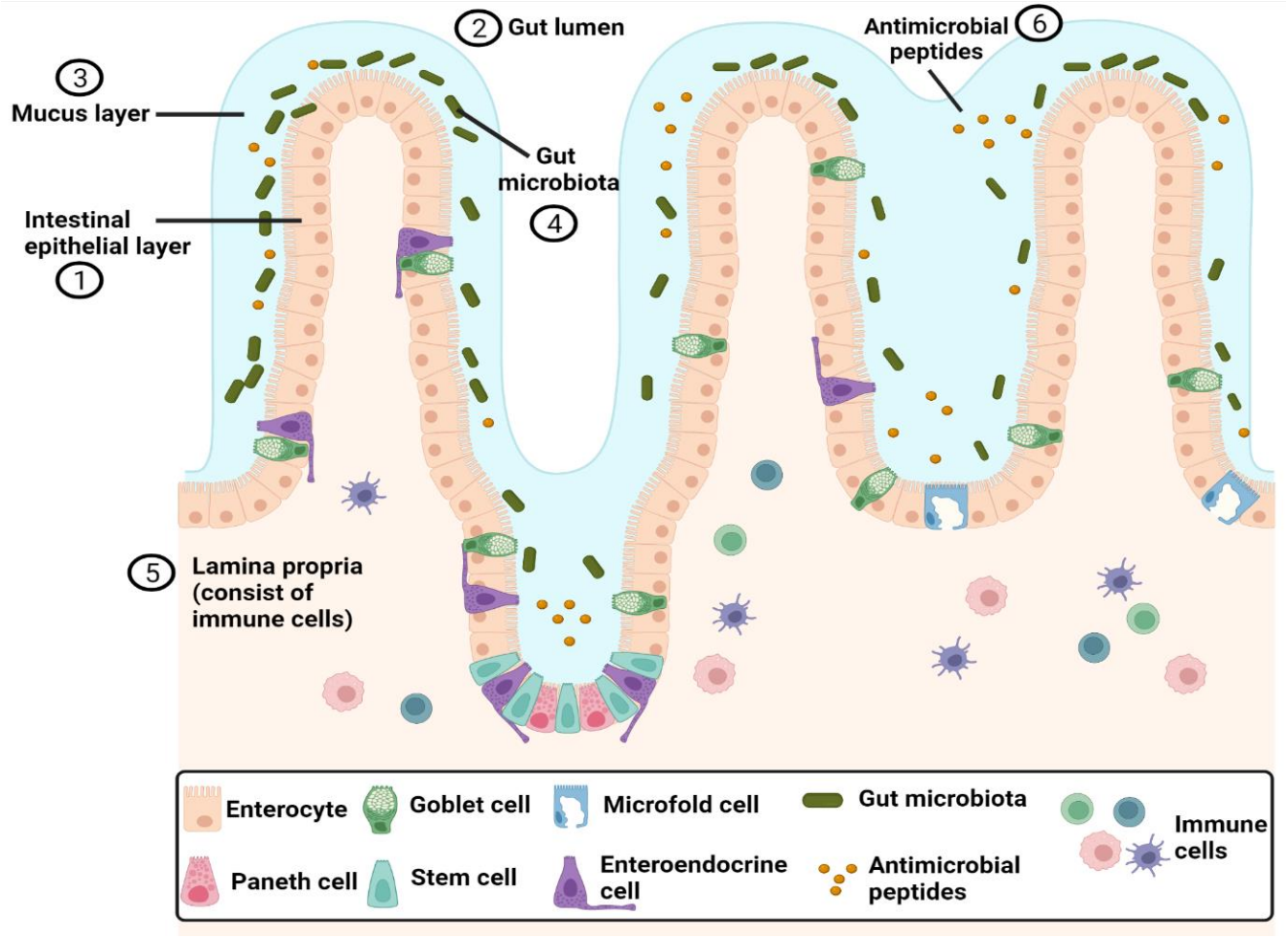

The intestinal epithelial layer (IEL) (1) is the first lining of gastrointestinal tract. It is formed by a single layer of specialized intestinal epithelial cells (enterocytes, goblet cells, paneth cells, microfold cells, stem cells and enteroendocrine cells) that physically separates the gut lumen (2) from the circulatory system. The IEL is lined by a mucous layer (3), where the gut microbiota (4) is embedded. The IEL orchestrates gut homeostasis by establishing communication between the gut microbiota and the underlying immune cells in lamina propria (5). The intestinal epithelial cells secrete several antimicrobial peptides (6) for host-defense. For references, see text. Own figure created using BioRender.com.

2.2 Implications of inflammation and oxidative stress in intestinal barrier

GIT is prone to inflammatory and oxidative damage owing to continuous contact with environmental stress factors. IECs exhibit specialized pattern-recognizing receptors (PRRs) such as the toll-like receptors (TLRs) and nucleotide oligomerization domain (NOD)-like receptors (NLRs) for identification of pathogen-associated molecular patterns (PAMPs) or damage-associated molecular patterns (DAMPs) (THOO et al., 2019). Subsequently, IECs

secrete various AMPs and pro-inflammatory signaling mediators such as cytokines, chemokines, and reactive oxygen species (ROS). These mediators are responsible for the differentiation, maturation, and activation of other cells of immune system (PENG et al., 2021; TURNER et al., 2014). Generally, oxidative stress can occur when an imbalance exists between the generation of ROS and the antioxidants available to scavenge (CHELI et al., 2011). ROS can directly damage the proteins, DNA, and lipids (CHELI and BALDI, 2011) or indirectly control certain transcription factors such as the nuclear factor-κB (NF-κB) (MORGAN et al., 2011).

NF-κB is described as the chief stimulator of infection and inflammation that is reported to activate more than 200 genes of pro-angiogenic factors, pro-inflammation, apoptosis, and inducible enzymes (GUO et al., 2009). These observations explain the relationship between inflammation and oxidative stress, which can trigger one another interchangeably (MORGAN and LIU, 2011). To a certain degree, physiological stress is necessary, however, in excess is detrimental. Occasionally, uncontrolled inflammation or oxidative stress can arise from defects in receptors, signal transduction, or during the *de novo* biosynthesis of pro-resolution mediators (SERHAN et al., 2008). Particularly, high local concentrations of cytokines such as the tumor necrosis factor (TNF)-α, interleukin (IL)-1β, and IL-6 are reported to compromise the IEL by downregulating the TJs and JAMs (CALDER et al., 2002). Subsequently, the leaky IEL stimulates leukocyte transmigration, disruption of barrier architecture and IEC maturation (THOO et al., 2019). Observations from human and animal studies have reported barrier defects to precede chronic inflammatory diseases (MARTINI et al., 2017). Therefore, the integrity of IEL is of paramount importance in the maintenance of gut but also the overall health.

2.3 Immunomodulatory nutrients for intestinal health

The pursuance of reducing the antibiotics and non-steroidal anti-inflammatory drugs (NSAIDs) has raised the interest in utilizing naturally existing bioactive compounds. These bioactive compounds are constituents of functional food, similar to conventional foods but provide additional therapeutic benefits. Thus, functional foods are described as food prepared using ‘scientific intelligence’ vital for optimal health (CENCIC et al., 2010). The European Food Safety Authority (EFSA) has categorized these natural bioactive or immunomodulatory compounds into, ‘plant extracts’, ‘prebiotics’, ‘probiotics’, ‘animal-by products’, and ‘other substances’ (IRTA, 2015). Plants have been the major source of energy since time immemorial in humans and animals. Certain compounds from whole or part of the plant exhibit

immunomodulatory properties and are commonly referred to as ‘phytobiotics’ or ‘botanicals’ (WINDISCH et al., 2008). A classic example of a plant- or marine-derived immunomodulatory compound is the essential fatty acid (EFA) such as the n-3 PUFAs. The common sources of n-3 PUFAs are marine phytoplankton, linseed oil (LO), and fish oil (FO) (DAS, 2006; SIMOPOULOS, 1991). Since several decades, n-3 PUFAs are routinely incorporated into human and animal diet in moderation for normal physiological functions. However, supplementation at a certain level result in achieving therapeutic effects. The n-3 PUFAs-enriched diet in livestock and poultry was shown to modulate the immune system, improve intestinal morphology, fertility, stress resistance, and performance (AGAZZI et al., 2004; ROSSI et al., 2010; SAVOINI et al., 2016; THANABALAN et al., 2021).

Further, pectins from citrus fruit peels are increasingly recognized for its multiple health-beneficial properties. Although the application of citrus pectin (CPn) as a feed additive is emerging, preliminary studies have reported to exhibit potential anti-inflammatory, antimicrobial and prebiotic properties (BEUKEMA et al., 2020; DE PAULA MENEZES BARBOSA et al., 2020; FAN et al., 2020; SAHASRABUDHE et al., 2018). Besides, the food processing industries utilize CPn as gelling agent and stabilizers for ages and is regarded safe for consumption (PARK et al., 2019). Moreover, GCS-100 and PectaSol-C are the two commercially available CPn-based drugs used for treating fibrosis in humans (SUTHAHAR et al., 2018). In the European Union, Italy is one of the leading producers of citrus fruits and after juicing, the peels are discarded as waste. These environmental wastes can otherwise be utilized as value-added, sustainable nutritional supplements in animal diet. Another prominent, animal-based nutritive compound is the milk-derived bioactive peptides and proteins (GIROMINI et al., 2019b). Recently, the exosomes present in milk are identified to carry cargoes of nucleic acid and peptides that improves the immune system, promotes intestinal barrier development, and prevent inflammatory diseases (GALLEY et al., 2020; GAO et al., 2021; WANG et al., 2019; ZEMPLENI et al., 2017). Currently, the milk-derived exosomes (MDEs) are gaining attention for targeted inflammatory diseases through diet (GALLEY and BESNER, 2020). Unlike antibiotics, these natural bioactive compounds are effective, environmentally friendly, and safe for improvising the immune system of animals, while eliminating stress and discomfort.

2.4 Omega-3 polyunsaturated fatty acids

2.4.1 Structure and molecular mechanism

Although n-3 PUFAs are widely known feed additive, its mechanism in intestinal barrier is poorly established, which limits the assessment of its efficacy. Therefore, presently, we outlined its possible modes of action in IEL based on the data derived from previous in vitro and in vivo studies. Generally, fatty acids are carbon chain structures of varying length, synthesized in the cytoplasm from Acetyl-CoA (LOTTENBERG et al., 2012). The two major fatty acid families as the omega-3 (n-3) and omega-6 (n-6) polyunsaturated fatty acids (PUFA) cannot be synthesized by animals, but obtained from the diet are called EFAs (BIRD et al., 2018; DAS, 2006). Basically, PUFAs are involved in cell signaling, immunomodulation, and formation of structural components in the phospholipid cell membranes (CALDER, 1998; RUSTAN and DREVON, 2005). An infection or injury triggers hydrolysis of PUFA from cell membranes to release certain lipid-based signaling molecules called eicosanoids (CALDER, 2009). The family eicosanoids orchestrate the initiation, progression, and resolution phases of the inflammatory responses.

Owing to the higher dietary ratio of n-6/n-3 PUFAs in animals, the eicosanoids are predominantly generated from n-6 arachidonic acid (ARA; C20:4n-6) by the enzymatic actions of cyclooxygenase (COX) and lipoxygenase (LOX) (CALDER, 2009; TILLEY et al., 2001; YEDGAR et al., 2007). The COX (COX-1/-2/-3) pathway generates 2-series prostaglandins (PGs) and thromboxanes (TXBs), while the LOX (5-/12-/15-LOX) generates hydroxyeicosatetraenoic acids (HETEs), lipoxins (LXs), 4-series leukotrienes (LTs), and other oxidative derivatives (LONE et al., 2013; YEDGAR et al., 2007). Similarly, the downstream derivatives of n-3 alpha-linolenic acid (ALA, C18:3n-3), specifically the eicosapentaenoic acid (EPA; C20:5n-3) generates 3-series PGs and TXBs via the COX-2 pathway, while hydroxyeicosapentaenoic acids (HEPEs) and 5-series LTs via the LOX (5-/12-/15-LOX) pathway (Figure 2). The ARA-derived pro-inflammatory eicosanoids are widely reported to alter the gut microbial composition, disrupt the intestinal barrier and play a central role in the pathogenesis of IBD (CALDER, 2009; DAS, 2006; SUGIHARA et al., 2018). Therefore, NSAIDs primarily target the inhibition of ARA and its derivatives mainly in the COX pathway. Conversely, EPA and docosahexaenoic acid (DHA; C22:6n-3) can replace ARA in the cell membranes and produce 100-fold weak pro-inflammatory eicosanoids for enhanced resolution of inflammation (CALDER, 2010, 2012, 2013; LEVY et al., 2001; SCHWAB and SERHAN,

2006). Furthermore, the newly identified downstream molecules of EPA such as the E-series resolvins (Rv)Es and DHA such as the D-series RvDs, maresins (MaRs), and protectins (PDs) act as an antagonist of inflammation (LEVY et al., 2001; SCHWAB and SERHAN, 2006; SERHAN et al., 2008; SERHAN and SAVILL, 2005) (Figure 2). These molecules not only terminate inflammation but scours inflammatory debris and stimulates antimicrobial defense for gut homeostasis (SERHAN et al., 2008). Moreover, recently ARA-derived PGs (PGD2, PGE2) and LX(A4) were identified to exert both pro-inflammatory and pro-resolution characteristics in a process called, 'class-switching' (SCHWAB and SERHAN, 2006; SERHAN et al., 2008; SERHAN and SAVILL, 2005). These key findings eventually enumerate the fact that both n-3 and n-6 PUFAs generate anti-inflammatory eicosanoids and supports pro-resolution. However, overwhelming data denotes n-3 PUFA as the strongest anti-inflammatory agent compared to n-6 PUFA. This could possible due to the difference in magnitude of action among the eicosanoids involved in resolution phase (Figure 2). Therefore, further studies are necessary to delineate the potency of pro-resolution eicosanoids to address the rationale behind n-3 PUFA's heightened anti-inflammatory actions.

Figure 2 Eicosanoid families of omega-3 and omega-6 polyunsaturated fatty acids involved in intestinal inflammation and resolution

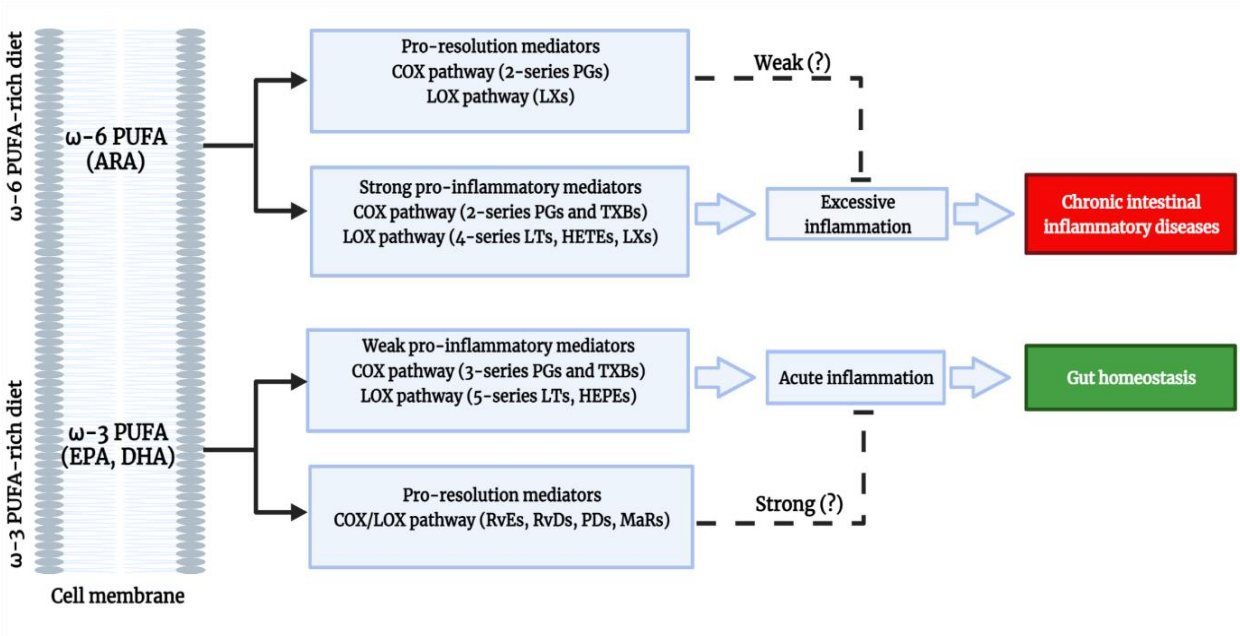

Eicosanoids are predominantly generated from the n-6 arachidonic acid (ARA) in phospholipid cell membranes by the enzymatic actions of cyclooxygenase (COX) and lipoxygenase (LOX). The COX pathway generates 2-series prostaglandins (PGs) and thromboxanes (TXBs), while the LOX generates lipoxins (LXs), hydroxyeicosatetraenoic acids (HETEs) and, 4-series leukotrienes (LTs) that occasionally stimulates excessive pro-inflammatory response leading to chronic intestinal inflammatory diseases. On the other hand, the n-3 eicosapentaenoic acid (EPA) stimulates acute inflammation by generating 3-series PGs and TXBs via the COX pathway, while hydroxyeicosapentaenoic acids (HEPEs) and 5-series LTs via the LOX pathway. Recently, certain ARA-derived PGs and LXs were identified to exert both pro-inflammatory and pro-resolution characteristics. Similarly, the newly identified downstream molecules of EPA such as the E-series resolvins (RvEs) and docosahexaenoic acid (DHA) such as the D-series resolvins (RvDs), maresins (MaRs), and protectins (PDs) are involved in pro-resolution. Both n-3 and n-6 polyunsaturated fatty acids (PUFA) supports pro-resolution, but overwhelming data reported n-3 PUFA as the strongest anti-inflammatory agent. This could be due to the difference in magnitude of action among the eicosanoids involved in the resolution phase of inflammation. For references, see text. Own figure created using BioRender.com.

2.4.2 Impact of n-3 PUFA on intestinal barrier under normal and stress conditions

***In vitro* studies**

The impact of n-3 PUFAs on the intestinal barrier under normal and inflammatory conditions was previously evaluated using different IEC models (Table 1). Particularly, the enterocyte models are widely utilized, as they are primarily involved in nutrition absorption, host-defence and are the most abundant cell type in IEL. In these experimental models, the pathophysiological events of barrier inflammation and oxidative stress are stimulated using different biological or chemical stressors. Some commonly applied stressors are pathogens, endotoxins, chemicals such as acetic acid, hydrogen peroxide (H_2O_2), dextran sulfate sodium (DSS), and 2,4,6-trinitrobenzene sulfonic acid (TNBS) (KIM et al., 1992; SUNDARAM et al., 2020). Moreover, these models are widely reported to mimic the cardinal signs of IBD (KIM and BERSTAD, 1992).

Accordingly, n-3 PUFA (ALA or EPA) treatment modulated the integrity and permeability of human Caco-2 cell monolayer in a dose-dependent manner (ROSELLA et al., 2000; USAMI et al., 2001). The epithelial integrity is determined by measuring the transepithelial electrical resistance (TEER) across the monolayer of IECs. Whereas the barrier permeability is assessed by measuring the paracellular flux of small molecules such as horseradish peroxidase (HRP), fluorescein-5-(6)-sulfonic acid (FS), or fluorescein isothiocyanate-labelled dextran 4kDa (FD4) between the TJ gap in the cell monolayer (ROSELLA et al., 2000; USAMI et al., 2001; WILLEMSEN et al., 2008). Further, pre-incubation of human T84 cells with n-3 PUFA (ALA, EPA, DHA) secured the monolayer integrity and permeability from the damage against IL-4 pro-inflammatory cytokine as indicated by increased TEER values and decreasing FD4 permeability compared to the control (WILLEMSEN et al., 2008). Similarly, the impact of heat-injury in the human Caco-2 cell monolayer was reduced by n-3 PUFA (EPA, DHA) pre-treatment. Specifically, EPA highly enhanced the barrier integrity (TEER) and expressions of different TJ proteins (Zonula occludens [ZO]-1, OCLN, CLDN-2), while decreased the barrier permeability to HRP flux compared to DHA (XIAO et al., 2013).

In the mechanically injured rat IEC-6 cells, n-3 PUFA (ALA, EPA, DHA, or docosapentaenoic acid) accelerated cell proliferation and wound healing by decreasing the level of pro-inflammatory eicosanoid, PGE2 and instead enhanced the expression of transforming growth factor (TGF)-β1 (RUTHIG et al., 1999, 2002). Further, n-3 PUFA (ALA,

EPA, DHA or FO) pre-treatment suppressed the expression of IL-1β-stimulated genes or proteins that involved in the pro-inflammatory response (COX-2, IL-6/-8, or inducible nitric oxide synthase [iNOS]) of Caco-2 cells and instead activated the protein expression of inhibitor of nuclear factor kappa B (IκB) and peroxisome proliferator-activated receptor(PPAR)γ (LETELLIER et al., 2008; REDDY et al., 2016; REIFEN et al., 2015a). Additionally, cell viability and the level of glutathione (GSH) antioxidant was enhanced, while the cell membrane damage was inhibited as indicated by a marked reduction in cytosolic lactate dehydrogenase (LDH) release (REDDY and NAIDU, 2016). Likewise, t-butyl hydroperoxide-induced Caco-2 cell membrane damage (LDH release), reduction in viability, and GSH level was recovered by n-3 PUFA (EPA, DHA) pre-treatment (REDDY and NAIDU, 2016). In another study, compared to EPA, DHA highly suppressed the expression of genes or proteins that involved in the pro-inflammatory response (NF-κβ1, IL-1R1/-6/-8) of human adult IECs (Caco-2 and NCM460 cells), fetal IECs (H4 cells), and neonate necrotizing enterocolitis (NEC)-IECs that challenged by IL-1β (WIJENDRAN et al., 2015).

Moreover, n-3 PUFA conferred antimicrobial activity against the common feed contaminants such as the mycotoxin deoxynivalenol (DON) and bacterial lipopolysaccharides (LPS). Accordingly, n-3 PUFA (EPA, DHA) pre-treatment of porcine IPEC-1 cells reversed the DON-induced damage on cell proliferation, viability, cell membrane (LDH release), TJ proteins (CLDN-1, ZO-1), and the monolayer integrity (TEER). Additionally, n-3 PUFA reduced the number of necrotic cells and the protein expression of molecules that involved in DON-induced apoptosis or necroptosis signaling such as the caspase-3/7, TNF receptor-1 (TNFR1), receptor-interacting protein kinase (RIPK)-1/-3, phosphorylated mixed lineage kinase-like protein (MLKL), phosphoglycerate mutase family 5 (PGAM5), dynamin-related protein 1 (Drp1) and high mobility group box-1 (HMBG1) (XIAO et al., 2020). Similarly, in our previous study, n-3 PUFA (EPA, DHA) treatment significantly enhanced the proliferation of porcine IPEC-J2 cells. It further inhibited the apoptosis (caspase-3/7) and secured the cell viability or cell membrane integrity (LDH release) that was damaged by different biological and chemical stressors as LPS, DSS, and H_2O_2 (SUNDARAM et al., 2020).

***In vivo* studies**

In accordance with cellular studies, n-3 PUFA secured the intestinal barrier and improved disease activity in both human and animal models of IBD (Table 1 and 2). At the intestinal level, disease activity is assessed by various parameters not limited to the expression of pro-

inflammatory mediators, intestinal weight/length (W/L) ratio, villus height/crypt depth (V/C) ratio, inflammatory cell infiltration, epithelial and mucosal morphology. Accordingly, in rat acetic acid-colitis, EPA administration significantly increased the intestinal fluid absorption and the expression of pro-inflammatory eicosanoids (PGE2, LTB4) (EMPEY et al., 1991). Conversely, in another study on the same disease model, n-3 PUFA reduced the expression of pro-inflammatory eicosanoids (PGE2, LTB4, TXB2), macrophage infiltration, mucosal, and tissue damage (CAMPOS et al., 2002). Following this, ALA supplementation in TNBS-colitis rats inhibited the protein expression of intercellular adhesion molecule-1 (ICAM-1), vascular cell adhesion molecule (VCAM-1), and vascular endothelial growth factor receptor-2 (VEGFR-2) that mediates leukocyte recruitment and angiogenesis in IBD (IBRAHIM et al., 2012).

Further, FO treatment supported the recovery of TNBS-, 1,3,5-trinitrobenzene (TNB) or DSS-induced colitis in murine models. Accordingly, FO reduced the gene or protein expression of pro-inflammatory eicosanoids (PGE2, COX-2, LTB4, or LTC4) (CAMUESCO et al., 2005; MBODJI et al., 2013; NIETO et al., 2002; REIFEN et al., 2015b; YUCEYAR et al., 1999) and molecules of cytokine signaling (TNF-α, IL-6 or NF-κB) (CAMUESCO et al., 2005; MBODJI et al., 2013; REIFEN et al., 2015b). The level of disease-specific enzymatic markers such as iNOS (CAMUESCO et al., 2005), alkaline phosphatase (CAMUESCO et al., 2005; NIETO et al., 1998; NIETO et al., 2002), γ-glutamyltransferase (NIETO et al., 1998) and myeloperoxidase (MPO) (CAMUESCO et al., 2005; NIETO et al., 1998; NIETO et al., 2002; REIFEN et al., 2015b; YUCEYAR et al., 1999) were also suppressed. Additionally, macroscopic injury of the intestinal mucosa (ulceration, necrosis, inflammation) (CAMUESCO et al., 2005; MBODJI et al., 2013; NIETO et al., 1998; NIETO et al., 2002; YUCEYAR et al., 1999), inflammatory cell infiltration (QIU et al., 2020; REIFEN et al., 2015b), colon wall thickness, and W/L ratio (QIU et al., 2020; YUCEYAR et al., 1999) were significantly reduced. Moreover, FO restituted the goblet cell abundance (CAMUESCO et al., 2005; NIETO et al., 1998; NIETO et al., 2002) GSH level (CAMUESCO et al., 2005), mucosal, and tissue integrity (CAMUESCO et al., 2005; MBODJI et al., 2013; NIETO et al., 1998; NIETO et al., 2002; YUCEYAR et al., 1999).

For the first time, DHA-derived MaR1 and EPA-derived RvE1 were shown to suppress the disease activity in murine colitis. Accordingly, MaR1 supplementation in DSS-colitis rats increased the expressions of different TJ proteins (ZO-1, OCLN), while inhibited the mucosal

damage, colon shortening, inflammatory cell infiltration, and expressions of different pro-inflammatory mediators (PGE2, MPO, ROS, TNF-α, IL-1β/-6). Importantly, MaR1 inhibited the protein expression of TLR4/NF-κB signaling (TLR4, p-NF-κB-p65) and instead activated the anti-inflammatory nuclear factor erythroid 2-related factor 2 (Nrf2)/heme oxygenase-1 (HO-1) signaling (QIU et al., 2020). Similarly, MaR1 intervention ameliorated the severity of acute and chronic DSS-colitis in mice by reducing epithelial loss, crypt damage, inflammatory cell infiltration, hyperaemia, colon wall thickness, colon shortening, and expression of pro-inflammatory genes or proteins (MPO, NF-κB, IL-1β, IL-6, TNF-α, interferon[INF]γ, ICAM-1). In the same study, MaR1 administration in TNBS-colitis mice significantly reduced the MPO activity, crypt damage, inflammatory cell infiltration, and edema (MARCON et al., 2013). Likewise, RvE1 facilitated tissue repair in peritonitis mice with TNBS-colitis, while significantly reduced the leukocyte infiltration, MPO activity, and the expression of genes corresponding to pro-inflammatory response (COX-2, TNF-α, IL-12p40, iNOS) (ARITA et al., 2005).

In rats with 5-fluorouracil-induced small intestinal injury, FO administration reduced the intestinal wall thickness, epithelial and mucosal damage, while improved goblet cell abundance and mucosal repair (V/C, periodic acid-Schiff's^{+} brush border, mitotic cells) (GAWISH et al., 2013). Likewise, in mice with 5-fluorouracil-induced mucositis, FO supplementation improved the mucosal architecture (villus height, crypt depth, V/C ratio), while ameliorated inflammatory cell infiltration and bacterial translocation across the intestinal barrier (GENEROSO SDE et al., 2015). In another study, DHA-enriched diet stimulated inflammatory response (IL-1α/-10) and facilitated pouch adaptation in the rats that underwent restorative proctocolectomy (DRZYMAŁA-CZYŻ et al., 2012). Similarly, n-3 PUFA supplementation improved the hydroxyproline level and tissue healing, while decreased the colonic burst pressure in rats with ischemic colon anastomoses (EKÇI et al., 2011).

Generally, a steep oxygen gradient exists in the intestinal barrier to support the sustenance of gut microbiota and other barrier functions. An imbalance in the gradient can instigate barrier degenerative diseases such as ischemic-reperfusion and NEC (GLOVER et al., 2016). In rats with ischemic-reperfusion, n-3 PUFA (EPA, DHA) administration facilitated intestinal tissue healing by increasing the protein levels of anti-inflammatory eicosanoids (PGE3, 8-Iso PGF3α, LTB5, TXB3, 17,18-EEP) and antioxidant enzymes such as the superperoxide dismutase (SOD) and catalase (CAT). Additionally, total tissue protein content

was increased, while the magnitude of mucosal damage and NO^{2-}/ NO^{3-} level was decreased (BRAHMBHATT et al., 2013).

Following, n-3 PUFA remediated the experimental NEC induced by hypoxia, formula feeding, or its combination in murine models. Accordingly, n3-PUFA (DHA or FO) intervention significantly decreased the gene or protein expression of pro-inflammatory mediators such as TLR2/4, LTB4, phospholipase A2-II, platelet-activating factor (PAF), and its receptor (PAFR). Additionally, mucosal damage, tissue necrosis, incidence of disease, and death were suppressed in the NEC-rat pups (AKISÜ et al., 1998; CAPLAN et al., 2001; LU et al., 2007). Moreover, n-3 PUFA (EPA, DHA) administration in maternal rats during gestation, significantly accumulated in the intestinal phospholipids of prematurely delivered rat pups. This subsequently ameliorated the impact of experimental NEC induced in rat pups by inhibited the gene expression of pro-inflammatory IκBα/β and instead activated the anti-inflammatory PPARγ. Besides, the gene expression of PGE2 and PGD2 receptors was increased, while the mucosal damage, inflammatory cell infiltration, and incidence of disease was decreased (OHTSUKA et al., 2011).

As observed in cellular studies, n-3 PUFA supported the recovery from bacterial infections in murine models. Specifically, FO administration in mice significantly reduced the *Citrobacter rodentium*-induced mucosal damage, inflammatory cell infiltration, enterocyte proliferation, apoptosis, and intestinal permeability to FD4. Also, FO increased the gene expression of anti-inflammatory cytokine IL-10, while suppressed the gene or protein expressions of pro-inflammatory cytokines and chemokines such as IL-6, IL-17A, IFNγ, monocyte chemoattractant protein-1 (MCP-1), keratinocyte cytokine, and macrophage inflammatory protein-2 (MIP-2) (HEKMATDOOST et al., 2013). Further, n-3 PUFA (EPA, DHA or FO) intervention in mice, attenuated the expression of genes or proteins involved in LPS-activated TLR4/NF-κB signaling (TLR4, MyD88, NF-κB-p65, NF-κB, transforming growth factor-β-activated kinase-1) and the downstream pro-inflammatory response (TNF-α, IL-1β/-6, INFγ or COX-2) (CAO et al., 2019; LIU et al., 2015). Besides, the expression of TJ proteins (E-cadherin, ZO-1, OCLN), n-3 PUFA receptor gene (G-protein coupled receptor 120), and tissue repair were significantly enhanced. The gene expression of anti-inflammatory cytokine IL-10, MUC2, and its regulatory gene, free fatty acid receptor-2 (FFAR-2) were also substantially increased (CAO et al., 2019).

Apart from infections, weaning imparts tremendous inflammatory and metabolic stress in pigs due to changes in gastrointestinal physiology. Previously, the administration of FO in pigs significantly downregulated the protein expression of pro-inflammatory eicosanoids (PGE, PGI2, TXB2) through n-3 PUFA enrichment in the intestinal phospholipids. Although the morphology of colonic mucosa remained stable, the crypt depth was significantly reduced (CAMPBELL et al., 1997) (Table 1). Further, FO administration during the course of gestation to lactation in sows markedly increased the n-3 PUFA levels in ileal phospholipids. The maternal diet subsequently instigated an age-dependent decrease in villus height (day-0), crypt depth (day-7), and HRP permeability (day 0-28) in the piglet ileum. These effects are reported to prevent the intestinal pathologies associated with IEL functioning during the neonatal period (BOUDRY et al., 2009).

In similar maternal physiology, supplementation of extruded LO temporarily increased the FD4/LPS permeability in the piglet jejunum explants until day-28 and thereafter decreased at day-52 (DESALDELEER et al., 2014). The distinct outcome of these two trials could have possibly aroused from a difference in LO formulation administered, dose-effect, or animal physiology. Nevertheless, the influence of maternal dietary n-3 PUFA on piglet intestinal development and health status is unclear and hence needs further investigations. In another study, FO administration in weaned piglets protected from LPS-induced damage on the intestinal barrier by enhancing the expressions of TJ proteins (OCLN, CLDN-1), villus height, and V/C ratio. Besides, the expression of genes corresponding to the TLR4 pathway such as the myeloid differentiation primary response 88 **(**MyD88), interleukin-1 receptor-associated kinase-1 (IRAK1), and TNFR-associated factor-6 (TRAF6) were suppressed. The expression of inflammatory genes as NOD2 and RIPK-2, and the expression of proteins as diamine oxidase, caspase-3, and heat shock protein-70 (HSP70) were also significantly downregulated (LIU et al., 2012). Furthermore, FO supported the remission of DSS-colitis in the early-weaned piglets by enhancing enterocyte mitosis and gene expression of PPARγ-responsive uncoupling protein-3 (UPC3) (BASSAGANYA-RIERA et al., 2006). Moreover, EPA intervention in piglets moderately supported the recovery of ileum ischemic injury by decreasing the expression of PGE2 protein and barrier flux to H^3-mannitol/C^{14}-inulin, while increased the expression of COX-2 gene and TEER values (JACOBI et al., 2012). In another study that administered FO in pigs, exhibited a significant reduction in LPS permeability across the ileal explants (MANI et al., 2013).

In clinical settings, n-3 PUFAs are administered either individually or as an immunological adjuvant for controlling different IBDs including Crohn's disease (CD), ulcerative colitis (UC), and distal proctocolitis (DP) (Table 2). Accordingly, in subjects with ethanol-induced duodenal injury, FO administration relieved macroscopic lesions by increased the protein expression of anti-inflammatory eicosanoid, LTC5 (SCHEPP et al., 1991). Also, EPA suppressed the mucosal expression of pro-inflammatory eicosanoid as LTB4 in pediatric UC under remission (SHIMIZU et al., 2003). Further, administration of FO in patients with active UC or DP, witnessed a marked reduction in disease activity as observed from improvements in clinical, endoscopic, and histological scores (ALMALLAH et al., 1998; DICHI et al., 2000; MCCALL TB, 1989; SEIDNER et al., 2005). In active UC or CD patients undertaking IBD medications, n-3 PUFA diet (FO, fish or EPA) reduced the disease activity (GRIMSTAD et al., 2011; LORENZ et al., 1989; SALOMON et al., 1990) and protein expression of pro-inflammatory eicosanoids (PGE2, PGI2, TXB2) (HILLIER et al., 1991) by incorporating in the mucosal phospholipids (GRIMSTAD et al., 2011; HILLIER et al., 1991; LORENZ et al., 1989). Similarly, the health status of UC patients in remission with or without IBD medication was improved by FO or EPA administration (LOESCHKE et al., 1996; PROSSOMARITI et al., 2017; SCAIOLI et al., 2018). Specifically, the disease activity and mucosal inflammation were remediated by activating the gene or protein expression of anti-inflammatory mediators such as IL-10, signal transducer and activator of transcription-3 (STAT3), and suppressor of cytokine signaling-3 (SOCS3). Additionally, the abundance of goblet cells, IL-22, and proteins that modulate the secretory and absorptive cell lineage such as the hairy and enhancer of split-1 (HES-1) and kruppel-like factor-4 (KLF-4) were also increased (PROSSOMARITI et al., 2017). On the contrary, few studies have reported that n-3 PUFA (FO, EPA, or DHA) had no beneficial effects in the patients with either active, quiescent, or remitted UC under IBD medications (BARBOSA et al., 2003; GREENFIELD et al., 1993; MIDDLETON et al., 2002). Of note, various factors could have contributed to the differential outcome of n-3 PUFA diet in patients such as the age, metabolic status, dose, or the impact of co-administered IBD medications. A schematic representation summarizing the anti-inflammatory and antioxidative mechanisms of n-3 PUFA through NF-κB inhibition in IEL is reported in the Figure 3.

Figure 3 Model summarizing the immunomodulatory mechanisms of omega-3 polyunsaturated fatty acids in the intestinal epithelium

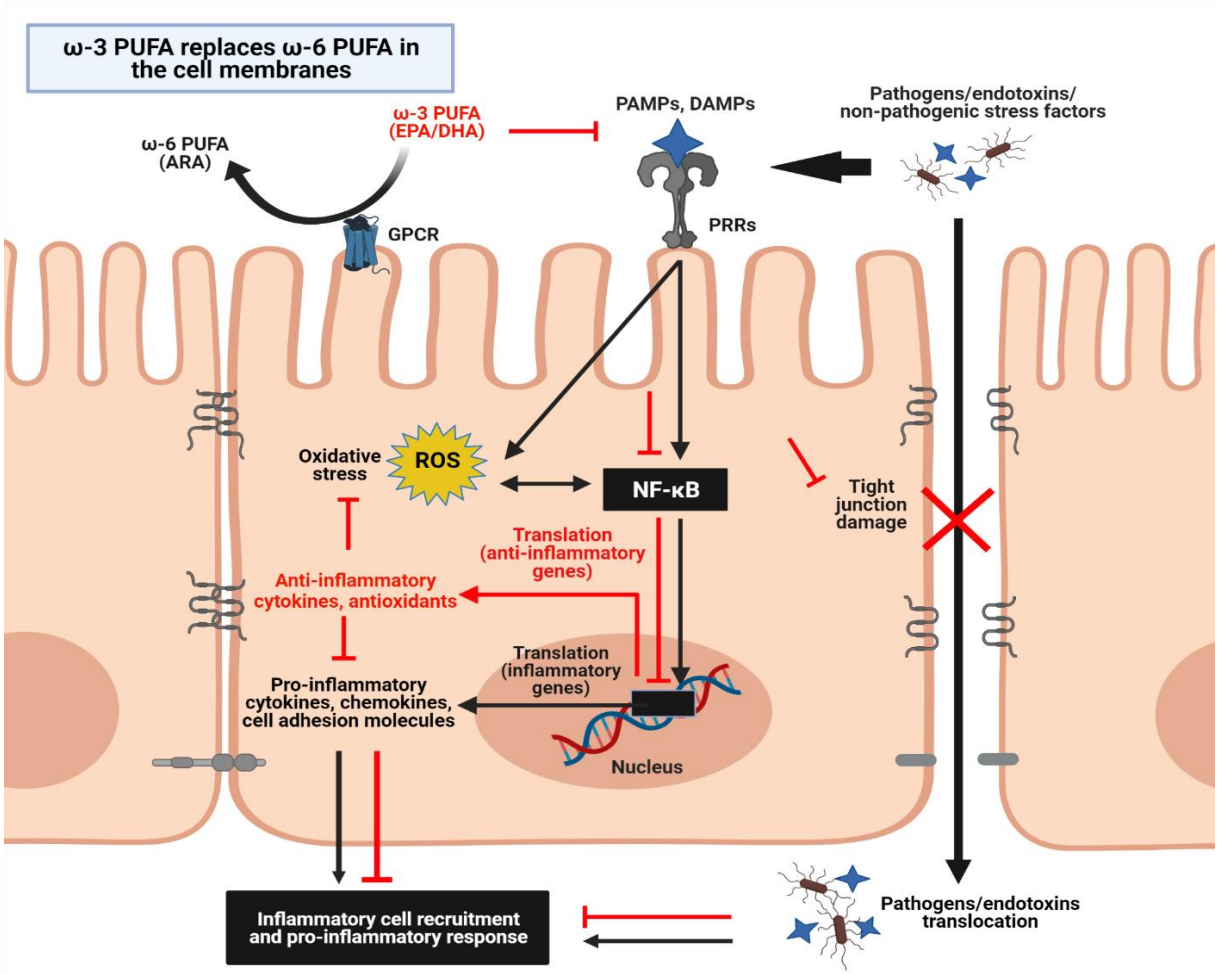

In arachidonic acid (ARA)-enriched cell membranes, during an infection or injury, pathogen-associated molecular patterns (PAMPs) or damage-associated molecular patterns (DAMPs) binds with the host-specific pattern-recognizing receptors (PRRs) and activate the nuclear factor-κB (NF-κB) signaling to release pro-inflammatory cytokines, chemokines and reactive oxygen species (ROS). Subsequently, these mediators recruit the inflammatory cells from lamina propria and exert a strong pro-inflammatory response. Pro-inflammation also damages the integrity of the epithelial barrier by disrupting the tight junction proteins. Loss of epithelial integrity aggravates inflammation by facilitating the translocation of luminal pathogens and endotoxins into the circulatory system (Black lines). Dietary supplementation of eicosapentaenoic acid (EPA) and docosahexaenoic acid (DHA) ameliorates the pro-inflammatory response by replacing ARA in specific cell membrane G-protein-coupled receptors (GPCR) and instead stimulates the production of anti-inflammatory cytokines and antioxidants (Red lines). For references, see text. Own figure created using BioRender.com.

2.5 Citrus pectin

2.5.1 Structure and molecular mechanism

CPn is a highly branched, complex heteropolysaccharide derived from the peels and pomace of citrus fruits. The structure of CPn involves a covalently linked, galacturonic acid backbone with three major polysaccharide units of homogalacturonan, rhamnogalacturonan, and substituted galacturonans (LECLERE et al., 2013; MAXWELL et al., 2012). Generally, the small intestine cannot assimilate native pectins due to its large molecular weight (60–300 kDa), complex structure, and higher degrees of esterification (DE~70%). However, pH or enzymatic treatment yields compounds of low molecular weight (15 kDa) and reduced DE (<5%). These modified CPn's exhibit enhanced intestinal absorption and transportation (COURTS, 2013; ELIAZ et al., 2019). Interest in utilizing CPn as a potential feed additive is emerging from the recent pieces of evidence on its anti-inflammatory, anti-microbial and prebiotic activities (BEUKEMA et al., 2020; LARA-ESPINOZA et al., 2018; PARK et al., 2019; RAMACHANDRAN et al., 2017). Owing to the complex physiochemical structure of CPn, its precise molecular mechanism is fairly established (PARK et al., 2019). However, previous reports on its ability to interact with TLRs, Galectin-3 (Gal-3) or produce short-chain fatty acids (SCFAs) could be attributed to part of its immunomodulatory mechanisms in the intestinal barrier (BEUKEMA et al., 2020; DO PRADO et al., 2019) (Figure 4). Interestingly, non-digestible carbohydrates (NDC) and LPS share a structural similarity, especially with respect to carbohydrate-containing regions that interact with IECs and other immune cells (DO PRADO et al., 2019). CPn belongs to the category of NDC and was shown to interact with TLR2/4 that resulted in modulating NF-κB in both IECs and immune cells (BEUKEMA et al., 2020; BEUKEMA et al., 2021; CHEN et al., 2006; DO PRADO et al., 2019; VOGT et al., 2016). Another mechanism by which CPn controls inflammation is by inactivating Gal-3 signaling proteins. Gal-3 belongs to the lectin family, a class of carbohydrate-binding proteins that dispersed in both intra- and extracellular regions. It possesses a unique carbohydrate-recognition domain (CRD) that binds to the β-galactoside sugars (BARONDES et al., 1994; MAXWELL et al., 2012). Gal-3 was reported to involve in the pathogenesis of microbial infections, cancer, and several other inflammatory diseases (DIAZ-ALVAREZ et al., 2017; HARA et al., 2020). The mechanism by which Gal-3 regulates inflammatory response is multifaceted. In intestine, it stimulates pro-inflammatory response by acting as ligands to TLRs of IECs (DIAZ-ALVAREZ and ORTEGA, 2017; SUN et al., 2020) (Figure 4B).

Previously, in rat pups, induction of experimental NEC was shown to activate Gal-3-mediated TLR4/NF-κB signaling (SUN et al., 2020). Alternatively, Gal-3 act as PRRs to pathogens or LPS and recruit immune cells for opsonization (DIAZ-ALVAREZ and ORTEGA, 2017) (Figure 4B). Of note, orally or intravenously administered CPn are able to cross the intestinal barrier and inhibit Gal-3 activity by binding its CRD region (Figure 4B) (NANGIA-MAKKER et al., 2002; PIENTA et al., 1995). Currently, the application of CPn as Gal-3 inhibitor is emerging as a novel strategy for treating cancer and other inflammatory diseases (DE BOER et al., 2014; ELIAZ and RAZ, 2019; MAXWELL et al., 2012; SUTHAHAR et al., 2018). From all these observations, it could be possible that certain carbohydrate regions of CPn, LPS, and Gal-3 that bind to IECs or immune cells are quite similar. This could have enabled CPn to prevent inflammation by competing with LPS or Gal-3 for the TLR-binding region (Figure 4A-B). Moreover, the SCFAs produced during the fermentation of dietary fibers such as CPn are reported to improve the intestinal barrier functions (DO PRADO et al., 2019).

2.5.2 Impact on intestinal barrier under normal and stress conditions

***In vitro* studies**

CPn self-assembles into dense hydrogel matrix on contact with mucin glycoproteins of IEL (SRIAMORNSAK et al., 2010) (Figure 4C). The gel-forming ability of CPn (DE94%, DE25%) was demonstrated using the commercially available mucins and on the mucosal surface of porcine colonic tissues. In this study, CPn-DE94% formed a gel matrix at the tissue surface, while CPn-DE25% permeated deeper towards the tissue wall. Besides, the net electrical charge of CPn influenced the rheological strength of the gel (LIU et al., 2005). Following, different oligosaccharides of CPn were shown to cross the Caco-2 cell monolayer based on the degree of polymerization in a transwell culture system. Particularly, only the short-chain galectins and arabinogalactans could transverse, but not the galacturonic acid (COURTS, 2013).

A recent study demonstrated the immunomodulatory behavior of in vitro digested citrus pulp on the intestinal barrier using IPEC-J2 cell model. Specifically, it inhibited the gene expressions of TLR4 and CLDN-1 and instead activated NOD1 under a stress-free environment (UERLINGS et al., 2020) (Table 3). Further, many studies demonstrated the barrier protective properties of CP under inflammatory conditions. Accordingly, CPn with different degrees of methyl esters (DM32%, DM59%, DM64%) secured the integrity (TEER) and reduced the permeability (lucifer yellow flux) of mouse CMT93 cell monolayer that was disrupted by the

pathogenic challenge of *C. rodentium*. Interestingly, using reporter cell assay, CPn was shown to activate the NF-κB/AP-1 signaling via TLR2 in CMT93 cells independent of *C. rodentium* challenge. Additionally, CPn imparted anti-adhesive effects on *C. rodentium* by interacting with the pathogen instead of CMT93 cells (BEUKEMA et al., 2021). Likewise, both native and enzymatically modified citrus residues prevented the Caco-2 cells from secreting IL-8 upon the pathogenic challenge of *Salmonella typhimurium* and *Listeria monocytogenes*. In this study, citrus treatment selectively supports the cellular adhesion of probiotics *(Lacticaseibacillus casei* and *Bifidobacterium lactis),* while repelled the pathogens (*S. typhimurium* and *L. monocytogenes)* (Figure 4C). Moreover, the enzymatically modified citrus residues exhibited enhanced antibacterial and prebiotic activities in comparison to the unmodified (DE PAULA MENEZES BARBOSA et al., 2020). In another study, CPn (DM30%, DM56%, DM74%) secured the integrity (TEER) of the T84 cell monolayer from the barrier disrupting agent as phorbol esters (VOGT et al., 2016).

***In vivo* studies**

Previously, CP administration in rats under normal physiology significantly increased the mucosal proliferation ($Ki67^+$ cells), intestinal length, weight, and the level of cecum SCFAs (FUKUNAGA et al., 2003) (Table 3). In agreement with cellular studies, CPn potentially ameliorated intestinal barrier inflammation under different stress conditions in animal models. Accordingly, in rats with methotrexate-colitis, supplementation of CPn reduced the intestinal barrier permeability, bacterial translocation, MPO expression, and intestinal water content. It further stimulated mucosal replenishment as indicated by an increase in mucosal wet weight, protein, and nucleic acid content (MAO et al., 1996). In the mice with acetic acid-colitis, CPn reduced the peritoneal granulocyte adhesion, intestinal tissue injury, ROS, and MPO expressions (MARKOV et al., 2011). Similarly, in mice with doxorubicin-induced ileitis, CPn-DM7% administration substantially reduced the crypt cell apoptosis, inflammatory cell infiltration, and protein expression of pro-inflammatory cytokines and chemokines (TNF-α, MCP-1, IL-6, chemokine C-X-C motif ligand[CXCL]-1) (SAHASRABUDHE et al., 2018). In DSS-colitis mice, supplementation of CPn or citrus residues (from juice extraction) decreased the expression of pro-inflammatory genes (TNF-α, IL-1β/-16, iNOS, ICAM-1) and colon W/L ratio. Additionally, CPn restituted the intestinal barrier integrity as observed from the increase in expression of MUC3 and TJ proteins (ZO-1, OCLN) (PACHECO et al., 2018). In a similar disease model of mice, dietary CPn (DE68.01±0.43%, DE41.61±0.12%, DE38.09±0.78%)

reduced the expression of pro-inflammatory proteins (IL-6/-17, MPO), intestinal permeability (FD4/LPS flux), inflammatory cell infiltration, colon W/L ratio, epithelial and mucosal damage. Additionally, CPn increased the goblet cell abundance, ZO-1 expression, and V/C architecture (FAN et al., 2020).

In another study, administration of CPn, its methanol extracts, or methanol residues in the DSS-colitis mice, attenuated the mucosal damage, inflammatory cell infiltration, colon shortening, and protein expression of pro-inflammation cytokines and chemokines (TNF-α, IL-1β/-6/-12/-17a, MCP-1 or CXCL-2), (ABE et al., 2018; KAWABATA et al., 2018; TINH et al., 2021). As observed earlier, CPn supported the recovery of barrier integrity by improving the goblet cell abundance (FAN et al., 2020; KAWABATA et al., 2018) and the expression of different TJ proteins (ZO-1/-2, OCLN, CLDN-3/-7, or JAM-A) (KAWABATA et al., 2018; TINH et al., 2021). In cats, CPn ameliorated the small intestinal ulceration and lesions commonly caused by the side effects of NSAIDs as indomethacin (SATOH et al., 2009). In chicken coccidiosis, CPn administration decreased the serosa thickness, the number of schizonts in the ileal enterocytes, and the gene expression of pro-inflammatory cytokine IL-12β. In addition to improvement in goblet cell abundance, V/C ratio, cecum weight, and levels of SCFAs, the gene expression of pro-inflammatory cytokines (INFγ, IL-1β) were also increased. Although CPn displayed beneficial effects to a certain extent, on the contrary, it also activated inflammatory response and decreased the growth performance of uninfected birds (WILS-PLOTZ et al., 2013). Following this, supplementation of citrus pulp in weaned piglets did not alter the intestinal morphology or inflammatory status (WEBER et al., 2008). In some of the *in vivo* trials, CPn administration significantly enhanced the level of the cecum or fecal SCFAs, which could have contributed to the changes observed in intestinal morphology or its immune status (KAWABATA et al., 2018; TINH et al., 2021; WILS-PLOTZ et al., 2013).

Figure 4 Model summarizing the immunomodulatory and antimicrobial mechanisms of citrus pectin in the intestinal epithelium

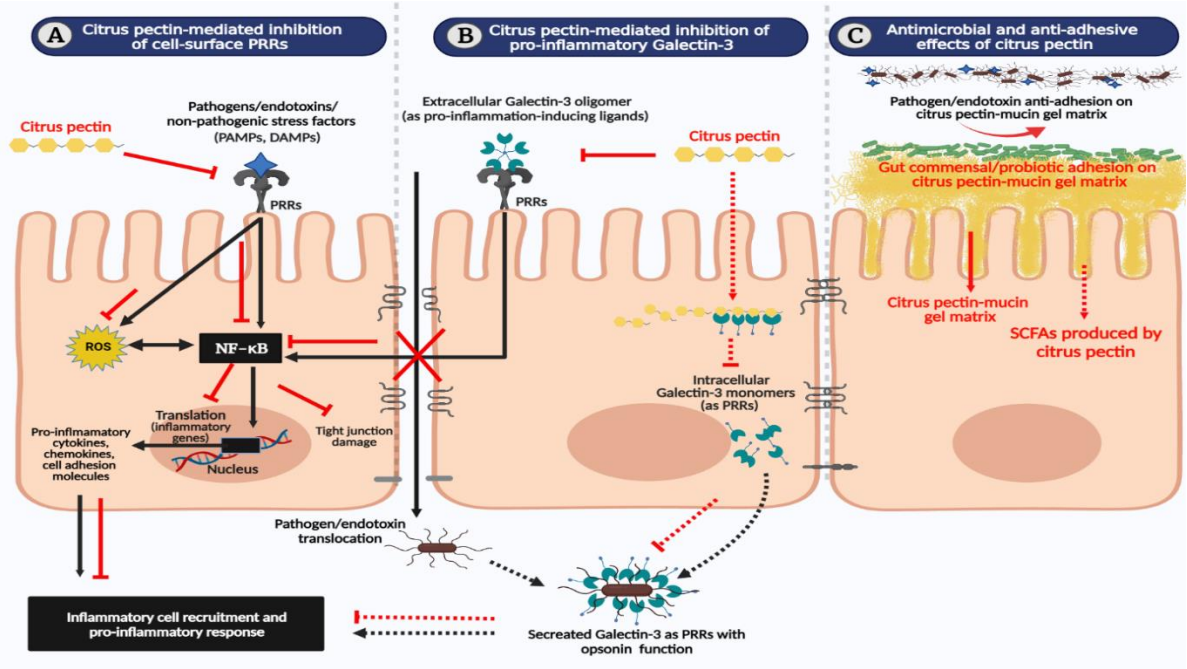

(A) Pathogen-associated molecular patterns (PAMPs) or damage-associated molecular patterns (DAMPs) activate the nuclear factor-κB (NF-κB)-mediated pro-inflammatory response and damages the epithelial integrity as described in figure. 2. (Black solid lines). Dietary citrus pectin (CPn) blocks the cell surface pattern-recognizing receptors (PRRs) and prevents the PAMPs or DAMPs from activating NF-κB (Red solid lines). (B) During infection or injury, extracellular Galectin-3 (Gal-3) acts as ligands to cell-surface PRRs and activates NF-κB-mediated pro-inflammatory response (Black solid lines). CPn can modify the cell-surface PRRs and prevent the Gal-3 from binding (Red solid lines). Alternatively, cells secrete intracellular Gal-3 that acts as PRRs to pathogens or endotoxins and recruits immune cells enabling opsonization (Black dotted lines). CPn can directly bind the intracellular Gal-3 and block its opsonin function (Red dotted lines). (C) CPn binds with mucin glycoproteins and forms gel-matrix that selectively support the adhesion of probiotics and gut commensals, while repel the pathogens (Red solid lines). Alternatively, CPn directly interacts with the pathogen and inhibits its growth or indirectly gives rise to short-chain fatty acids (SCFAs) that protects barrier health (Red dotted line). Abbreviations: ROS, Reactive oxygen species. For references, see text. Own figure created using BioRender.com.

Table 1 Effects of omega-3 polyunsaturated fatty acids in the intestinal barrier cell and animal models

Model of study	**Stress by**	**n-3 PUFA assessed**	**Immune response and morphological changes**	**Reference**
In vitro				
Human Caco-2 cells	Non-stimulated	EPA	↑phospholipid n-3 PUFAs; ↓HRP flux; =(TEER, LDH release)	(ROSELLA et al., 2000)
Human Caco-2 cells	Non-stimulated	ALA, EPA	↑(FS flux, LDH release) in EPA; ↓TEER	(USAMI et al., 2001)
Human T84 cells	IL-4	ALA, EPA, DHA	↑TEER; ↓FD4 flux	(WILLEMSEN et al., 2008)
Human Caco-2 cells	Heat	EPA, DHA	↑(phospholipid n-3 PUFA, TEER, ZO-1, OCLN, CLDN-2); ↓HRP flux	(XIAO et al., 2013)
Rat IEC-6 cells	Mechanical wound	ALA, EPA, DPA, DHA	↑(cell proliferation and migration in wound healing, TGF-β1); ↓PGE2	(RUTHIG and MECKLING-GILL, 1999, 2002)
Human Caco-2 cells	IL-1β	ALA, EPA, DHA	↓(IL-6, IL-8, iNOS); ↑(IκB, PPARγ)	(LETELLIER et al., 2008)
Human Caco-2 cells	IL-1β	ALA, FO	↓(COX-2, IL-8, iNOS) in ALA treatment; =FO treatment	(REIFEN et al., 2015a)
Human Caco-2 cells	t-BHP or IL-1β	EPA, DHA	↑(cell viability, GSH); ↓(LDH release, IL-8)	(REDDY and NAIDU, 2016)
Human Caco-2 cells, human NCM460 cells, fetal H4 cells or	IL-1β	EPA, DHA	↓(NF-κβ1, IL-18, IL-6, IL-1R1)	(WIJENDRAN et al., 2015)

neonate NEC-IEC cells				
Porcine IPEC-1 cells	DON	EPA, DHA	↑(cell proliferation, viability, TEER, CLDN-1, ZO-1); ↓(LDH release, FD4 flux, caspase-3/8, necrotic cells, ROS); ↓necroptosis signaling molecules (TNFR1, RIPK-1/3, MLKL, PGAM5, Drp1, HMGB1)	(XIAO et al., 2020)
Porcine IPEC-J2 cells	LPS, DSS or H_2O_2	EPA, DHA	↑(cell proliferation, viability); ↓(LDH release, caspase-3/7); =NO_2^-	(SUNDARAM et al., 2020)
In vivo				
Rat	Acetic acid-colitis	EPA	↑(fluid absorption, PGE2, LTB4); =(mucosal ulceration, tissue damage)	(EMPEY et al., 1991)
Rat	Acetic acid-colitis	Not specified	↓(PGE2, LTB4, TXB2, mucosal and tissue damage, macrophage infiltration); =LTC4	(CAMPOS et al., 2002)
Rat	TNBS-colitis	ALA	↓(ICAM-1, VCAM-1, VEGFR-2); =HO-1	(IBRAHIM et al., 2012)
Rat	TNBS-colitis	FO	↓(AP, MPO, γ-GT, colon weight/length ratio, colon wall thickness, mucosal ulceration, tissue damage); ↑(goblet cells, epithelial repair)	(NIETO et al., 1998)
Rat	TNB-colitis	FO	↓(LTB4, LTC4, MPO, mucosal ulceration and inflammation)	(YUCEYAR et al., 1999)
Rat	TNBS-colitis	FO	↑(phospholipid n-3 PUFAs, goblet cells with matured mucin granules, tissue repair); ↓(AP, MPO, PGE2, LTB4, mucosal necrosis, tissue damage)	(NIETO et al., 2002)
Rat	TNBS-colitis	FO	↓(COX-2, PGE2, LTB4, NF-κB, TNF-α); =(IL-1β, PPARγ, mucosal damage, inflammatory cell infiltration)	(MBODJI et al., 2013)
Rat	TNBS- or DSS-colitis	FO	↑(phospholipid n-3 PUFAs, MPO); ↓(COX-2, IL-6, TNF-α); =(mucosal necrosis)	(REIFEN et al., 2015b)
Rat	DSS-colitis	FO	↓(disease activity, colon weight/length ratio, mucosal ulceration, crypt dilation, goblet cell depletion, inflammatory cell infiltration, tissue damage, MPO, iNOS, AP, COX-2, LTB4, TNF-α,); ↑GSH; =IL-1β	(CAMUESCO et al., 2005)

Rat	DSS-colitis	MaR1	↓(disease activity, colon shortening, mucosal damage, inflammatory cell infiltration, PGE2, MPO, ROS, TLR4, p-NF-κB-p65, TNF-α, IL-6, IL-1β); ↑(ZO-1, OCLN, Nrf2, HO-1)	(QIU et al., 2020)
Rat	5-FU-small intestinal injury	FO	↑(V/C architecture, mitotic cells, goblet cells, periodic acid-Schiff's^{+} brush border); ↓(intestinal wall thickness, mucosal damage, epithelial sloughing)	(GAWISH et al., 2013)
Rat	Restorative proctocolectomy	DHA	↑(IL-1α, IL-10, pouch adaptation and inflammation); =(IL-6, IL-12)	(DRZYMAŁA-CZYŻ et al., 2012)
Rat	Ischemic colon anastomoses	Not specified	↑(tissue healing, hydroxyproline level); ↓colonic burst pressure	(EKÇI et al., 2011)
Rat	Ischemic reperfusion	EPA, DHA	↑(phospholipid n-3 PUFAs, total tissue protein, SOD, CAT, PGE3, 8-Iso PGF3α, LTB5, TXB3, 17,18-EEP); ↓(mucosal damage, NO^{2-}/ NO^{3-}); =(IL-6, IL-8, INFγ, TNF-α, MPO, neutrophil infiltration)	(BRAHMBHATT et al., 2013)
Neonate mice	Hypoxia-induced NEC	FO	↓(mucosal damage, platelet-activating factor, LTB4)	(AKISÜ et al., 1998)
Neonate rats	Hypoxia, formula feed-induced NEC	DHA	↓(phospholipase A2-II, platelet-activating factor receptor, tissue necrosis, incidence of disease and death); =(epithelial apoptosis, iNOS)	(CAPLAN et al., 2001)
Neonate rats	Hypoxia, formula feed-induced NEC	DHA	↓(TLR2/4, platelet-activating factor receptor, tissue necrosis, incidence of disease); =phospholipase A2-II	(LU et al., 2007)
Maternal rats	Formula feed-induced NEC	EPA, DHA	↑(phospholipid n-3 PUFAs, PGE2 receptor, PGD2 receptor, PPARγ) and ↓(IκBα/β, mucosal damage, inflammatory cell infiltration, incidence of disease) in premature rat pups	(OHTSUKA et al., 2011)
Mice	Acute or chronic DSS-colitis	MaR1	↓(disease activity, MPO, NF-κB, IL-1β, IL-6, TNF-α, INFγ, ICAM-1, crypt damage, inflammatory cell infiltration, colon wall thickness, colon shortening, hyperaemia and tissue damage)	(MARCON et al., 2013)
Mice	TNBS-colitis	MaR1	↓(tissue damage, MPO, crypt damage, inflammatory cell infiltration, edema)	(MARCON et al., 2013)
Peritonitis mice	TNBS-colitis	RvE1	↑(tissue repair); ↓(leukocyte infiltration, COX-2, TNF-α, IL-12p40, iNOS, MPO); =(INF-γ, IL-4, IL-10, TGF-β)	(ARITA et al., 2005)

Mice	5-FU-induced mucositis	FO	↓(intestinal permeability to bacterial translocation, mucosal damage, lesions, apoptosis, inflammatory cell infiltration); ↑(villus height, crypt depth, V/C ratio)	(GENEROSO SDE et al., 2015)
Mice	*Citrobacter rodentium*	FO	↑(phospholipid n-3 PUFAs, IL-10); ↓(mucosal damage, inflammatory cell infiltration, apoptotic cells, $Ki67^{+}$ enterocytes, MIP-2, keratinocyte cytokine, MCP-1, IFN-γ, IL-6, IL-17A, FD4 intestinal permeability); =(mucosal adherent *C. rodentium* count, TNF-α, TGF-β, FoxP3)	(HEKMATDOOST et al., 2013)
Mice	LPS	FO	↓(COX-2, TLR4, MyD88, NF-κB, IL-1β, IL-6, TNF-α); =(iNOS, MCP-1)	(LIU et al., 2015)
Mice	LPS	EPA, DHA	↑(E-cadherin, ZO-1, OCLN, GPR120, FFAR-2, MUC2, IL-10, V/C ratio, tissue repair); ↓(NF-κB-p65, TAK1, INFγ, TNF-α, IL-1β, IL-6); =TLR4	(CAO et al., 2019)
Pigs	Non-stimulated	FO	↑phospholipid n-3 PUFAs; ↓(PGE, PGI2, TXB2, crypt depth); =(colonic mucosal morphology)	(CAMPBELL et al., 1997)
Sows	Non-stimulated	LO	↑phospholipid n-3 PUFA in sow ileum; ↓(δ-5/-6 desaturase, HRP flux until day 28, villus height at day 0, crypt depth at day 7) in piglet ileum; =ileum enterocyte maturation in piglets	(BOUDRY et al., 2009)
Sows	Non-stimulated	Extruded LO	↑(FD4/LPS permeability between day 0-28 in piglet jejunum explant); =(FD4/LPS permeability at day-52, IL-8, TNF-α in LPS-challenged piglet jejunum explant)	(DESALDELEER et al., 2014)
Weaned piglets	LPS	FO	↑(phospholipid n-3 PUFAs, villus height, V/C ratio, OCLN, CLDN-1); ↓(diamine oxidase, TNF-α, PGE2, caspase-3, HSP70, NF-κB-p65); ↓TLR4 signaling molecules (TLR4, MyD88, IRAK1, TRAF6, NOD2, RIPK-2)	(LIU et al., 2012)
Weaned piglets	DSS-colitis	FO	↑(mitotic figures in enterocytes, UPC3, disease remission); =(mucosal damage, PPARγ, PGC1-α, TNF-α, keratinocyte growth factor)	(BASSAGANYA-RIERA and HONTECILLAS, 2006)
Suckling piglets	Ischemic-injury	EPA	↓PGE2; ↑(TEER, H^{3}-mannitol/C^{14}-inulin flux, COX-2); =mucosal damage	(JACOBI et al., 2012)

Pigs	LPS	FO	↓LPS permeability and =TEER in ileum explants	(MANI et al., 2013)

The arrow indicates an increase (↑) or decrease (↓) in the level or activity of the different parameters analyzed, "=" symbol designates unchanged parameters. ALA: Alpha-linolenic acid; AP: Alkaline phosphatase; CAT: Catalase; COX: Cyclooxygenase; DHA: Docosahexaenoic acid; DON: Deoxynivalenol; Drp1: Dynamin-related protein 1; DSS: Dextran sulphate sodium; 17,18-EEP: 17,18-Epoxyeicosatetraenoic acid; EPA: Eicosapentaenoic acid; FD4: Fluorescein isothiocyanate-labelled dextran 4kDa; FFAR-2: Free fatty acid receptor-2; FO: Fish oil; FS: Fluorescein sulfonic acid; 5-FU: 5-Fluorouracil; GPR: G-protein coupled receptor; GSH: Glutathione; γ-GT: γ-Glutamyltransferase; HMGB1: High mobility group box-1 protein; HO-1: Heme oxygenase-1; H_2O_2: hydrogen-peroxide; HRP: Horseradish peroxidase; HSP70: Heat shock protein-70; IκB: Inhibitor of nuclear factor kappa B; ICAM-1: Intercellular adhesion molecule-1; IEC: Intestinal epithelial cells; IL: Interleukin; INFγ: Interferon γ; iNOS: Inducible nitric oxide synthase; IRAK1: Interleukin-1 receptor-associated kinase-1; 8-Iso PGF3α: 8-Iso prostaglandin F3α; LDH: Lactate dehydrogenase; LPS: Lipopolysaccharides; LT: Leukotriene; MaR: Maresin; MCP-1: Monocyte chemoattractant protein-1; MIP-2: Macrophage inflammatory protein-2; MLKL: Phosphorylated mixed lineage kinase-like protein; MPO: Myeloperoxidase; MUC: Mucin; MyD88: Myeloid differentiation primary response 88; NEC: Necrotizing enterocolitis; NF-κB: Nuclear factor-κB; NO^{2-}/ NO^{3-}: Nitrite/nitrate; NOD: Nucleotide-binding oligomerization domain-containing protein; Nrf2: Nuclear factor erythroid 2-related factor 2; OCLN: Occludin; PGAM5: Phosphoglycerate mutase family 5; PG: Prostaglandin;PGC1-α: PPARγ co-activator 1-α; PPAR: Peroxisome proliferator-activated receptor; PUFA: Polyunsaturated fatty acid; RIPK: Receptor-interacting protein kinase; ROS: Reactive oxygen species; RvE: E-series resolvin; SOD: Superperoxide dismutase; TAK1: Transforming growth factor-β-activated kinase-1; TEER: transepithelial electrical resistance; TGF: Transforming growth factor; TNB: 1,3,7-Trinitrobenzene; TNBS: 2,4,6-Trinitrobenzene sulfonic acid; TNF: Tumour necrosis factor; TNFR1: Tumour necrosis factor receptor-1;TRAF6: Tumour Necrosis Factor Receptor-Associated Factor-6;TXB: Thromboxane; UPC3: PPARγ-responsive gene uncoupling protein-3; V/C: Villus height/crypt depth; VCAM-1: Vascular adhesion molecule-1; VEGFR-2: Vascular endothelial growth factor-2; ZO: Zonula occludens

Table 2 Effects of omega-3 polyunsaturated fatty acids in intestinal barrier of patients with inflammatory bowel disease

Clinical study	Under IBD medications	n-3 PUFA assessed	Immune response and morphological changes	Reference
Ethanol-induced duodenum lesions	No	FO	↑LTC5; ↓endoscopic and histologic lesions; =(PGE2, PGI2, TXB2)	(SCHEPP et al., 1991)
Pediatric UC in remission	Yes	EPA	↓LTB4; =histological score	(SHIMIZU et al., 2003)
Active DP	No	FO	↑clinical, endoscopic and histological remission	(ALMALLAH et al., 1998)
Active UC	No	FO	↑clinical and histological remission	(MCCALL TB, 1989)
Active UC	No	FO	↑endoscopic remission; =clinical and histological score	(DICHI et al., 2000)
Active UC	No	FO	↑clinical, endoscopic and histological remission	(SEIDNER et al., 2005)
Active UC or CD	Yes	FO	↑phospholipid n-3 PUFAs, clinical, endoscopic and histological remission	(LORENZ et al., 1989)
Active UC or CD	Yes	FO	↑phospholipid n-3 PUFAs; ↓(PGE2, PGI2, TXB2)	(HILLIER et al., 1991)
Active UC	Yes	Salmon fillet	↑phospholipid n-3 PUFAs, clinical, endoscopic and histological remission	(GRIMSTAD et al., 2011)
Active UC	Yes	EPA	↑clinical and endoscopic remission	(SALOMON et al., 1990)
UC in remission	No	FO	↑temporary clinical, macroscopic and histologic remission; delayed early relapse	(LOESCHKE et al., 1996)
UC in remission	Yes	EPA	↑endoscopic and histological remission	(SCAIOLI et al., 2018)
UC in remission	Yes	EPA	↑(IL-10, SOCS3, IL-22, HES-1, KLF-4, goblet cell abundance, endoscopic and histological remission); ↓phospho-STAT3; =(STAT3, Ki67, c-MYC, LGR5)	(PROSSOMARITI et al., 2017)

Active UC or in remission	Yes	FO	=(bleeding, disease relapse, endoscopic and histological score)	(GREENFIELD et al., 1993)
Active UC	Yes	FO	=endoscopic and histologic scores	(BARBOSA et al., 2003)
Quiescent UC	Yes	EPA, DHA	=(disease relapse, endoscopic and histological score)	(MIDDLETON et al., 2002)
The arrow indicates an increase (↑) or decrease (↓) in the level or activity of the different parameters analyzed, "=" symbol designates unchanged parameters. CD: Crohn's disease; COX: Cyclooxygenase; c-MYC: c-Myelocytomatosis proto-oncogene; DP: Distal proctocolitis; HES-1: Hairy and enhancer of split-1; IBD: Inflammatory bowel disease; IL: Interleukin; Ki67: Cell proliferation marker; KLF-4: Kruppel-like factor-4; LGR5: Leucine-rich repeat-containing G-protein coupled receptor 5; LT: Leukotriene; PG: Prostaglandin; PUFA: Polyunsaturated fatty acid; p-STAT3: Phosphorylated signal transducer and activator of transcription 3; SOCS3: Suppressor of cytokine signalling-3; STAT3: Signal transducer and activator of transcription-3; TXB: Thromboxane; UC: Ulcerative colitis				

Table 3 Effects of citrus pectin in the intestinal barrier cell and animal models

Model of study	Stress by	CPn assessed	Immune response and morphological changes	Reference
In vitro				
Human T84 cells	Phorbol esters	CPn (DM30%, DM56%, DM74%)	↑TEER	(VOGT et al., 2016)
Human Caco-2 cells	*Salmonella typhimurium (pathogen), Listeria monocytogenes (pathogen), Lacticaseibacillus casei (probiotic), Bifidobacterium lactis (probiotic)*	CPn or citrus residues after juice/pectin extraction	↓(IL-8, pathogen adhesion and invasion); ↑probiotic adhesion	(DE PAULA MENEZES BARBOSA et al., 2020)
Mouse CMT93 cells	*Citrobacter rodentium*	CPn (DM32%, DM59%, DM64%)	↓(pathogen adhesion, LY flux); ↑TEER	(BEUKEMA et al., 2021)
Porcine IPEC-J2 cells	Non-stimulated	Fermented citrus pulp	↓(TLR4, CLDN-1); ↑NOD1	(UERLINGS et al., 2020)
In vivo				
Rats	Non-stimulated	CPn	↑($Ki67^+$ cells, intestinal length and weight, cecum SCFAs, mucosal wet weight, protein and DNA content)	(FUKUNAGA et al., 2003)
Rats	MTX-colitis	CPn	↓(organ water content, MPO, intestinal permeability, bacterial translocation); ↑(mucosal protein, DNA and RNA content)	(MAO et al., 1996)
Mice	Acetic acid-colitis	CPn	↓(ROS, MPO, granulocyte adhesion, colon damage)	(MARKOV et al., 2011)
Mice	DOX-ileitis	CPn (DM7%)	↓(TNF-α, MCP-1, CXCL1, IL-6, inflammatory cell infiltration, crypt cell apoptosis); =(IL-10, cecum SCFAs)	(SAHASRABUDHE et al., 2018)
Mice	DSS-colitis	CPn or citrus residues after juice extraction	↓(TNF-α, IL-1β, IL-16, iNOS, ICAM-1, colon W/L ratio); ↑(MUC3, ZO-1, OCLN)	(FAN et al., 2020)

Mice	DSS-colitis	CPn (DE68.01±0.43%, DE41.61±0.12%, DE38.09±0.78%)	↓(IL-6, IL-17, MPO, FD4/LPS flux, epithelial erosion, ulceration, inflammatory cell infiltration, colon W/L ratio); ↑(ZO-1, goblet cells, crypt and villus structure); =OCLN	(PACHECO et al., 2018)
Mice	DSS-colitis	CPn, CPn methanol extracts or methanol residues	↓(TNF-α, IL-1β, IL-6, CXCL2, IL-17a, ulceration, erosion, inflammatory cell infiltration, colon shortening); ↑(ZO-2, OCLN, CLDN-3/-7, JAM-A)	(TINH et al., 2021)
Mice	DSS-colitis	Methanol extracted CPn	↓(IL-6, MCP-1, CXCL2, epithelial damage, inflammatory cell infiltration, colon shortening); ↑(ZO-1/-2, CLDN-3/7, crypt structure, goblet cells); =IL-17a	(KAWABATA et al., 2018)
Mice	DSS-colitis	CPn	↓(TNF-α, IL-12, colon shortening)	(ABE et al., 2018)
Cats	IND-small intestinal lesions	CPn	↓mucosal ulceration and lesions	(SATOH et al., 2009)
Chicken	*Eimeria maxima* coccidiosis	CPn	↓(IL-12β, serosa thickness, schizont count in enterocytes); ↑(IFN-γ, IL-1β, goblet cell abundance, V/C ratio, cecum weight, cecum SCFAs); =(MUC2, IL-8, INFγ)	(WILS-PLOTZ et al., 2013)
Weaned piglets	Non-stimulated	Citrus pulp	= (IL-6, IL-1β, TNF-α, IFN-γ, IL-10, SOCS3)	(WEBER et al., 2008)

The arrow indicates an increase (↑) or decrease (↓) in the level or activity of the different parameters analyzed, "=" symbol designates unchanged parameters. CLDN: Claudin; CPn: Citrus pectin; CXCL: Chemokine C-X-C motif ligand; DE: Degree of esterification; DM: Degrees of methyl esterification; DOX: Doxorubicin; DSS: Dextran sulphate sodium; FD4: Fluorescein isothiocyanate-labelled dextran 4kDa; ICAM-1: Intercellular adhesion molecule-1; IFNγ: Interferon γ; IL: Interleukin; IND: Indomethacin; iNOS: Inducible nitric oxide synthase; JAM: Junctional adhesion molecule; Ki67: Cell proliferation marker; LPS: Lipopolysaccharides; LY: Lucifer yellow; MCP-1: Monocyte chemotactic protein-1; MPO: Myeloperoxidase; MUC: Mucin; MTX: Methotrexate; NF-κB: Nuclear factor-κB; OCLN: Occludin; ROS: Reactive oxygen species; SCFAs: Short-chain fatty acids; SOCS3: Suppressor of cytokine signalling-3; TEER: Transepithelial electrical resistance; TLR: Toll-like receptor; TNBS: 2,4,6-Trinitrobenzene sulfonic acid; TNF: Tumour necrosis factor; TJ: Tight junction; W/L: Weight/length; ZO: Zonula occludens

3 Aims of the study

I. To determine the effects of omega-3 polyunsaturated fatty acids (n-3 PUFA) as the eicosapentaenoic acid (EPA) and docosahexaenoic acid (DHA) in the porcine IPEC-J2 cells under lipopolysaccharides (LPS) stress conditions by cell-based assays on viability, cytotoxicity and apoptosis.

II. To determine the biological pathways regulated by n-3 PUFA in the IPEC-J2 cells under LPS stress conditions by transcriptomic and proteomic analysis.

III. To establish a model of chicken embryonic intestinal epithelial cell culture for evaluation of citrus pectin against LPS stress by viability assay.

Figure 5 Schematic workflow of the study

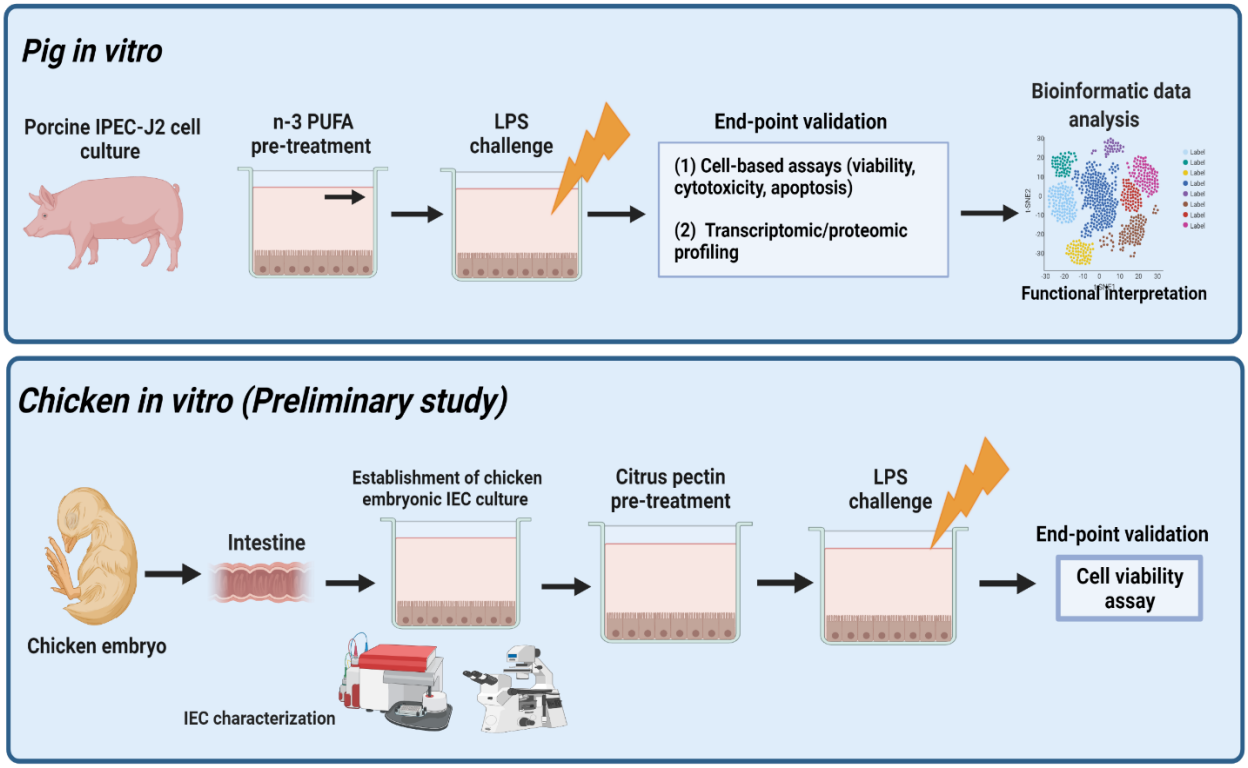

IPEC-J2: Porcine small intestinal cell line; n-3 PUFA: Omega-3 fatty acids; LPS: Lipopolysaccharides; IEC: Intestinal epithelial cells

4 Materials and methods

4.1 Cell-based assays for n-3 PUFA assessment

4.1.1 Porcine IPEC-J2 cell culture

IPEC-J2 is a non-transformed cell line, derived from the jejunum epithelium of unsuckled piglet (DSMZ, Germany). Cell passages of 24 – 28 were used for the experiments. Cells were cultured in complete medium consisting 1:1 mixture of Dulbecco's modified Eagle's medium with stable L-Glutamate and Ham's F-12 mixture (DMEM/F12) (Immunological science), supplemented with 15 mM of 4-(2-hydroxyethyl)-1-piperazineethanesulfonic acid (HEPES) (Sigma Aldrich), 5% heat-inactivated fetal bovine serum (FBS) (Immunological science) and 1% penicillin (100 U/mL)/streptomycin (100 mg/mL) (Euroclone). Cells were seeded at a density of 2×10^6 cells in 15 mL culture media in T-75 cm^2 culture flask (Corning) and maintained at 37°C under humidified atmosphere of 5% CO_2. At complete confluency, cells were trypsinated with 5 mL trypsin-Ethylenediaminetetraacetic acid (EDTA) (Sigma Aldrich). Subsequently, the viable cells were counted in a haemocytometer by tryphan blue (Sigma Aldrich) staining. Further, the cells were seeded at a density of 3×10^4 cells/well in 96-well plates (Corning). Cells were allowed to adhere 24 h prior to the treatments.

4.1.2 IPEC-J2 cell treatments

- **Dose-response study**

Cells were treated with increasing concentrations of EPA or DHA (0-200 µM) in the basal DMEM medium for 24 h. Similarly, the cells were exposed to different stressors as *Salmonella typhimurium* LPS (0-100 µg/mL), DSS (0-10%) for 24 h and H_2O_2 (0-10 mM) for 1 h. All the chemicals were purchased from Sigma Aldrich.

- **Cellular challenge**

Cells were pre-treated 24 h with or without DHA (3.3 µM), EPA (6.7 µM) and DHA:EPA (1:2; 10 µM) in DMEM medium supplemented with 0.05% FBS. The FBS concentration was chosen based on a preliminary study with a range of 0-1% up to 48 h. The concentration of 0.05% FBS optimally supported cell attachment and growth. Subsequently, the cells were challenged with LPS (50 µg/mL) and DSS (2%) for 24 h, whereas H_2O_2 (1 mM) for 1 h individually to induce inflammatory and oxidative damage.

4.1.3 Cell viability assay by MTT

Cell viability was determined by quantification of mitochondrial oxidoreductase using the 3-(4,5-dimethylthiazol-2-yl)-2,5-diphenyltetrazolium bromide (MTT) assay method. At the end of cellular treatments, the supernatant was replaced with 150 µL/well of MTT buffer (Sigma Aldrich) prepared in 1x PBS (0.25 mg/mL) and incubated at 37°C for 2 h. The end-product so obtained was dissolved in an equal volume of absolute dimethyl sulfoxide (DMSO) (Sigma Aldrich) and the optical density (OD) was measured at 570 nm in a colorimetric microplate reader (BioRad). Cells without any treatment was included as control, which represents 100% viability. For colorimetric measurements DMSO was used as a blank. Cell viability was calculated using the formula,

$$\text{Cell viability (\%)} = (OD_{treatment} - OD_{blank} / (OD_{control} - OD_{blank}) \times 100$$

4.1.4 Lactate dehydrogenase assay

Cell membrane integrity was estimated by assessing the amount of cytosolic lactate dehydrogenase (LDH) released into the culture media. At the end of cellular treatments, 50 µL of the supernatant was mixed with an equal volume of LDH buffer (CytoTox 96®, Promega) in a 96-well plate and incubated for 30 minutes in dark at room temperature (RT). Subsequently, colorimetric measurement was performed in a colorimetric microplate reader (Bio-Rad) at 490 nm.

4.1.5 Nitric oxide activity

The amount of cellular nitric oxide (NO) release in the culture media was estimated by Griess test. For this, 50 µL of cell supernatant was incubated with an equal volume of Griess reagent for 10 minutes at RT in dark. Then 50 µL of reaction stop solution was added and incubated as before. The end-point was colorimetrically measured at 490 nm as per the manufacturer's instructions (Promega).

4.1.6 Apoptosis assay

Cellular apoptosis was determined by accessing the intracellular caspase-3/7 activity. For this, the cells were seeded at a low density of 2×10^4 cells/well in a black 96-well plate and the treatments were performed as described in the section 4.2.2. Thereafter, supernatant was replaced with 100 µL/well assay reagent and incubated at 37°C for 30 minutes. Subsequently,

the fluorescence was measured at $499_{Ex}/521_{Em}$ in a fluorescence microplate reader (BioTek) as per manufacturer's instructions (Apo-ONE®, Promega).

4.1.7 Statistical analysis

The values of half inhibitory concentrations (IC_{50}) were calculated by non-linear regression analysis using the GraphPad Prism software (Version 8). The treatment effects were assessed by one-way ANOVA with post-hoc Bonferroni or Dunnett's test. At least three independent experiments were performed with IPEC-J2 cells, whereas two independent experiments performed for chicken cells with three technical replicates. All data are expressed in mean ± SEM and a value of $p < 0.05$ was considered statistically significant.

4.1.8 Cell sample collection for bioinformatic analysis

For RNA-seq analysis, cells were seeded in complete medium at a density of 3.5×10^5 cells/well in 6-well plates and allowed to adhere for 24 h prior to the treatments. At 80% confluency, cells were then treated with or without DHA:EPA (1:2 ratio, 10 µM, 2 mL/well) reconstituted in DMEM media with 0.05% FBS for 24 h. Subsequently, the cells were challenged with LPS (10 µg/mL, 2 mL/well) reconstituted in DMEM media for 24 h. Cells without any treatment was included as the control. After the treatments, cells in 6-well plates were washed thrice with sterile 1x PBS and stored at -80°C until use. For proteomic analysis, cells were seeded at a density of 1.5×10^6 cells/T-75 cm^2 flask and treatments were performed as before but in 15 mL treatment volumes. After cell treatments, samples were collected in cell culture flasks and stored as before

4.2 Cell sample processing and analysis for transcriptomics study

4.2.1 RNA isolation

Cell samples in the 6-well plates were defrosted from -80°C to RT for 10 minutes. RNA isolation was performed using the RNeasy Mini Kit (50) (Qiagen) as per the manufacturer's instructions with slight modifications. Accordingly, cells were rinsed with 350 µL RLT lysis buffer and transferred to RNase-free 1.5 mL eppendorf tubes. Following, 350 µL/well of 70% ethanol was added to the cells and scraped using a cell scraper. The cell lysate so obtained was then transferred to the same 1.5 mL tubes as before. The well plates were checked under a microscope to ensure complete cell detachment. Following, 700 µL of the cell lysate was transferred to a spin-column, centrifuged at 8000 rpm for 1 minute and subsequently, the flow-

through (FT) was discarded. Then 350 µL of RW1 buffer was added to the column, centrifuged at 8000 rpm for 1 min and the FT discarded. To digest the DNA, 80 µL of working DNase I (Qiagen) solution was added to the column and incubate at RT for 15 minutes. After incubation, 350 µL of RW1 buffer was added to the column, centrifuged at 8000 rpm for 1 min and FT discarded. Then, the column was washed twice with 500 µL RPE buffer to remove any DNA debris by centrifugation at 8000 rpm for 1 min, and the FT discarded as before. Centrifugation step was repeated with empty column to remove any excess liquid. The column consisting RNA was transferred to a new DNase/RNase-free 1.5 mL eppendorf tube. RNA was eluted by adding 30 µL RNase-free water to the column, incubated for 5 minutes at RT and then centrifuge at 8000 rpm for 2 minutes. Samples were stored at -80°C until use.

4.2.2 Quality and quantity assessment of the RNA samples

The concentration of RNA samples was measured using the Nanodrop (ThermoFisher Scientific) (Table 4). Following, the integrity of RNA samples was assessed by agarose gel electrophoresis. About, 200 ng of RNA sample was mixed with 2 µL of 6x DNA-loading dye (Sigma Aldrich) and loaded into 1% Borax agarose gel prepared in 1x Borax buffer. Similarly, 5 µL of gene ruler (1Kb plus Thermofisher) was mixed with 1 µL of 6x DNA-loading dye and loaded alongside the samples. The RNA bands were allowed to resolve in the gel electrophoresis with 1x Borax running buffer for 20 minutes at 120V. After the electrophoresis, nucleic acid staining was performed by incubating the gel in SYBR gold stain diluted in running buffer (50 mL, 1:10 ratio, pH 7-8.5) for 40 minutes with gentle shaking. Subsequently, the 28S and 18S bands corresponding to the rRNA subunits were visualized under a UV illuminator (Figure 6). Detection of these two bands is a preliminary quality check for RNA samples prior to the RNA-seq analysis.

Table 4 Concentrations of the RNA samples

No.	Samples	Concentration (ng/µL)	A 260/280	A 260/230
1	Control 1	248.6	2.08	2.15
2	Control 2	261.7	2.08	1.97
3	Control 3	253.6	2.08	1.83
4	LPS 1	293.1	2.09	1.9
5	LPS 2	163.4	2.08	1.66
6	LPS 3	150.5	2.08	1.75
7	n-3 PUFA 1	82.1	2.09	1.45
8	n-3 PUFA 2	141.7	2.08	1.61
9	n-3 PUFA 3	191.7	2.08	1.97
10	n-3 PUFA+LPS 1	108.5	2.07	1.81
11	n-3 PUFA+LPS 2	124.5	2.07	1.29
12	n-3 PUFA+LPS 3	141	2.06	1.55

Figure 6 RNA samples visualized by agarose gel electrophoresis

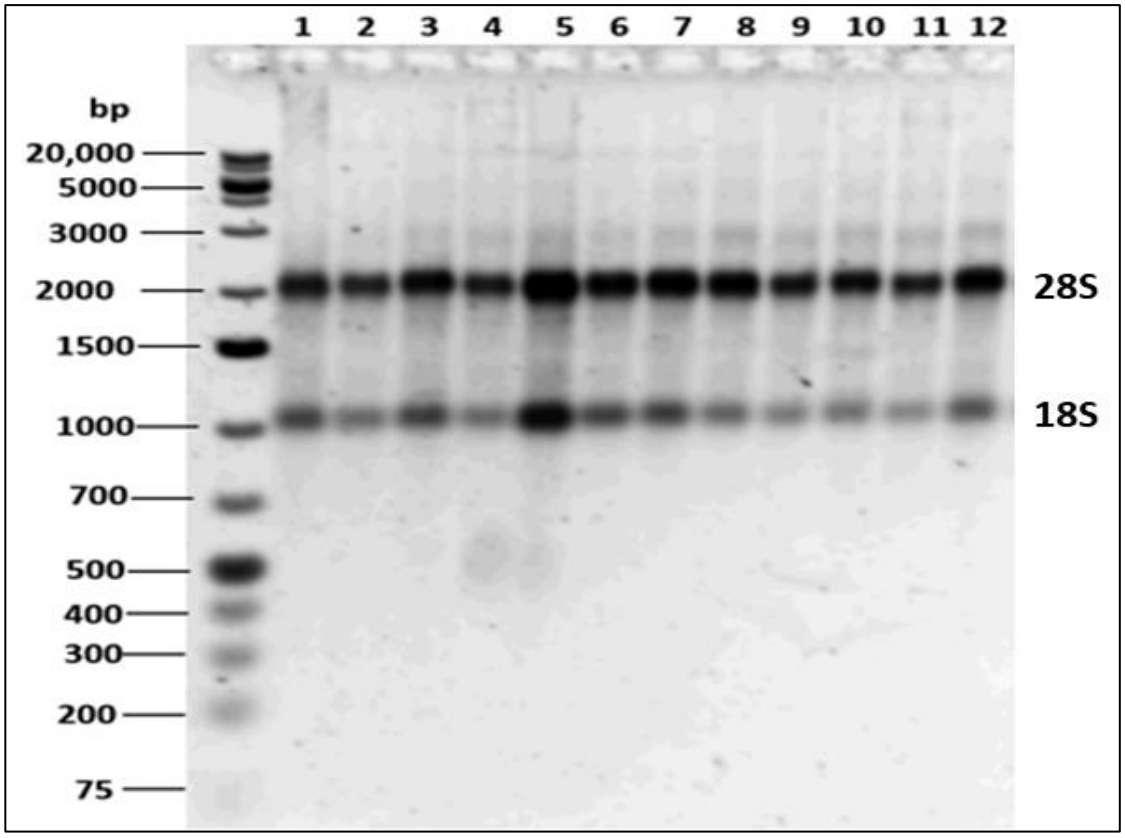

The total RNA extracted from the IPEC-J2 cells were resolved by agarose gel electrophoresis. As a preliminary quality assessment of the RNA samples, the 28S and 18S rRNA subunits were visualized.

4.2.3 cDNA library preparation and RNA sequencing

The integrity of RNA samples was assessed by capillary electrophoresis (Fragment analyzer, Advanced Analytical Technologies, Inc., USA). Then the cDNA libraries were generated as described in our previous publication (JIMENEZ-MUNGUIA et al., 2021) using the QuantSeq 3′ mRNA-Seq Library Prep Kit (Lexogen, Austria). Firstly, the RNA samples (250 ng) were reverse transcribed into cDNA using the oligodT primers from QuantSeq 3′ mRNA-Seq Library Prep Kit (Lexogen, Austria), following the manufacturer's instructions. Then the RNA template was removed and the second strand was subsequently synthetized using the random hexamer that consist of Illumina-compatible linker sequences at its 5′ end. The double stranded DNA library so obtained was purified by magnetic beads provided in the kit. The libraries were further amplified by PCR using the single indexing i7 primers that generates uniquely tagged libraries for sequencing multiple libraries together. The number of PCR cycles for each library was determined using the PCR Add-on kit from Illumina (Lexogen). The amplified libraries were again purified by magnetic beads and then the quality was assessed in fragment analyzer. Following, the libraries were subjected to single-end sequencing (75 bp) in the Illumina NextSeq with a minimal depth of 8 million reads per sample.

4.2.4 Bioinformatic analysis of RNA-seq data

Fastq files obtained from sequencing was aligned against the reference genome (Sus scrofa) to generate gene counts using STAR aligner tool. The differential gene expression analysis was performed using the edgeR package in R studio. Further, filtering of statistically significant differentially expressed genes (DEGs) and comparison between the treatments group were carried out in Excel (MS office). DEGs were selected based on the following parameters: average logCPM (count per million) ≥ 3, logFC (fold change) beyond ±1 and *p*-value < 0.01. Volcano plots were generated using the OMnalysis web application (http://lbmi.uvlf.sk/omnalysis), to visualize the distribution of DEGs across different treatment groups. Venn diagram was created using the Microsoft PowerPoint to display the number of common and uniquely regulated DEGs between the treatment groups. The DEGs were further categorized based on their involvement in different biological processes using the OMnalysis tool. The biological pathways regulated by the DEGs were analyzed using the peer-reviewed Reactome server (https://reactome.org). Heat mapping function of Prism 9 (Graphpad, USA) was used to compare the expression level of DEGs involved in Gene Ontology (GO) biological processes and Reactome pathways.

4.2.5 Validation of differentially expressed genes by real-time PCR.

RNA samples were reverse transcribed using the RevertAid RT reverse transcription kit (Thermo Fisher Scientific, USA). For this, 1 µL of RNA was mixed with 100 pMol of random hexamer and heated at 65°C for 5 minutes. Then, 4 µL of 5x reaction buffer, 2 µL of dNTP (10 mM), 1 µL of RevertAid reverse transcriptase (200 U) and 0.5 µL of RiboLock RNase inhibitor (20 U) were added (Thermo Fisher Scientific, USA). The reaction mixture was initially incubated at 25°C for 10 minutes, followed by 42°C for 1 h and finally at 70°C for 10 minutes. For preliminary qRT-PCR validation, 4 genes were chosen from the RNA-seq analysis that were either significantly up or downregulated. Primers for the PCR analysis were designed using the Geneious Pro software (Biomatters, USA) (Table 5). PCR reaction mixture consisted 6 ng of cDNA, 1x qPCR GreenMaster with highROX (Jena Bioscience, Germany), gene-specific primers (10 pMol) and RNase-free water that made up to 20 µL of final volume. The amplification cycle was as follows: 95°C – 10 minutes, 40 × 95°C – 15 s, 50 – 60°C – 30 s (annealing temperature varied according to the primers used), 72°C for 30 s (signal capture), melting curve 60°C to 95°C - 0.3 % temperature increment/s (StepOnePlus, Thermo Fisher Scientific, USA). The gene expressions (ΔΔCt) were normalized against the β-2-microglobulin (house-keeping gene) as described before (JIMENEZ-MUNGUIA et al., 2021). The ΔΔCt values were converted to logFC (http://www.endmemo.com/algebra/log2.php).

Table 5 PCR primers used in this study

Genes	Forward primer	Tm (°C)	Product size (bp)
NFKB1	(F) TCGCTGCCAAAGAAGGACAT		102
	(R) TAGCGTTCAGACCTTCACCG		
TRPC1	(F) GCCTCCGACATTCCAGGTTT		180
	(R) TACATTGCCGGGCTAGTTCC	55	
YWHAZ	(F) CCCAGAGAAAGCCTGCTCTC		181
	(R) TTCCCCTCCTTCTCCTGCTT		
PSME1	(F) AGTATTTCTCTGAGCGGGGC		107
	(R) ATCCCGGTACTCTGCCTCAT		

4.3 Cell sample processing and analysis for proteomics study

4.3.1 Protein isolation

Cells ($2.5*10^6$ cells) collected in culture flask (Section 4.8) was scraped in 2.5 mL of lysis buffer and transferred to 15 mL falcon. To recover any remaining cells, the flask was finally rinsed with another 1.5 mL of lysis buffer and transferred to the same falcon. The cells were resuspended in the buffer by gently pipetting, followed by a short vortex. The cell samples were then incubated at 95°C for 15 minutes in a water bath with shaking. After incubation, the samples were sonicated for 10 minutes in a sonicator bath (at maximum power) followed by centrifugation at 15000 rpm for 10 minutes at 20°C. The supernatant consisting the whole cell lysate was transferred to sterile microfuge tubes and stored at -80°C until used. The lysis buffer consists of 2% SDS (Sigma Aldrich), 10% 1M Tris-HCl (100 mM) (Sigma Aldrich), 10% 1M DTT (100 mM) (Roche), 10% 1x protease inhibitor (SigmaFAST Protease inhibitor cocktail), and the remaining volume made up with Milli-Q water (final p.H-6.8).

4.3.2 Quantity and quality assessment of the protein samples

- Protein concentrations were measured using the Pierce 660nm Protein Assay Kit (Thermo Scientific) (Table 7). Pre-diluted Protein Assay Standards (Bovine Serum Albumin, Thermo Scientific) were used to build the calibration curve with a concentration range of 125-2000 µg/mL (Figure 7, Table 6). About 10 µL of the standard or sample was added to 150 µL assay reagent in a 96-well plate. The samples were shortly mixed in a plate shaker and incubated for 5 minutes at RT. Subsequently the absorbance was measured at 660 nm in a spectrophotometer as per the manufacturer's instructions.

Table 6 Calibration curve obtained by Pierce 660 nm Protein Assay Reagent

No.	Concentration (µg/µL)	Absorbance at 660 nm
1	0.125	0.0974
2	0.25	0.1386
3	0.50	0.1889
4	0.75	0.2465
5	1.0	0.3265
6	1.5	0.4461
7	2.0	0.5704

Figure 7 Linear regression used to evaluate the concentrations of the protein samples

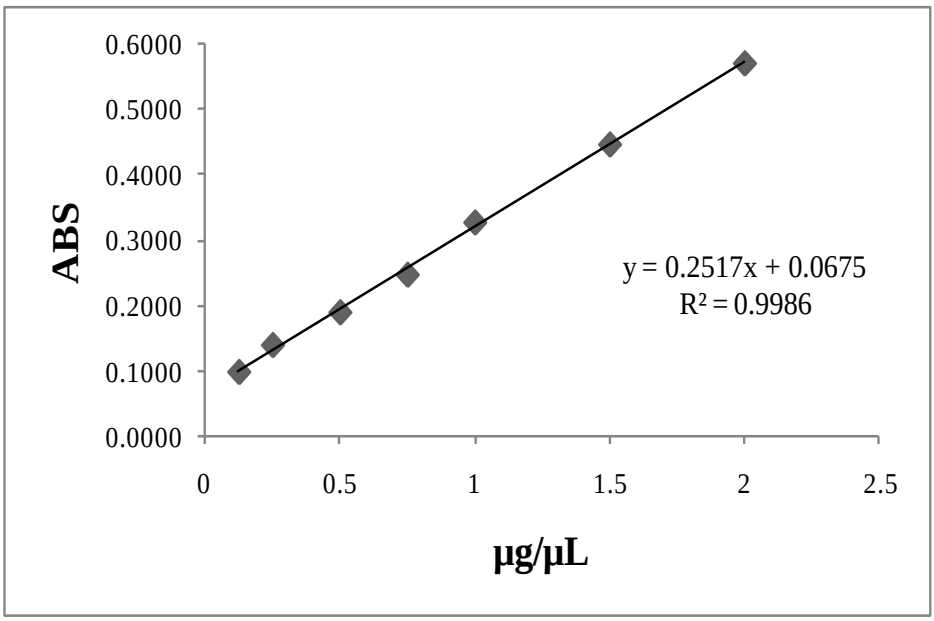

Table 7 Concentrations of the protein samples

No.	Samples	Absorbance at 660 nm	Concentration of 1:10 dilution (µg/µL)	Concentration (µg/µL)	Final concentration (µg)
1	Control 1	0.1281	0.2408	2.41	240.76
2	Control 2	0.1273	0.2376	2.38	237.58
3	Control 3	0.1230	0.2205	2.21	220.50
4	Control 4	0.1243	0.2257	2.26	225.67
5	LPS 1	0.1325	0.2582	1.29	129.12
6	LPS 2	0.1255	0.2304	2.30	230.43
7	LPS 3	0.1391	0.2845	1.42	142.23
8	LPS 4	0.1157	0.1915	1.91	191.50
9	n-3 PUFA 1	0.1370	0.2761	2.76	276.12
10	n-3 PUFA 2	0.1299	0.2479	2.48	247.91
11	n-3 PUFA 3	0.1236	0.2229	2.23	222.88
12	n-3 PUFA 4	0.1294	0.2459	2.46	245.93
13	n-3 PUFA+LPS 1	0.1206	0.2110	2.11	210.97
14	n-3 PUFA+LPS 2	0.1289	0.2439	2.44	243.94
15	n-3 PUFA+LPS 3	0.1245	0.2265	2.26	226.46
16	n-3 PUFA+LPS 4	0.1211	0.2130	2.13	212.95

- The integrity of protein samples was assessed by visualization in the SDS-PAGE (Bio-Rad). For the gel electrophoresis, 2 µL of sample was mixed with reducing Laemmli buffer (1:1 ratio) and boiling at 100°C for 5 minutes. Then centrifuged at 16000g for 5 minutes. The samples were loaded into the pre-cast protein gel (Any kD™ Mini-PROTEAN® TGX, Bio-Rad) along with 3 µL of protein ladder (All Blue pre-stained protein standard, Bio-Rad). Additionally, reference milk samples (3.3, 16.5 and 33 µg) were loaded into the gel and resolved at 150V for 1 h in a pre-made 1x Tris-Glycine-SDS running buffer (ThermoFisher). After the resolution, the gel was rinsed with deionized water and then stained with 20 mL of SimplyBlue SafeStain (ThermoFisher) for 1 h. Then the bands were visualized by boiling the gel for 1 minute in ultrapure water following the microwave protocol as per the manufacturer's instructions (Figure 8).

Figure 8 Protein samples visualized by SDS-PAGE

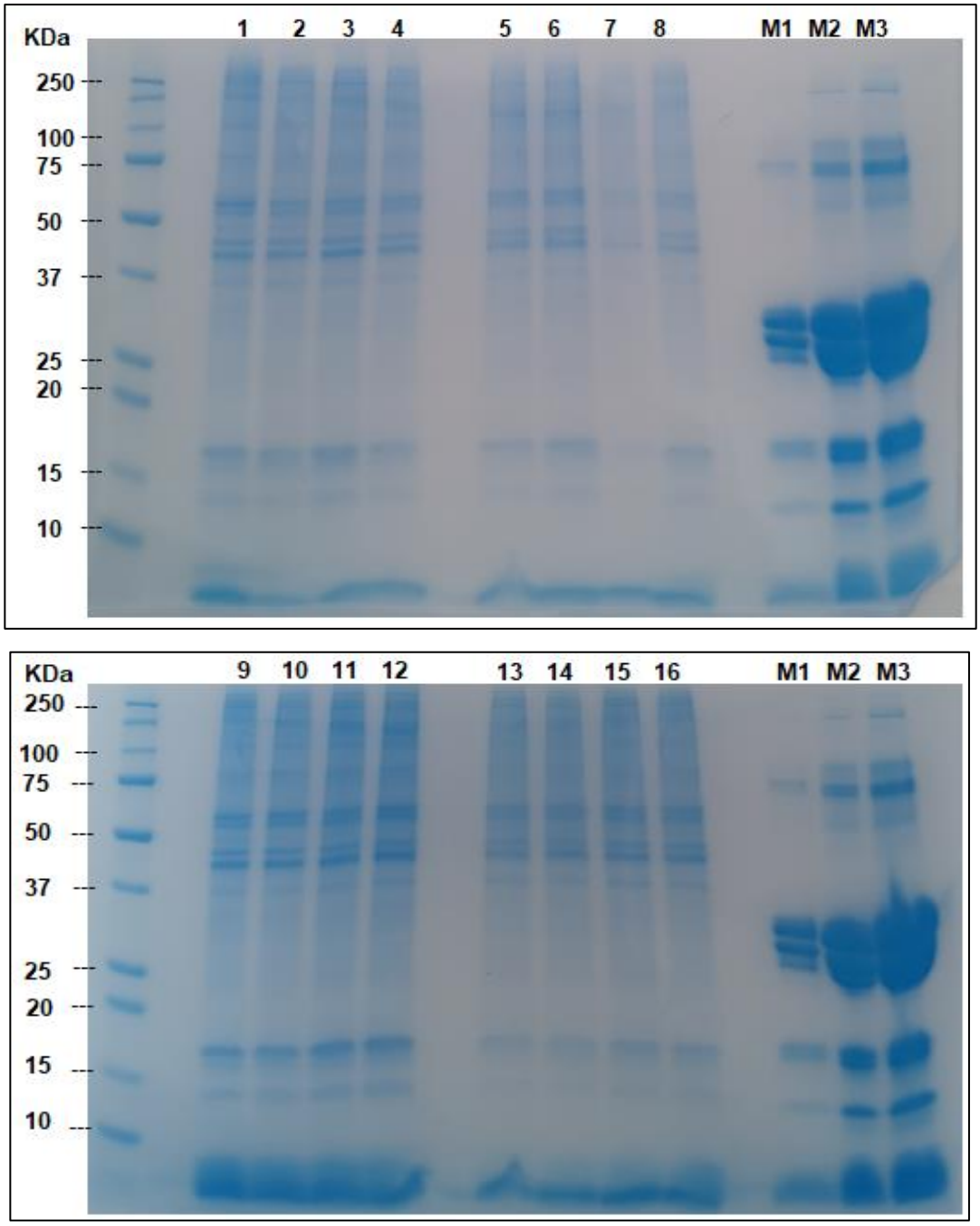

The total protein extracted from the IPEC-J2 cells were resolved by SDS-PAGE. The lanes 1-16 represents the protein samples resolved with 2 µL unknown concentration. M1 (3.3 µg), M2 (16.5µg) and M3 (33 µg) lanes are the reference milk sample with known concentration.

4.3.3 Filter Aided Sample preparation (FASP) for proteomic analysis

Protein extracts were subjected to on-filter reduction, alkylation, and trypsin digestion according to the filter-aided sample preparation (FASP) protocol. Accordingly, the protein extracts were diluted in the Tris-Urea buffer (8 M urea, 100 mM Tris-HCl adjusted to pH 8.8) and loaded onto Amicon Ultra-0.5 centrifugal filter units with a 3 kDa cut-off membrane (Millipore, Billerica, MA, USA), and centrifuged at 13000g for 15 minutes. The concentrates were then diluted in the same buffer and centrifugation repeated. Proteins in the filter was then reduced with 10 mM DTT for 30 minutes and then alkylated in 50 mM iodoacetamide for 20 minutes. After six washes (3 times in Tris-Urea buffer and 3 times in 50 mM ammonium bicarbonate), trypsin solution was dispensed on the filter (1:100 enzyme-to-protein ratio) consisting the samples, and incubated at 37°C overnight. After trypsin digestion, the peptides were collected by centrifugation followed by an additional wash with an elution solution (20% acetonitrile plus 1% formic acid). Finally, the peptide mixture was dried and reconstituted in 0.2% formic acid to a final concentration of 2 µg/µL. The concentration of peptide mixture was estimated by measuring the absorbance at 280 nm in a NanoDrop 2000 spectrophotometer (Thermo Scientific, San Jose, CA, USA), using dilutions of the MassPREP *E. Coli* Digest Standard (Waters, Milford, MA, USA) to generate a calibration curve.

4.3.4 LC-MS/MS analysis

The analyses were carried out using a Q Exactive mass spectrometer (Thermo Scientific) interfaced with an UltiMate 3000 RSLCnano LC system (Thermo Scientific). After loading, the peptide mixtures (4 µg per run) were concentrated and desalted on a trapping pre-column (Acclaim PepMap C18, 75 µm × 2 cm nanoViper, 3 µm, 100 Å, Thermo Scientific), using 0.2% formic acid at a flow rate of 5 µL/minute. Subsequently, the peptide separation was performed at 35°C using a C18 column (Acclaim PepMap RSLC C18, 75 µm × 50 cm nanoViper, 2 µm, 100 Å, Thermo Scientific) at a flow rate of 250 nL/minute with a 245 minutes gradient from 2 to 37.5% eluent B (0.2% formic acid in 20% acetonitrile) in eluent A (0.1% formic acid). MS data were acquired using a data-dependent Top12 method, dynamically choosing the most abundant precursor ions from the survey scan under the direct control of Xcalibur software (version 3. 1.66.10 SP2), where a full-scan spectrum (from 300 to 2,000 m/z) was followed by tandem mass spectra (MS/MS). The instrument was operated in positive mode with a spray voltage of

1.8 kV and a capillary temperature of 275°C. Survey and MS/MS scans were performed in the Orbitrap with a resolution of 70,000 and 17,500 at 200 m/z, respectively. The automatic gain control was set to 1,000,000 ions and the lock mass option was enabled on a protonated polydimethylcyclosiloxane background ion as an internal recalibration for accurate mass measurements. The dynamic exclusion was set to 30 seconds. Higher Energy Collisional Dissociation (HCD) performed at the far side of the C-trap, was used as a fragmentation method by applying a 25eV value for normalized collision energy. An isolation width of m/z 2.0. Nitrogen was used as the collision gas.

4.3.5 Bioinformatic analysis of proteomics data

Protein and peptide identification was performed using Proteome Discoverer (version 2.4, Thermo Scientific) and Sequest-HT as search engine for protein identification according to the following criteria: Database UniprotKB: taxonomy *Sus Scrofa* (Taxon identifier: 9823, 120,707 sequences, release_2021_03); Enzyme: trypsin, with two missed cleavages allowed; Precursor mass tolerance: 10 ppm; Fragment mass tolerance: 0.02 Da; Charge states: +2, +3, and +4; Static modification: cysteine carbamidomethylation; Dynamic modification: methionine oxidation and acetylation (Acetyl), loss of Methionine (Met-loss) and loss of Methionine-loss+Acetylation (Met-loss+Acetyl) on N-Terminal. Protein significance and peptide validation (false discovery rate, FDR, <1%) were performed with the percolator algorithm. Peptide and protein grouping were allowed according to the Proteome Discoverer algorithm by applying the strict maximum parsimony principle. Differential analysis was performed comparing two experimental groups at a time; in particular, (i) LPS *vs* control, (ii) n-3 PUFA *vs* control, and (iii) n-3 PUFA+LPS *vs* control. Each group was composed of four biological replicates. A standard workflow was set using the Proteome Discoverer 2.4 to evaluate the label-free (LFQ) and precursor ion quantification. Precursor ion abundances were calculated using intensity as an abundance parameter, that was normalized to evaluate the significance of abundance ratio among the identified proteins in two different experimental groups. Precursor ion quantification was performed only if the ions were detected in at least 50% of the samples in an experimental group. The fold ratio was calculated by pair-wise ratio-based method and the maximum allowed fold ratio was set to 100. The abundance ratio was log-transformed (log_2) and differential proteins were predicted using the t-test (background based) and adjusting the p-value (FDR) with the Benjamini-Hochberg method.

4.4 Establishment of chicken embryonic intestinal cell culture

4.4.1 Cell isolation from intestinal tissues

Four days old fertile chicken eggs (n = 30) were purchased from a commercial hatchery and maintained in a semi-automated, humidified incubator at 37.5°C. After 12 days of incubation, the embryos were removed from the eggs and sacrificed immediately by decapitation. The whole intestine was dissected free from mesenteries and connective tissues, and then washed in 1x PBS supplemented with 1% penicillin/streptomycin. Further, the intestine was longitudinally cut open exposing the mucosal epithelium and then segmented into ~0.5 cm fragments. The tissue pieces were then forced through a sterile 100 µm cell strainer using a cell scraper. The cell suspension was then centrifuged at a minimal speed of 800 rpm for 5 minutes at RT. The cell pellet so obtained was resuspended in complete medium and seeded on collagen-coated culture flasks (Figure 9). The cell culture was then maintained at 37°C in a humidified atmosphere with 7.5% CO_2. Complete culture medium consisted 1:1 ratio of DMEM/F12 supplemented with 10% heat-inactivated FBS, 1% penicillin-streptomycin, 1% L-Glutamine (29 mg/mL), 0.2% ITS (5 mg/mL insulin, 5 mg/mL transferrin, 5 µg selenium) and 5 µL EGF (Epidermal growth factor) (20 µg/5 µL).

Note: This experiment was performed at the University of Veterinary Medicine and Pharmacy in Košice (Slovakia). As Slovakia is free from ethical clearance to conduct studies on chicken embryos, an application for the same is not applicable for the present study.

4.4.2 Cell detachment and staining for flow cytometry

In order to visualize the tight junction proteins by flow cytometry, the cells were detached by calcium chelation method from the cell culture flasks. Calcium chelation preserves the cell junction structure during detachment process. For this, at 80% confluency, cells were incubating with 2.5 mM EDTA in Ca^{2+}/Mg^{2+}-free PBS for 20-25 minutes at 37°C. Concentration of EDTA for cell detachment was chosen based on a preliminary test with a range of 1-30 mM. Post detachment, the cells were counted by tryphan blue staining in a haemocytometer. About 10^6 cells/mL were fixed with 4% paraformaldehyde for 10 minutes at RT with gentle shaking. After fixation, the cells were stained with Rabbit anti-E cadherin antibody (LSBio, USA) in blocking solution (1:200 dilution in 1% BSA) for 2 h at RT. Following, cells were stained with a secondary antibody, Protein A conjugated with Alexa 647 fluorophore (1:500 dilution in 1% BSA) for 45 minutes at 4°C. The labelled cells were analysed

in the BD Accuri™ C6 (Accuri Cytometers, USA) using BD Accuri C6 software. The cells stained with only secondary antibody was used as a control in gating analysis to check if any non-specific interaction exist.

Figure 9 Establishment of primary intestinal epithelial cell culture from chicken embryos

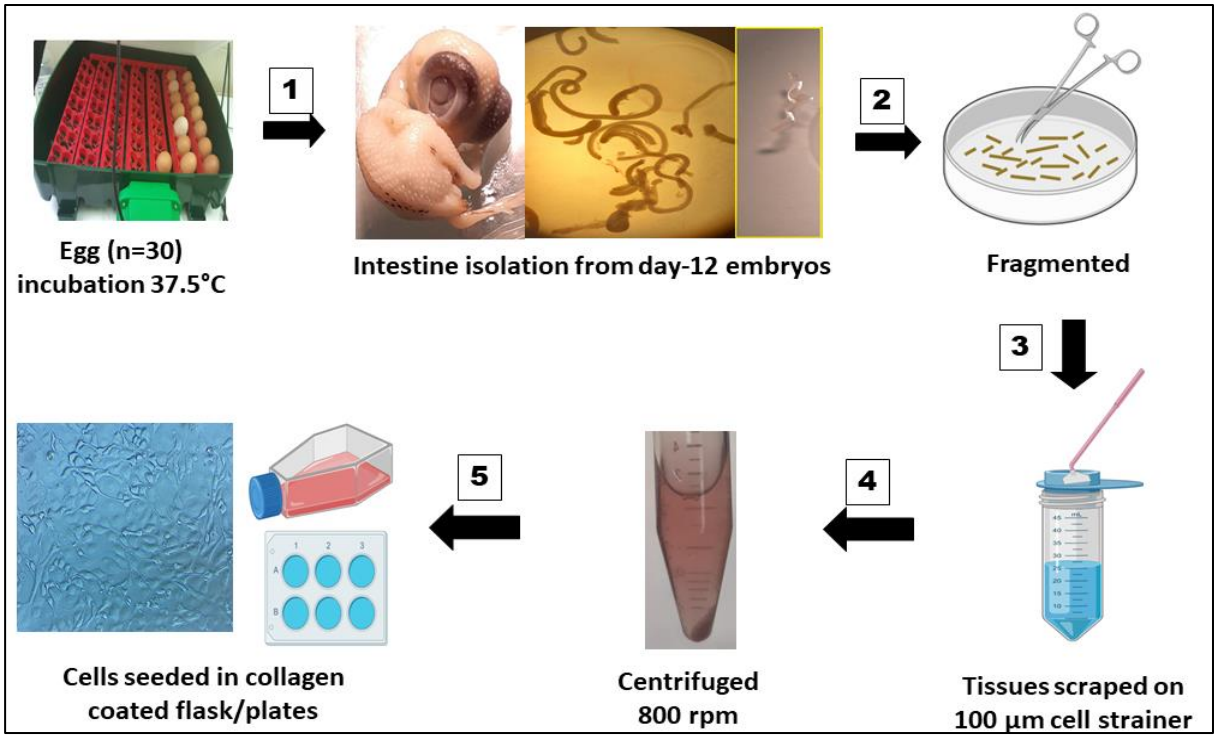

Schematic representation of the method of establishing primary intestinal cell culture from the chicken embryos by mechanical tissue disruption method. (1) Embryos were developed from the chicken eggs by incubating in an automatic incubator. Whole intestine was dissected out from the 12-days old embryos. (2) Intestine was longitudinally dissected and cut into ~0.5 cm pieces. (3) Tissues were forced through 100 µm cell strainer using a cell scraper. (4) Cell filtrate centrifuged at 800 rpm to obtain cell pellet. (5) Cells resuspended in culture medium and seeded onto collagen-coated culture flasks/plates.

4.4.3 Chicken primary intestinal cell treatments

- **Dose-response study**

Cells were seeded at a density of 3×10^4 cells/well in 96-well plates (Corning) and allowed to adhere 24 h prior to the treatments. Following, chicken primary intestinal epithelial cells (IECs) or porcine IPEC-J2 cells were treated with increasing concentrations of *Salmonella typhimurium* LPS (0–50 or 100 µg/mL) or citrus pectin (0-5 mg/mL) in DMEM medium for 24 h. All the chemicals for cell treatments were purchased from Sigma Aldrich.

- **Cellular challenge**

Cells were seeded as before followed by pre-treatment with citrus pectin (2.5, 0.6, or 0.15 mg/mL) and then challenged against LPS (25 or 50 µg/mL). Cells without any treatment were included as a control which represented 100% viability.

4.4.4 Cell viability assessment by XTT

At the end of the cellular treatments, cell viability was determined by the XTT (2,3-bis-(2-methoxy-4-nitro-5-sulfophenyl)-2H- tetrazolium-5-carboxanilide) assay for chicken IECs. For this, 100 µL of cell supernatant was mixed with 50 µL of XTT buffer and then incubated at 37°C for 2 h. After incubation, the absorbance was measured at 450-500 nm in a colorimetric plate reader as per manufacturer's instructions (PanReac, AppliChem). For IPEC-J2 cells, the viability assay was performed following the methods described earlier in the section. Cell viability was calculated as described before in the section (Section 4.3).

5 Results

5.1 Assessment of n-3 PUFA effects in the porcine IPEC-J2 cells by cell-based assays

5.1.1 Dose-response effect of different test compounds on the IPEC-J2 cell viability

As shown in the figure 10(a-b), the concentrations between 6.25-50 µM of EPA and DHA, significantly increased the cell viability while, it abruptly decreased at 200 µM compared to the control (0 µM, 100% viability; $p < 0.05$). The dose-response curves of LPS, DSS and H_2O_2 are reported in the figure 11(a-c). 24 h exposure of LPS did not affect the IPEC-J2 cell viability until 25 µg/mL (Figure 11a) and DSS until 0.62% (Figure 11b). Later, it decreased in a dose-dependent manner between 50-100 µg/mL for LPS and 1.25-10% for DSS. Similar such dose-dependent effect was observed for 1 h acute challenge of H_2O_2 as shown in the figure 11c. Subsequently, the dose-response curves of the stressors were used to estimate the IC_{50} values that corresponds to 62.02 µg/mL for LPS, 2.07% for DSS, and 1.53 mM H_2O_2 respectively. Based on these values, the concentrations of 50 µg/mL LPS, 2% DSS, and 1 mM H_2O_2 below the IC_{50} were chosen for further nutrient assessment.

Figure 10 Dose-response effect of EPA and DHA in the IPEC-J2 cells

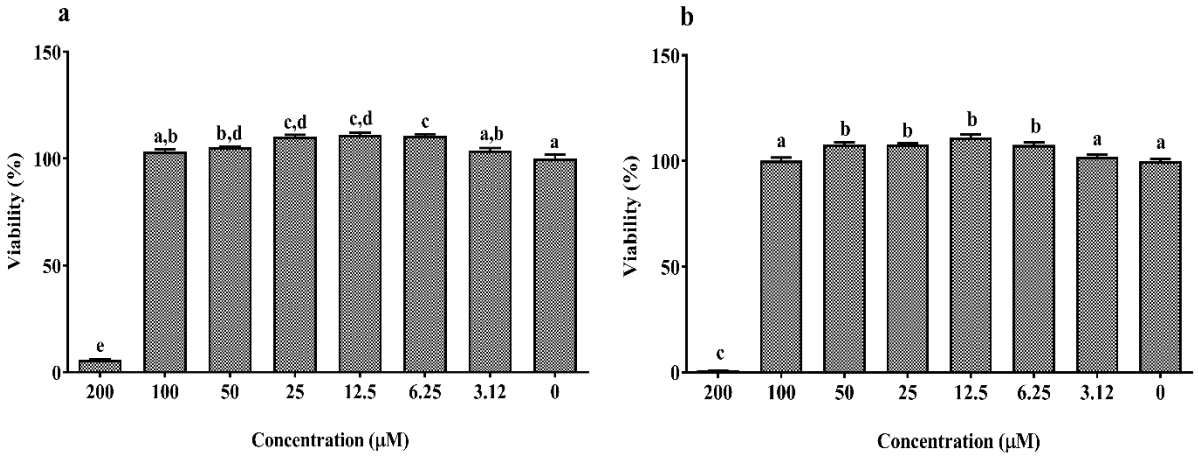

Viability of IPEC-J2 cells treated with (a) EPA and (b) DHA (0-200 µM for 24 h. Data are presented as mean ± SEM (n = 3, one-way ANOVA). Statistically significant difference among the treatments is denoted by different letters, where $p < 0.05$.

Figure 11 Dose-response effect of LPS, DSS and H_2O_2 in the IPEC-J2 cells

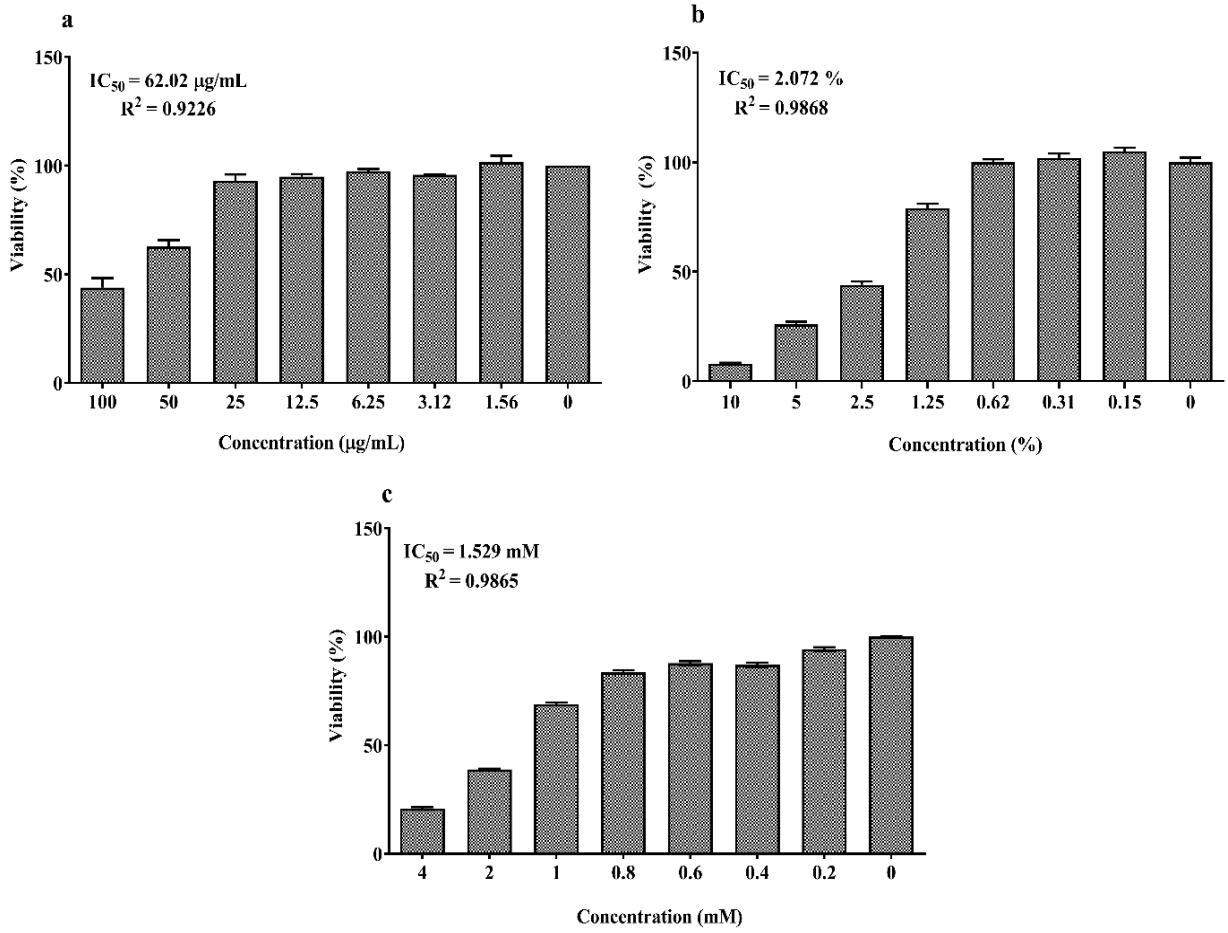

Viability of IPEC-J2 cells treated with (a) LPS (0-200 µM) for 24 h; (b) DSS (0-10%) for 24 h, and (c) H_2O_2 (0-4 mM) for 1 h. Data are presented as mean ± SEM (n = 3, one-way ANOVA). The 50% inhibitory concentrations (IC_{50}) were calculated by non-linear regression analysis and R^2 represents the goodness of fit.

5.1.2 Viability effects of EPA and DHA on IPEC-J2 cells challenged by different stressors

MTT based viability assay was used to determine the treatment effects on mitochondrial metabolic activity of IPEC-J2 cells. Pre-treatment of cells with EPA (6.7 µM) and DHA:EPA (1:2; 10 µM) increased the mitochondrial activity against LPS stress, while DHA did not have an impact compared to the control (0 µM, $p < 0.05$) (Figure 12a). Similar such mitochondrial protection was observed for cells pre-treated with DHA (3.3 µM), EPA (6.7 µM) and their combination, DHA:EPA (1:2; 10 µM) from the damage of 24 h DSS (Figure 3b) and 1 h H_2O_2 stress (Figure 12c) compared to the control (0 µM, $p < 0.05$).

Figure 12 n-3 PUFA impact on the viability of IPEC-J2 cells under different stress conditions

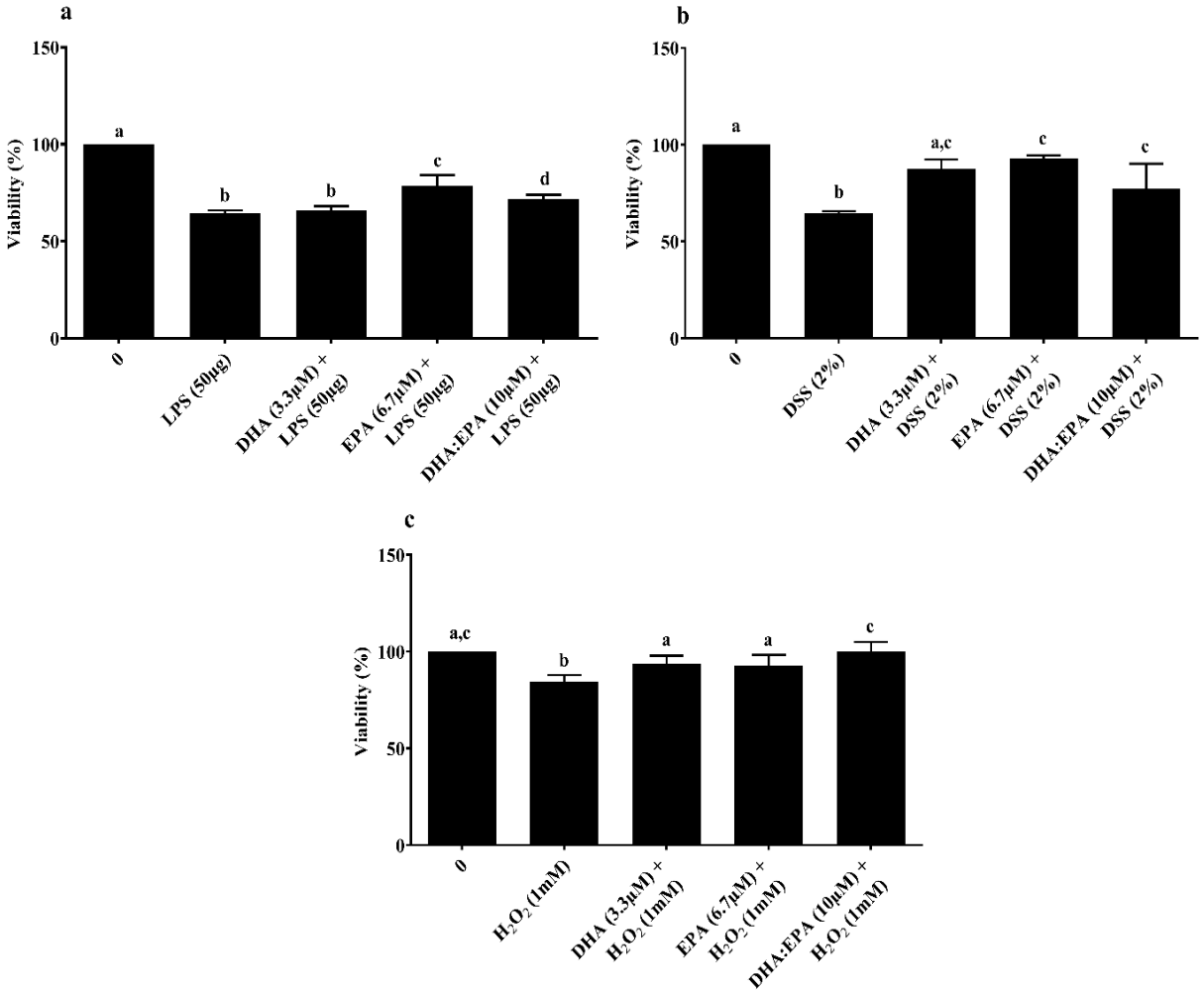

Effects of DHA (3.3 µM), EPA (6.7 µM) and DHA:EPA (1:2; 10 µM) pre-treatment (24 h) on the viability of IPEC-J2 cells challenged by (a) LPS (50 or 100 µg/mL) for 24 h; (b) DSS (2%) for 24 h and (c) H_2O_2 (1 mM) for 1 h. Data are presented as mean ± SEM (n = 3, one-way ANOVA). Statistically significant difference among the treatments is denoted by different letters, where $p < 0.05$.

5.1.3 Effects of EPA and DHA on LDH and NO activity of IPEC-J2 cells challenged by different stressors

LDH assay was performed to determine the treatment effects on cell membrane integrity. Neither the individual DHA (3.3 µM)/EPA (6.7 µM) nor its combination DHA:EPA (1:2; 10 µM) were able to recover the membrane integrity from 24 h LPS (Figure 13a) and DSS

challenge (Figure 13b) ($p < 0.05$). As shown in the figure 13c, pre-treatment of the cells with DHA (3.3 µM), EPA (6.7 µM) and DHA:EPA (1:2; 10 µM) were able to significantly maintain the membrane integrity against 1 h H_2O_2 challenge compared to the control (0 µM, $p < 0.05$). The NO activity in the culture media was tested by Griess reagent. Unlikely, the NO content in the culture media was below the detection limit (< 2.5 µM) for all the treatments as shown in the representative figure 15.

Figure 13 n-3 PUFA impact on the membrane integrity of IPEC-J2 cells under different stress conditions

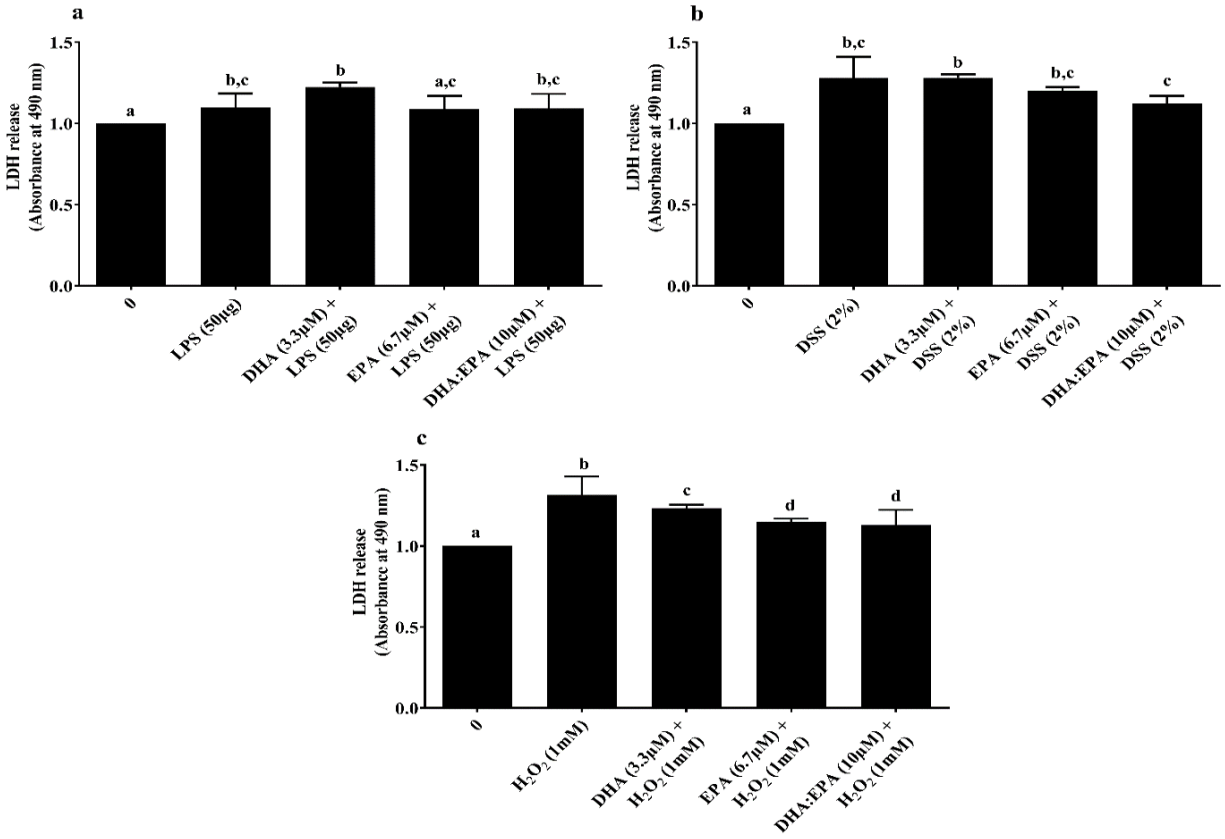

Effects of DHA (3.3 µM), EPA (6.7 µM) and DHA:EPA (1:2; 10 µM) pre-treatment (24 h) on the membrane integrity of IPEC-J2 cells challenged by (a) LPS (50 µg/mL) for 24 h; (b) DSS (2%) for 24 h and (c) H_2O_2 (1 mM) for 1 h. Data are presented as mean ± SEM (n = 3, one-way ANOVA). Statistically significant difference among the treatments is denoted by different letters, where $p < 0.05$.

5.1.4 Effects of EPA and DHA on apoptosis of IPEC-J2 cells exposed to different stressors

The intracellular caspase-3/7 activity was estimated to elucidate the treatment effects on apoptosis of IPEC-J2 cells. 24 h challenge of 50-100 µg/mL LPS (Figure 14a) and 2% DSS (Figure 14b) significantly increased the caspase-3/7 activity by 2-fold compared to the control (0 µM) while, the 24 h DHA:EPA (1:2; 10 µM) pre-treatment remarkably reduced this activity in IPEC-J2 cells ($p < 0.05$). Also, the reduction of caspase-3/7 activity was comparatively higher for 50 µg/mL over 100 µg/mL of LPS. On the contrary, no caspase-3/7 activity was observed for H_2O_2 challenge (not shown).

Figure 14 n-3 PUFA impact on the caspase-3/7 activity of LPS-infected IPEC-J2 cells

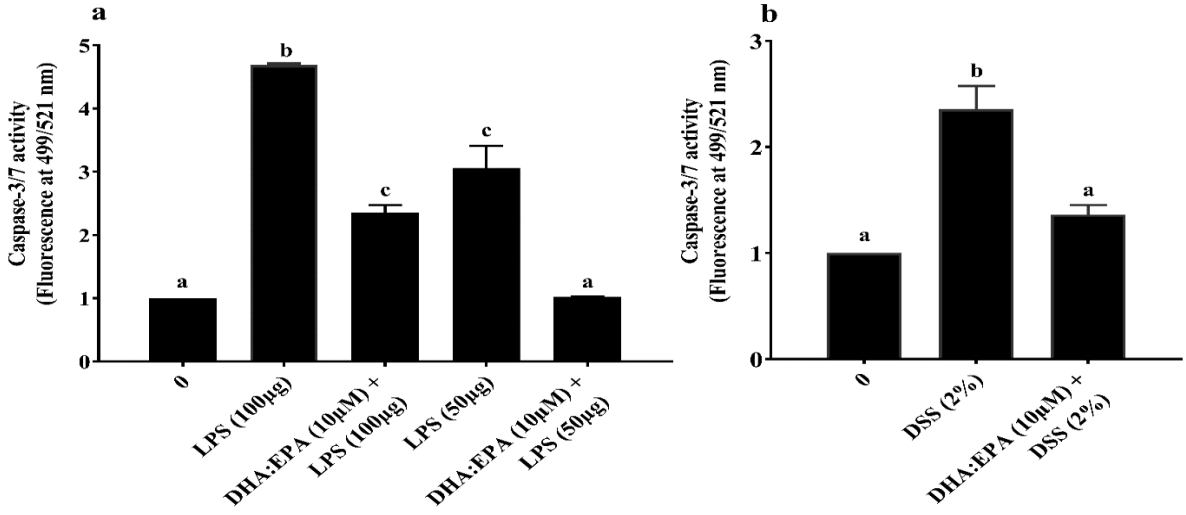

Effects of DHA:EPA (1:2; 10 µM) pre-treatment (24 h) on the apoptosis of IPEC-J2 cells challenged by (a) LPS (50 or 100 µg/mL) and (b) DSS (2%) for 24 h. Data are presented as mean ± SEM (n = 3, one-way ANOVA). Statistically significant difference among the treatments is denoted by different letters, where p < 0.05.

Figure 15 Nitric oxide activity of IPEC-J2 cells stressed with LPS

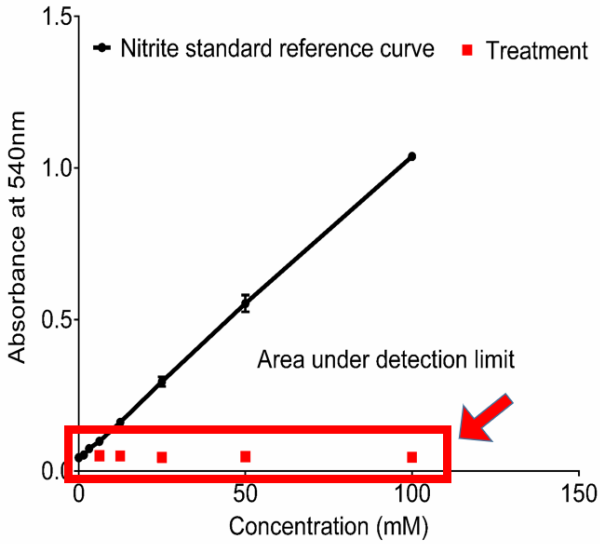

Effects of DHA (3.3 µM), EPA (6.7 µM) and DHA:EPA (1:2; 10 µM) pre-treatment (24 h) on the NO activity of IPEC-J2 cells challenged by LPS (50 µg/mL) for 24 h. Data are presented as mean ± SEM (n = 3).

5.2 Transcriptomic analysis of LPS-infected cells with or without n-3 PUFA pre-treatment

5.2.1 Differentially expressed genes

Totally, twelve cDNA libraries were constructed with three biological replicates for the treatment groups, (i) n-3 PUFA *vs* control, (ii) LPS *vs* control, (iii) n-3 PUFA+LPS *vs* control. The cDNA libraries generated for the RNA-seq analysis had optimal fragment size between 150-300 nt. In total, between 11,790-11,798 genes were mapped for each of the treatment group. The genes with minimum average logCPM (count per million) ≥ 3, logFC (fold change) ranging beyond ± 1 and *p*-value ≤ 0.01 were considered statistically significant, differentially expressed genes (DEGs) in each of the treatment group on comparison against the control (Figure 16A-C). To visualize the DEGs between the three treatment groups, volcano plots were generated using the OMnalysis web application developed by our team (http://lbmi.uvlf.sk/omnalysis) (TYAGI et al., 2021). As shown in the volcano plot (Figure 16), n-3 PUFA+LPS treatment induced the broadest transcriptional change in the IPEC-J2 cells (Figure 16C) followed by LPS (Figure 16B), whereas n-3 PUFA evoked the narrowest change (Figure 16A).

As shown in the figure 17B, 51 DEGs (23 upregulated and 28 downregulated) were identified in the IPEC-J2 cells after n-3 PUFA treatment (logCPM ≥ 3, logFC ≥ 1 or ≤ -1, $p \leq 0.01$). In the LPS challenged cells, 75 DEGs (46 upregulated and 29 downregulated) were detected. Likewise, 173 (45 upregulated and 128 downregulated) DEGs were detected in the LPS challenged cells pre-treated with n-3 PUFA. Between all of the three treatment groups, only 7 DEGs were commonly identified as shown in the Venn diagram (Figure 17A). Moreover, 18 DEGs were uniquely regulated in the n-3 PUFA treated cells. In the LPS challenged cells, 21 DEGs were uniquely identified. Similarly, 99 DEGs were uniquely regulated in the LPS-induced cells pre-treated with n-3 PUFA (Figure 17A). A preliminary validation of 4 genes identified in the RNA-seq analysis with qRT-PCR method, confirmed the consistency of gene expression (Figure 18A-B).

Figure 16 DEPs identified in the porcine IPEC-J2 cells exposed to n-3 PUFA, LPS or n-3 PUFA+LPS.

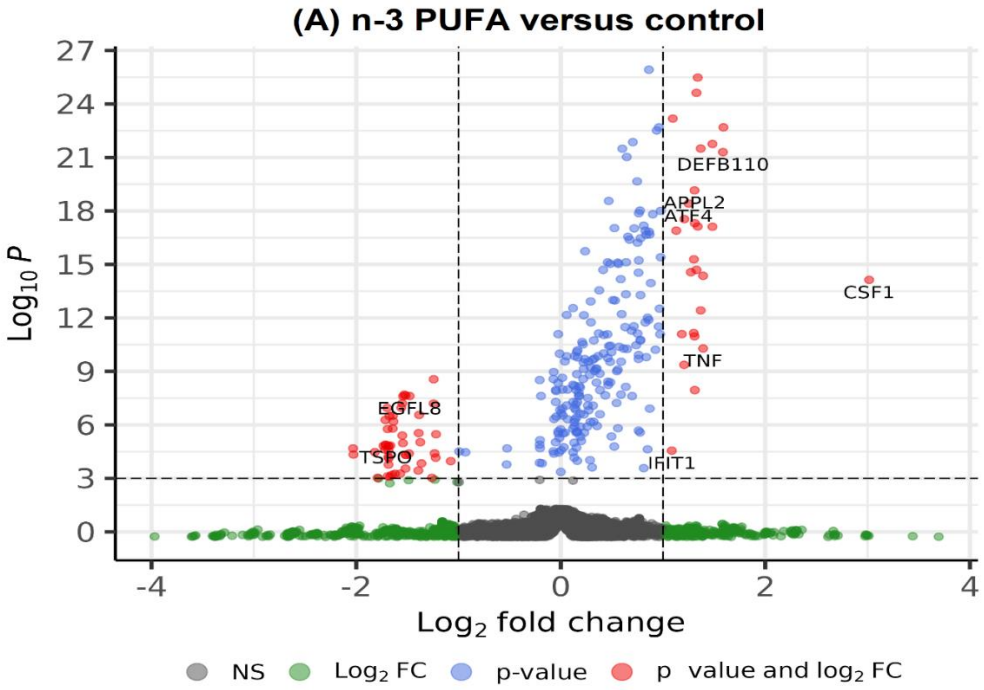

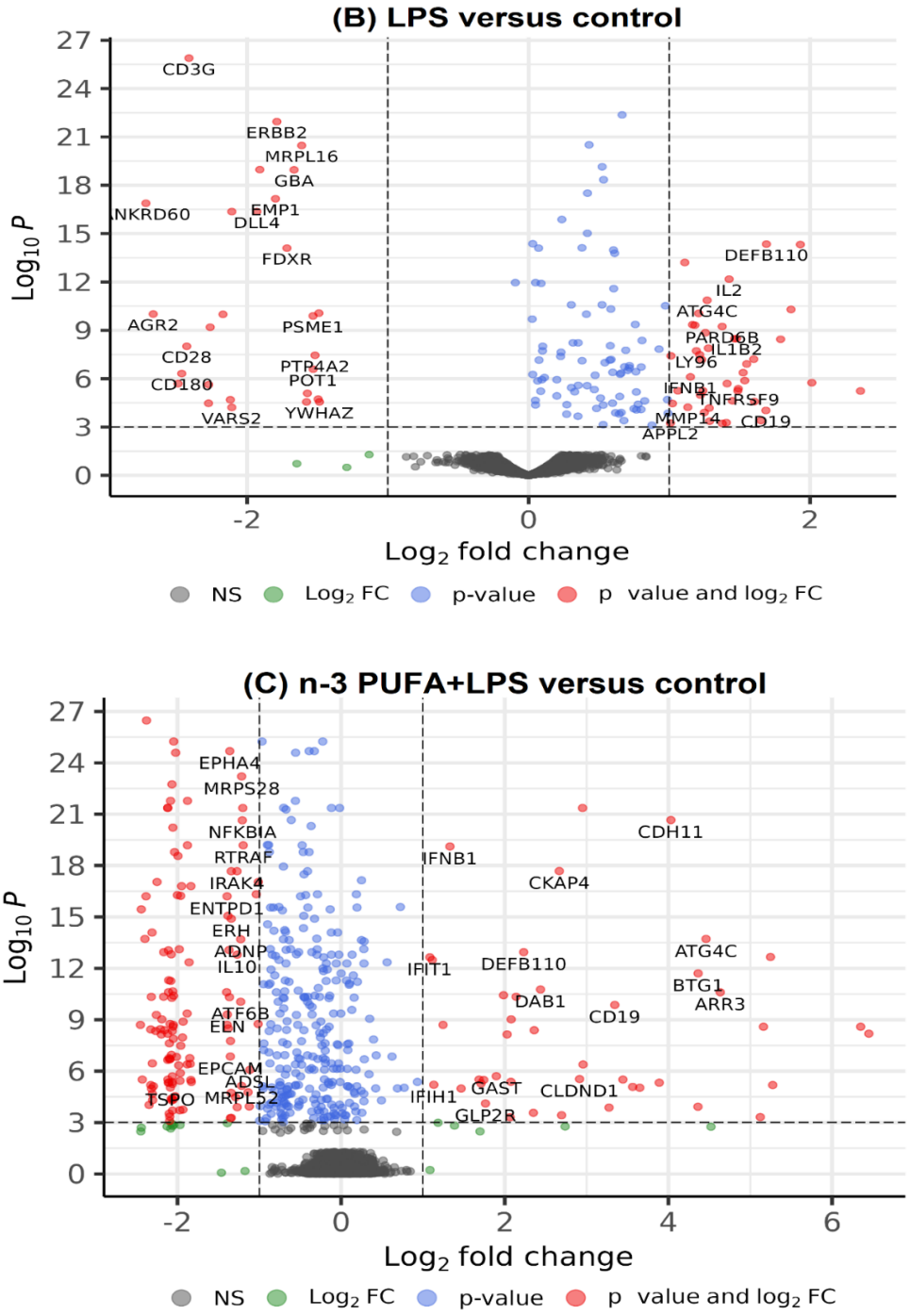

Volcano plot representation of differentially expressed genes (DEGs) identified in IPEC-J2 cells after n-3 PUFA (A), LPS (B) or n-3 PUFA pre-treatment and LPS challenge (C) in comparison against the control. Red dots represent the DEGs that are significantly up or downregulated (n =3, logCPM ≥ 3, logFC ≥ 1 or ≤ -1, p ≤ 0.01), while the green, blue and grey dots collectively represent the non-significant DEGs. The volcano plots were prepared using the OMnalysis application.

Figure 17 Common and uniquely regulated DEGs between the treatment groups

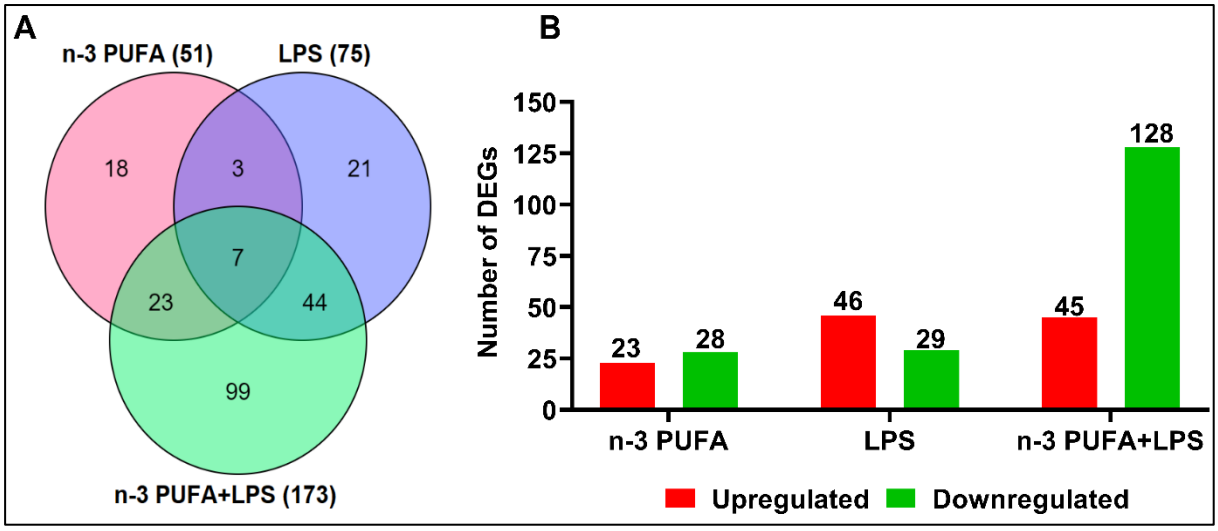

(A) Venn diagram represents the number of common and unique DEGs identified in the n-3 PUFA, LPS and n-3 PUFA+LPS treatment groups. (B) Bar represents the number of up and downregulated DEGs identified in each treatment group. Red denotes the upregulated DEGs while, the green denotes the downregulated DEGs (n =3, logCPM ≥ 3, logFC ≥ 1 or ≤ -1, p ≤ 0.01).

Figure 18 Preliminary validation of DEGs from RNA-seq analysis with qRT-PCR

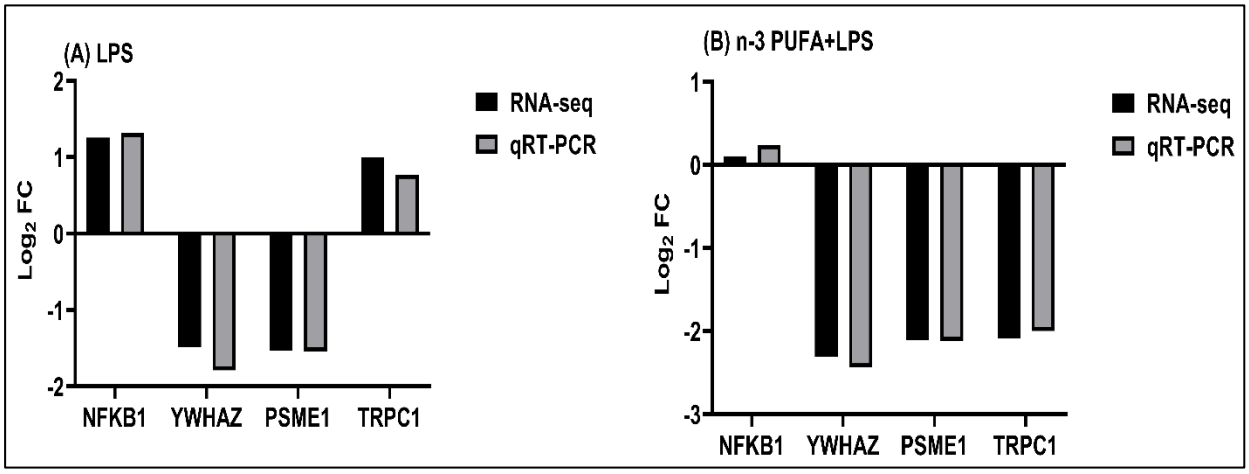

Consistence of the expression of 4 highly up or downregulated DEGs in the RNA-seq was checked against the qRT-PCR analysis.

5.2.2 Gene ontology annotations and pathway enrichment analysis

Gene Ontology (GO) annotation was performed using the OMnalysis to functionally capture the transcriptional dynamics of IPEC-J2 cells at different treatment conditions (n-3 PUFA, LPS, or n-3 PUFA+LPS). GO analysis provides the details of the DEGs in three categories - biological process, cellular components and molecular functions in which it participates. In the present study, GO analysis revealed the enrichment of DEGs in several cellular process. Specifically, the biological process that related to the enterocyte proliferation, apoptosis, cell-junction organization, oxidative stress, and inflammatory response were assessed. To further enumerate the role of n-3 PUFA in intestinal barrier inflammation, the major inflammatory pathways that activated by LPS was assessed. To this, the pathway enrichment analysis was performed for each of the three treatment groups using the peer-reviewed, Reactome pathway database. The top ten pathways in which majority of the genes were mapped are reported in the Table 8, 9 and 10. For the analysis, only the pathways that satisfy the statistical filtering of $p < 0.05$ after correction with Benjamani-Hochberg method were considered.

Table 8 List of top 15 Reactome database pathways identified in the n-3 PUFA treated cells

No.	Pathway identifier	Pathway name	Entities found	Entities total	Entities FDR	Reactions found	Reactions total	Reactions ratio
1	R-HSA-1280215	Cytokine Signaling in Immune system	19	1092	1.49E-04	88	710	0.05203
2	R-HSA-6783783	Interleukin-10 signaling	6	86	7.76E-04	2	15	0.001099
3	R-HSA-168256	Immune System	27	2684	0.004196	130	1625	0.119083
4	R-HSA-449147	Signaling by Interleukins	12	643	0.004196	60	493	0.036128
5	R-HSA-1059683	Interleukin-6 signaling	3	17	0.007152	15	20	0.001466
6	R-HSA-1482883	Acyl chain remodeling of DAG and TAG	3	18	0.007152	2	8	5.86E-04
7	R-HSA-373753	Nephrin family interactions	3	25	0.014189	3	13	9.53E-04
8	R-HSA-909733	Interferon alpha/beta signaling	6	188	0.014189	2	24	0.001759
9	R-HSA-8979227	Triglyceride metabolism	4	66	0.014189	3	24	0.001759
10	R-HSA-6783589	Interleukin-6 family signaling	3	30	0.019103	19	34	0.002492
11	R-HSA-1483206	Glycerophospholipid biosynthesis	6	222	0.025477	4	133	0.009746
12	R-HSA-9609736	Assembly and cell surface presentation of NMDA receptors	3	49	0.06443	4	23	0.001685
13	R-HSA-9020956	Interleukin-27 signaling	2	13	0.065508	8	20	0.001466
14	R-HSA-913531	Interferon Signaling	7	394	0.068917	21	71	0.005203
15	R-HSA-428540	Activation of RAC1	2	15	0.068917	4	4	2.93E-04

Table 9 List of top 15 Reactome database pathways identified in the LPS-induced cells

No.	Pathway identifier	Pathway name	Entities found	Entities total	Entities FDR	Reactions found	Reactions total	Reactions ratio
1	R-HSA-168256	Immune System	48	2684	4.62E-09	328	1625	0.119083
2	R-HSA-1280215	Cytokine Signaling in Immune system	28	1092	1.30E-07	148	710	0.05203
3	R-HSA-449147	Signaling by Interleukins	21	643	3.23E-07	113	493	0.036128
4	R-HSA-1059683	Interleukin-6 signaling	6	17	3.62E-07	18	20	0.001466
5	R-HSA-5660668	CLEC7A/inflammasome pathway	4	8	3.14E-05	2	4	2.93E-04
6	R-HSA-112411	MAPK1 (ERK2) activation	4	12	1.33E-04	1	3	2.20E-04
7	R-HSA-110056	MAPK3 (ERK1) activation	4	13	1.61E-04	1	4	2.93E-04
8	R-HSA-5357769	Caspase activation via extrinsic apoptotic signalling pathway	5	32	1.93E-04	5	17	0.001246
9	R-HSA-9614085	FOXO-mediated transcription	7	110	5.33E-04	9	85	0.006229
10	R-HSA-5602358	Diseases associated with the TLR signaling cascade	5	42	5.33E-04	9	15	0.001099
11	R-HSA-5260271	Diseases of Immune System	5	42	5.33E-04	9	15	0.001099
12	R-HSA-6785807	Interleukin-4 and Interleukin-13 signaling	9	211	6.23E-04	21	47	0.003444
13	R-HSA-5602498	MyD88 deficiency (TLR2/4)	4	26	0.001281	2	2	1.47E-04
14	R-HSA-5357801	Programmed Cell Death	9	238	0.001281	9	197	0.014436
15	R-HSA-5603041	IRAK4 deficiency (TLR2/4)	4	27	0.001281	2	2	1.47E-04

Table 10 List of top 15 Reactome database pathways identified in the LPS-induced cells pre-treated with n-3 PUFA

No.	Pathway identifier	Pathway name	Entities found	Entities total	Entities FDR	Reactions found	Reactions total	Reactions ratio
1	R-HSA-9614085	FOXO-mediated transcription	11	110	3.30E-04	14	85	0.006229
2	R-HSA-168256	Immune System	64	2684	4.85E-04	360	1625	0.119083
3	R-HSA-1280215	Cytokine Signaling in Immune system	31	1092	0.01747	137	710	0.05203
4	R-HSA-5603029	IkBA variant leads to EDA-ID	3	8	0.036134	2	2	1.47E-04
5	R-HSA-5579026	Defective CYP11A1 causes AICSR	3	9	0.036134	1	1	7.33E-05
6	R-HSA-5602358	Diseases associated with the TLR signaling cascade	5	42	0.036134	10	15	0.001099
7	R-HSA-5260271	Diseases of Immune System	5	42	0.036134	10	15	0.001099
8	R-HSA-2395516	Electron transport from NADPH to Ferredoxin	3	10	0.038847	2	2	1.47E-04
9	R-HSA-1362409	Mitochondrial iron-sulfur cluster biogenesis	4	25	0.038847	4	6	4.40E-04
10	R-HSA-449147	Signaling by Interleukins	20	643	0.038847	80	493	0.036128
11	R-HSA-196108	Pregnenolone biosynthesis	4	27	0.039017	4	9	6.60E-04
12	R-HSA-9617828	FOXO-mediated transcription of cell cycle genes	4	27	0.039017	4	22	0.001612
13	R-HSA-933542	TRAF6 mediated NF-kB activation	4	30	0.046543	3	4	2.93E-04
14	R-HSA-5603027	IKBKG deficiency causes anhidrotic ectodermal dysplasia with immunodeficiency (EDA-ID) (via TLR)	2	3	0.046543	1	1	7.33E-05
15	R-HSA-5602636	IKBKB deficiency causes SCID	2	3	0.046543	1	1	7.33E-05

5.2.3 DEGs involved in the enterocyte proliferation

In total, 14 genes (6 upregulated and 8 downregulated) were identified related to cell proliferation from the GO terms, 'Epithelial cell proliferation (GO:0050673)', 'Positive regulation of cell population proliferation (GO:0008284)', and 'Negative regulation of epithelial cell proliferation (GO:0050680)' (Figure 19, Panel A). Challenge with LPS, upregulated the gene expression of ITGAV (Integrin alpha V) and IRF(Interferon regulatory factor)6, while downregulated the DLL4 (Delta Like Canonical Notch Ligand 4) and CD28 (T-Cell-Specific Surface Glycoprotein). ITGAV is an integral membrane receptor, that mediates the cell-extracellular matrix (ECM) interactions. Earlier, knockdown of ITGAV induced cell cycle arrest and reduced cell proliferation in adipose tissue stem cells (MORANDI et al., 2016; PAOLI et al., 2013). Whereas, IRF6 is a member of the IRF family of transcription factors, that associated with epithelial cell proliferation and differentiation (KWA et al., 2014). Recently, IRF6 promoted Notch-induced proliferation and transformation in mammary epithelial cells (ZENGIN et al., 2015b). The LPS-downregulated DLL4 gene, encodes the ligand of Notch receptor 3. DLL4 is one of the essential growth factors secreted by IECs for balancing the cell proliferation and turnover via Notch signaling (THOO et al., 2019). Overexpression of DLL4 was associated with anti-proliferation in lung cancer cells (LIU et al., 2018b). Besides, CD28 that downregulated by LPS, is a glycoprotein expressed on T cell surface. It regulates the T cell proliferation and apoptosis by controlling the T cell receptor(TCR)/CD3 signaling (WALKER LS, 1998). Although, n-3 PUFA was unable to alter the expression of these genes, it slightly enhanced the LPS-induced suppression on DLL4 (by 1.07-fold) in the infected cells.

Furthermore, 6 genes were uniquely regulated in the LPS-infected cells pre-treated with n-3 PUFA. Specifically, the downregulated PDCD10 (Programmed Cell Death 10), PHB2 (Prohibitin 2), and EPCAM (Epithelial cell adhesion molecule) genes were associated with cell proliferation (MERKWIRTH et al., 2008; SCHNELL et al., 2013; SUN et al., 2021; YOU et al., 2013). EPCAM is a transmembrane glycoprotein that establishes homotypic cell-cell adhesion in epithelia. Loss of EPCAM is associated with reduced cell proliferation and delayed cell cycle progression (SCHNELL et al., 2013). On the other hand, PDCD10 exhibits both pro- and anti-apoptotic functions. Earlier, PDCD10 silencing induced endothelial proliferation and angiogenesis through vascular endothelial growth factor (VEGF) activation and DLL4-Notch

signaling inhibition (YOU et al., 2013). In another study, overexpression of PDCD10 induced proliferation and metastasis of hepatocellular carcinoma cells by binding the catalytic subunit of protein phosphatase (PP)2A (SUN et al., 2021). Besides, PHB2 encodes the protein that localized in the inner mitochondrial membrane. Loss of PHB2 impaired the cell proliferation and stimulated resistance towards apoptosis in mouse embryonic fibroblasts (MERKWIRTH et al., 2008).

In addition, the anti-inflammatory IL10 cytokine was uniquely downregulated in the infected cells pre-treated with n-3 PUFA. IL10 is known to protect from excessive tissue damage during inflammations. Recently, loss of PP2A aggravated LPS-induced lung injury in mice, which intern resulted in IL10-dependent sensitization of lung epithelial apoptosis (SUN et al., 2019). These observations suggest that, LPS infection could have induced cell proliferation via Notch signaling by regulating the IRF6 (ZENGIN et al., 2015a) and DLL4 genes (THOO et al., 2019). In turn, n-3 PUFA might have inhibited stress-induced proliferation by controlling the PDCD10, DLL4, EPCAM, and IL10 genes through Notch signaling or by protein phosphatase activity. In agreement to this speculation, in the present study, PPP1CA (Protein phosphatase 1 catalytic subunit alpha) that encodes one of the three subunits of serine/threonine PP1 was downregulated only in the LPS-infected cells pre-treated with n-3 PUFA. Moreover, n-3 PUFA uniquely upregulated TNF, ADAM(A Disintegrin and Metallopeptidase)10, and NCK1 (Non-catalytic region of tyrosine kinase adaptor protein 1) genes in the uninfected cells. TNF (Tumor necrosis factor) is a multifunctional cytokine that belongs to the TNF superfamily. It stimulates epithelial cell proliferation to facilitate tissue repair in mucosal injury. Earlier, treatment of rat gastric mucosal epithelial cell line (RGM-1) with increasing concentration of TNF-α, promoted cell proliferation without inducing apoptosis (LUO et al., 2005).

Besides, the n-3 PUFA-induced ADAM10 and NCK1 genes are involved in epithelial proliferation and morphogenesis. ADAM10 is a member of the ADAM family of transmembrane proteins, that proteolytically release various cell surface proteins including the TNF cytokine and E-cadherin cell adhesion protein (SCHNELL et al., 2013). On the other hand, NCK1 is a cytoplasmic adaptor protein that involved in receptor tyrosine kinase signaling. Earlier, NCK1 promoted cell proliferation in corneal epithelial cells (PAENSUWAN et al., 2022). The outcome of present study suggests the differential behavior of n-3 PUFA in normal and infected enterocytes. Specifically, n-3 PUFA promoted epithelial cell proliferation

and morphogenesis in normal state, whereas during infection it suppressed the stress-induced cell proliferation.

5.2.4 DEGs involved in the enterocyte apoptosis

In the GO biological process, 'Apoptotic process (GO:0006915)', 23 genes (9 upregulated and 14 downregulated) were identified (Figure 19, Panel B). Specifically, LPS upregulated the gene expression of BTG(B-cell translocation gene)1, ITGAV, TNFRSF9, and IL2 whereas, suppressed the CD3G and CD28. Among these genes, n-3 PUFA inhibited the expression of TNFRSF9 and IL2 in the infected cells. Besides, n-3 PUFA highly amplified the expression of LPS-activated BTG1 (by 3.7-fold) while, uniquely induced the BTG2 in infected cells. BTG1 and BTG2 encodes anti-proliferative proteins, that regulates various cellular process including the maintenance of homeostasis under stress conditions (YUNIATI et al., 2019). TNFRSF9 (CD137) is a member of the TNF receptor family, that controls the T cell proliferation and survival (OTANO et al., 2021). TNFRSF9 and CD28 co-stimulates regulates the T cell survival and apoptosis by activating the TCR/CD3 signaling (OTANO et al., 2021; WALKER LS, 1998). It was also reported that the cells that downregulate CD28, undergoes apoptosis (WALKER LS, 1998). Besides, in a process called activation-induced cell death, IL2 triggers Fas/FasL-mediated apoptosis in the activated T cells (ESSER MT, 1997; REFAELI Y, 1998). Notably, the genes TNFRSF9, IL2, CD3G, CD28, and FASLG (Fas ligand) related to T cell apoptosis were downregulated in the infected cells pre-treated with n-3 PUFA.

Further, in both normal and infected cells, n-3 PUFA treatment upregulated the expression of IFIT(Interferon-induced protein with tetratricopeptide repeats)3, while downregulated the expression of DPEP1 (Dipeptidase 1), PPP1CA, and CKMT1A (Mitochondrial creatine kinase-1) genes. IFIT3 encodes an anti-viral protein upon stimulation of Interferon (IFN) receptor or Toll-like receptor (TLR). The knockdown of IFIT3 in lung epithelial cells, induced cell apoptosis by suppressing the caspase-3/8/9 and BAX (BCL2 Associated X, Apoptosis Regulator) expressions (HSU et al., 2013). Besides, n-3 PUFA-induced downregulation of PPP1CA was 1.7-fold higher in infected cells compared to the uninfected cells. PPP1CA controls several cellular processes including apoptosis by regulating the BCL-2 (B-cell lymphoma 2) family of apoptotic proteins (GARCIA et al., 2003). Further, the gene CKMT1 transfers high energy phosphatase from mitochondria to the cytosolic carriers. CKMT1 is highly expressed in various cancers and knockdown of which, triggers apoptotic cell death by mitochondrial depolarization (DATLER C, 2014).

Moreover, the genes PHB2, PDCD10 and CLU (Clusterin) were uniquely downregulated in the infected cells pre-treated with n-3 PUFA. As described in the GO cell proliferation, downregulation of PDCD10 and PHB2 genes induces apoptosis resistance. Whereas, CLU is a multifunctional acute-phase protein, expressed by various antigen-presenting cells (FALGARONE et al., 2009). Distinct isoforms of CLU were reported to influence NF-κB signaling and BAX-mediated apoptosis (FALGARONE and CHIOCCHIA, 2009). However, in the LPS-infected cells pre-treated with n-3 PUFA, the anti-apoptotic FAIM (Fas Apoptotic Inhibitory Molecule) was downregulated while, the pro-apoptotic AIFM1 (Apoptosis Inducing Factor Mitochondria Associated 1) was upregulated. FAIM was reported to ameliorate Fas killing by enhancing the CD40-mediated NF-κB activation (KAKU et al., 2009). Presently, the expression of CD40 was highly upregulated only in the infected cells pre-treated with n-3 PUFA. On the other hand, AIFM1 was reported to activate the caspase-3 mediated apoptosis (LIU et al., 2018a). The regulation of these genes in the apoptosis process is not clear, however LPS could have stimulated apoptosis by controlling Fas/caspase signaling in the enterocytes. In agreement to this speculation, in our previous study LPS induced the caspase-3/7 activity in IPEC-J2 cells which was counteracted by n-3 PUFA pre-treatment (SUNDARAM et al., 2020). Presently, FASLG was downregulated and the caspase-related genes were unexpressed, which supports the possibility of n-3 PUFA-aided apoptosis termination via Fas/caspase inhibition in the infected cells.

5.2.5 DEGs of cellular components involved in cell junction organization

IEL is formed by a single layer of intestinal epithelial cells (IECs), interconnected by different protein complexes such as the tight junctions (TJs), adherens junctions (AJs) and desmosomes. TJs consist of transmembrane proteins as the occludin, claudins, and junctional adhesion molecules (JAM), that governs the paracellular permeability of epithelium. AJs mainly consist of Ca^{2+}-dependent cell-cell adhesion molecules as cadherins and catenins, that controls the epithelial stability and dynamic cellular movements (MEGE et al., 2017). First step in a bacterial infection is the host-cell attachment and infiltration by disruption of the cell junction proteins. To understand the impacts of n-3 PUFA on cell junction architecture under LPS stress, the DEGs related to the cell junction proteins were searched. Accordingly, the terms, ‘Cell junction (GO:0030054)’, ‘Cell-cell junction (GO:0005911)’ and ‘Adherens junction (GO:0005912)’ were identified in the analysis of GO cellular components (Figure 19,

Panel C). In total, 16 genes (10 upregulated and 6 downregulated) were identified of which several were commonly shared between the three GO terms (Figure 19, Panel C).

Specifically, LPS upregulated the expression of important regulatory genes of the cell junctions such as the CDC42SE1 (CDC42 Small Effector 1), PARD6B (Partitioning defective 6 homolog beta), ITGAV and ARR3 (Arrestin 3). Notably, Par6 is a membrane protein that primarily localized at the TJs of the intestinal epithelium (NOLAN et al., 2008). Whereas, Cdc42 is one of the three members of Rho-family GTPases, that regulates the formation of apical cell-cell junction and apical-basal polarization by interacting with the Par6 (NOLAN et al., 2008; WALLACE et al., 2010). ITGAV is an integral membrane protein that regulates the cell-ECM interactions (DESGROSELLIER et al., 2010). Whereas, ARR3 is involved in terminating the signal transduction by activated G protein-coupled receptors (GPCR). Notably, pre-treatment with n-3 PUFA, highly enhanced the expression of LPS-induced CDC42SE1 (by 1.8-fold), PARD6B (by 2-fold) and ARR3 (3.2-fold) in the infected cells.

Additionally, n-3 PUFA upregulated the expression of ITGB3 (Integrin Subunit beta 3), CLDN1 (Claudin 1) and CDH11 (Cadherin 11) genes, while downregulated the GNAI2 (G Protein Subunit Alpha I2) gene only in the LPS-infected cells. The ITGAV and ITGB3 genes activated in the infected cells, are the subunits of Alpha-v beta-3 ($\alpha_V\beta_3$) integrin receptors, that mediates the cell-ECM interactions (DESGROSELLIER and CHERESH, 2010). While, GNAI2 is the subunit of Guanine nucleotide-binding proteins (G proteins), that involved in several transmembrane-mediated signalling (KLIEWER et al., 2017).

Combinedly, in both infected and uninfected cells, n-3 PUFA downregulated the expression of EPHA4 (Ephrin type-A receptor 4) and PPP1CA genes. In fact, n-3 PUFA induced downregulation on PPP1CA gene was 1.7-fold higher in the infected cells compared to uninfected cells. Earlier, PPP1CA is reported to inhibit TJ assembly by interacting with the occludin protein, suggesting its similar role in the present study (SETH et al., 2007). On the other hand, EPHA4 belongs to the ephrin receptor subfamily, that reported to control developmental events in axon guidance including the formation and disassembly of cell junctions (BEAMISH et al., 2018). Interestingly, in the uninfected cells, n-3 PUFA uniquely upregulated the ADAM10 and NCK1 genes. ADAM10 is a metallopeptidase that reported to cleave many cell surface proteins including the cell junction E-cadherin protein (MARETZKY

et al., 2005). While, NCK1 is a signal protein that participates in the receptor tyrosine kinase signaling (BEAMISH et al., 2018).

Figure 19 DEGs involved in the enterocyte proliferation, apoptosis and cell junction organization

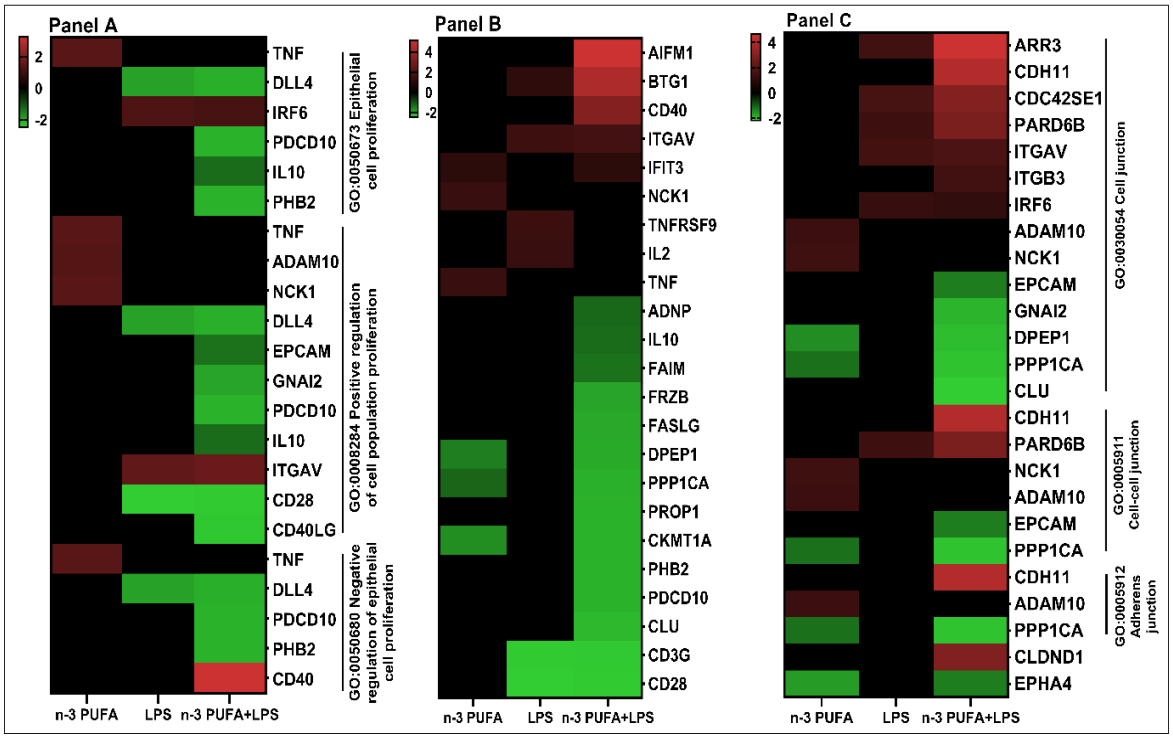

Heatmap of DEGs enriched in the GO biological process of enterocyte proliferation (Panel A), apoptosis (Panel B), and cell junction organization (Panel C). Red denotes upregulation, green denotes downregulation and black denotes no significant change in the gene expression. Scaling represents the range of log fold change (Log FC) values.

5.2.6 DEGs involved in the innate and adaptive immune responses

The GO biological process, 'Innate immune response (GO:0045087)' and 'Adaptive immune response (GO:0002250)' were identified related to the immune responses (Figure 20, Panel D). Eight genes, APPL2 (Phosphotyrosine interacting with PH domain and leucine zipper 2), DEFB110 (Beta defensin 110), TLR4, TLR8, CD14, LY96 (Lymphocyte antigen 96, also known as MD-2), MYD88 (Myeloid differentiation factor 88), and CD59 related to the innate immune response was upregulated by LPS (Figure-1). Among these genes, TLR4, TLR8, CD14, LY96, and MYD88 are involved in the TLR signaling (KAWASAKI et al., 2014). APPL2 is an important adaptor protein that controls the TLR4 signalling and secretion of

pro/anti-inflammatory cytokines in macrophages (YEO et al., 2016). None of these pro-inflammatory genes were induced by n-3 PUFA, except the DEFB110. DEFB110 is a β-Defensin antimicrobial protein, primarily secreted by epithelial cells in the intestinal mucosa (BALS, 2000). Notably, n-3 PUFA inhibited all TLR-related genes induced by LPS except the CD14, CD59 and DEFB110. In fact, n-3 PUFA amplified the expression of CD14 and CD59 by 1.8-fold, while DEFB110 by 1.4-fold. CD14 is the co-receptor of TLRs (KAWASAKI and KAWAI, 2014), whereas the membrane-bound CD59 protects the self-cells from complement membrane attack complex (MAC) that activated during infections (KOLEV et al., 2010). Furthermore, n-3 PUFA uniquely upregulated CD40, while downregulated the SOCS1 (Suppressor of Cytokine Signaling 1) and IFNL3 (IL28B) genes in the infected cells. CD40 is expressed by various antigen-presenting cells, that establishes B cell-mediated humoral immune response (LEE et al., 2003). Whereas, SOCS1 is a negative regulator of cytokine signaling in the Janus Kinase-signal transducer and activator of transcription proteins (JAN-STAT) and TLR inflammatory pathways (INAGAKI-OHARA et al., 2013). The n-3 PUFA-induced IFNL3 (Interferon lambda 3) is a pro-inflammatory cytokine. In addition to DEFB110, n-3 PUFA activated two other antimicrobial genes, IFIT1 and IFIT3 in both normal and infected cells. Notably, IFIT1 and IFIT3 negatively regulates the activation of LPS-mediated TLR4 signaling in macrophages (JOHN et al., 2018).

In the GO of adaptive immune response (Figure 20, Panel D), LPS upregulated the expression of IL1B, IL2, IL6, CD1A, and CD19 genes while, downregulated the CD3G and CD28 genes. Except CD1A, none of these genes were activated by n-3 PUFA. However, in the uninfected cells, n-3 PUFA uniquely induced the expression of pro-inflammatory cytokine gene, TNF and the NCK1 signaling protein. On the other hand, n-3 PUFA inhibited the LPS-induced pro-inflammatory cytokines (IL1B, IL2, and IL6), while amplified the expression of CD19 and CD1A by 2-fold. CD19 is a cell surface transmembrane protein, that controls B cell differentiation and immunoglobulin secretion (DEPOIL et al., 2008). CD1A is also a transmembrane protein expressed in various antigen-presenting cells, that delivers lipid antigens to the T cells (MITCHELL et al., 2021).

5.2.7 DEGs involved in oxidative stress

In the GO biological process, ‘Response to oxidative stress (GO:0006979)’, five genes (4 upregulated and 1 downregulated) were identified (Figure 20, Panel D). LPS upregulated the expression of ITGAV, which was unable to alter by n-3 PUFA in infected cells. Under

different physiological conditions, integrins engage in epidermal-growth factor signaling and generate reactive oxygen species for the regulation of cell survival and apoptosis (GIANNONI et al., 2008). Besides, in the infected cells pre-treated with n-3 PUFA, the genes PDCD10 and CCS (Copper Chaperone For Superoxide Dismutase) were uniquely downregulated. PDCD10 modulates cellular apoptosis and overexpression of this gene is associated with oxidative stress (YOU et al., 2013). Whereas, CCS is a copper chaperone that delivers Cu ions to the antioxidant, Cu/Zn superperoxide dismutase (SOD1). Recently, CCS was suggested to cross-react with the ATOX1 (Antioxidant 1 Copper Chaperon) and exchange Cu ions (MATSON DZEBO et al., 2016). Even though CCS was downregulated by n-3 PUFA, interestingly, ATOX1 was remarkably amplified by 5.8-fold in the infected cells (logFC 5.24) compared to the uninfected cells (logFC 0.90) [Although ATOX1 expression in uninfected cells is below the logFC ± 1 cut-off that applied in DEG analysis, it is considered for comparison due to closeness to this range]. ATOX1 was known to ameliorate the LPS-induced oxidative stress, NF-κB and Mitogen-activated protein kinase (MAPK) signaling in macrophages (KIM et al., 2018; MATSON DZEBO et al., 2016). Moreover, n-3 PUFA downregulated the expression of DPEP1 in the normal cells, whose suppression was enhanced by 1.3-fold in the infected cells. DPEP1 encodes the Dipeptidase 1 glycoprotein, that hydrolyses various biomolecules including the glutathione antioxidant (KOZAK et al., 1982).

5.2.8 DEGs involved in the Toll-like receptor signaling pathway

In the Reactome pathway enrichment analysis, totally 19 genes (9 upregulated and 10 downregulated) were identified related to the TLR signaling of innate immune response (Figure 20-Panel E, Figure 21). Specifically, CD14, LY96 (also known as MD-2), and TLR4 genes were highly expressed in the LPS-infected cells, that encodes the cell surface pattern recognition receptors (PRRs) for identification of PAMPs as the LPS (AIN et al., 2020). The membrane-bound CD14 initially binds the LPS and transfers it to the LY96-TLR4 complex (AIN et al., 2020). None of these genes were induced by n-3 PUFA; however, it inhibited the activation of LY96 and TLR4, while enhanced the CD14 expression (by 1.8-fold) in the infected cells (Figure 20-PanelE, Figure 21B). The interaction between LPS and TLR4 subsequently stimulated the intracellular activation of MyD88-dependent pathways. MyD88 is an adaptor protein that interacts with the Interleukin-1 receptor-associated kinase (IRAK)1/4 and activates the Transforming growth factor-β activated kinase 1 (TAK1) (AIN et al., 2020). This results in the downstream activation of IkappaB kinase (IKK) and MAPK for the

transcription of pro-inflammatory genes (AIN et al., 2020; AZAM et al., 2019). Particularly, IKK pathway activates the NF-κB mediated transcription, whereas MAPK pathway triggers the activator protein-1 complex (AP-1) induced transcription (KAWASAKI and KAWAI, 2014).

Presently, LPS induced the expression of MyD88, IRF6, NKAP (NF-kappa-B-activating protein) and NFKB1 (Nuclear Factor Kappa B Subunit 1) in the infected cells. IRF6 is an epithelial-specific transcription factor, recently identified to modulate the TLR signaling by interacting with the IRAK1 and MyD88 (KWA et al., 2014). Besides, NKAP and NFKB1 are involved in recruiting the NF-κB complexes. Notably, n-3 PUFA inhibited these genes in the infected cells and instead uniquely downregulated the expression of IRAK4, CHUK, IKBKG, NFKBIA and NFKBIZ that involved in NF-κB activation. Specifically, CHUK encodes the inhibitor of NF-κB kinase subunit alpha (IKK-α), IKBKG encodes the inhibitor of NF-κB kinase subunit gamma (IKK-γ), which along with the inhibitor of NF-κB kinase subunit beta (IKK-β), forms the three subunits of IKK complex (KAWASAKI and KAWAI, 2014).

On the other hand, NFKBIA encodes the NF-κB inhibitor alpha (IκBα) and NFKBIZ encodes the NF-κB inhibitor zeta (IκBζ). Both IκBα and IκBζ belongs to the IkappaB (IκB) family that inhibits the NF-κB activation (OECKINGHAUS et al., 2009). The primary role of IKK complex is to activate the NF-κB and facilitate its nuclear translocation by phosphorylating the IκB (KAWASAKI and KAWAI, 2014). Earlier, IκBζ promoted IL6 activation but inhibited the TNF expression in response to LPS (HORBER et al., 2016). In the present study similar observation was made, suggesting the possible influence of IκBζ on the expression of IL6 and TNF genes. Further, the expression of MAPK12, FOS (Fos proto-oncogene, AP-1 transcription factor subunit), FOSL2 (FOS like 2, AP-1 transcription factor subunit), and ATF6B (Atrial fibrillation, familial, 1) that involves in the MAPK signaling was uniquely downregulated in the infected cells pre-treated with n-3 PUFA. Notably, FOS, FOSL2, and ATF6B belongs to the AP-1 family of transcription factors (FAN et al., 2021).

To re-establish the barrier homeostasis, it is necessary to neutralize the TLR signaling. The genes, CD180, SIGIRR (Single Ig IL-1 receptor-related molecule), and SOCS1 were identified related to the negative regulation of TLR4 signaling (TKACIKOVA et al., 2020). LPS downregulated the expression of CD180, which was unable to alter by n-3 PUFA in the infected cells. On the other hand, SOCS1 was downregulated only in the infected cells pre-

treated with n-3 PUFA. Interestingly, n-3 PUFA upregulated the expression of SIGIRR in the normal cells, whereas the expression of this gene was absent in the infected cells.

Figure 20 DEGs involved in immune response, oxidative stress, TLR and cytokine signaling pathways

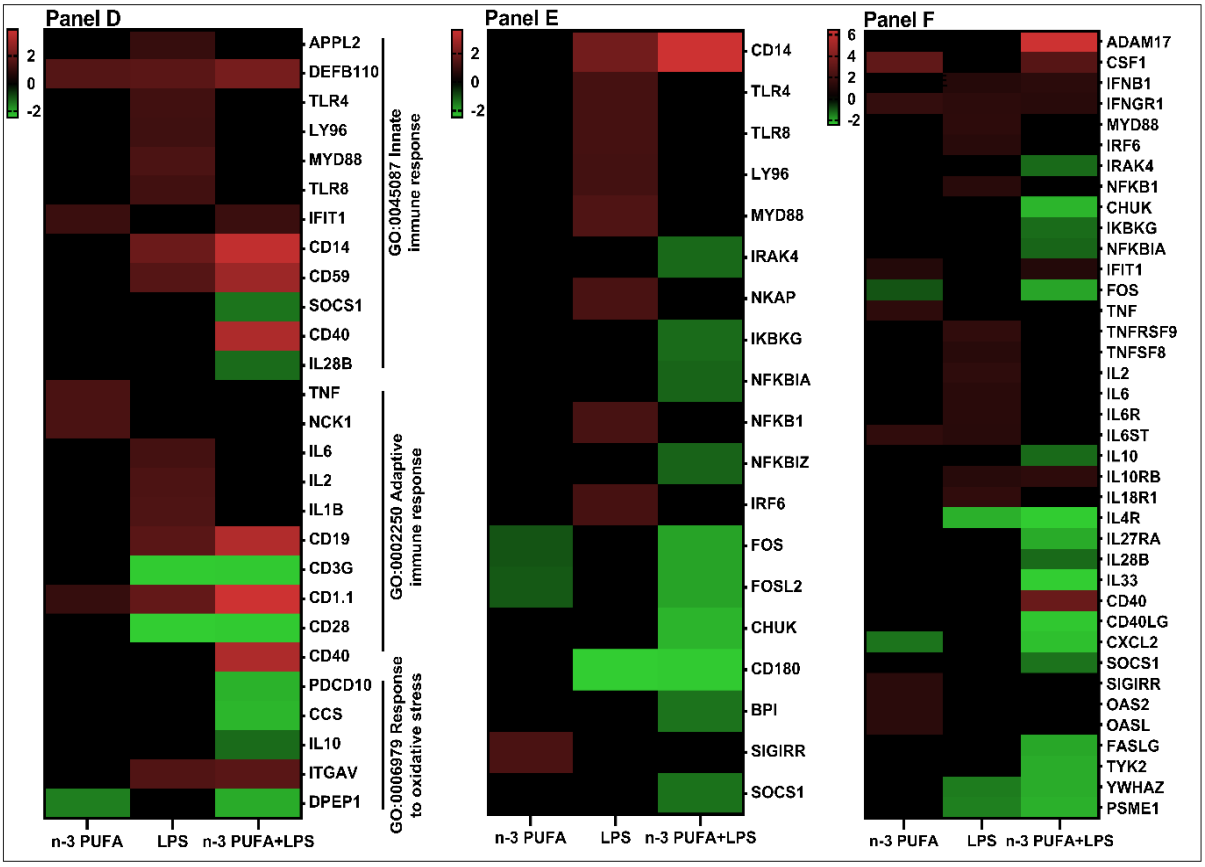

Heatmap of DEGs enriched in the GO biological process of immune response and oxidative stress (Panel D), TLR signaling (Panel E), and cytokine signaling (Panel F) pathways. Red denotes upregulation, green denotes downregulation and black denotes no significant change in the gene expression. Scaling represents the range of log fold change (LogFC) values.

Figure 21 Gene interaction network of the TLR signaling pathway

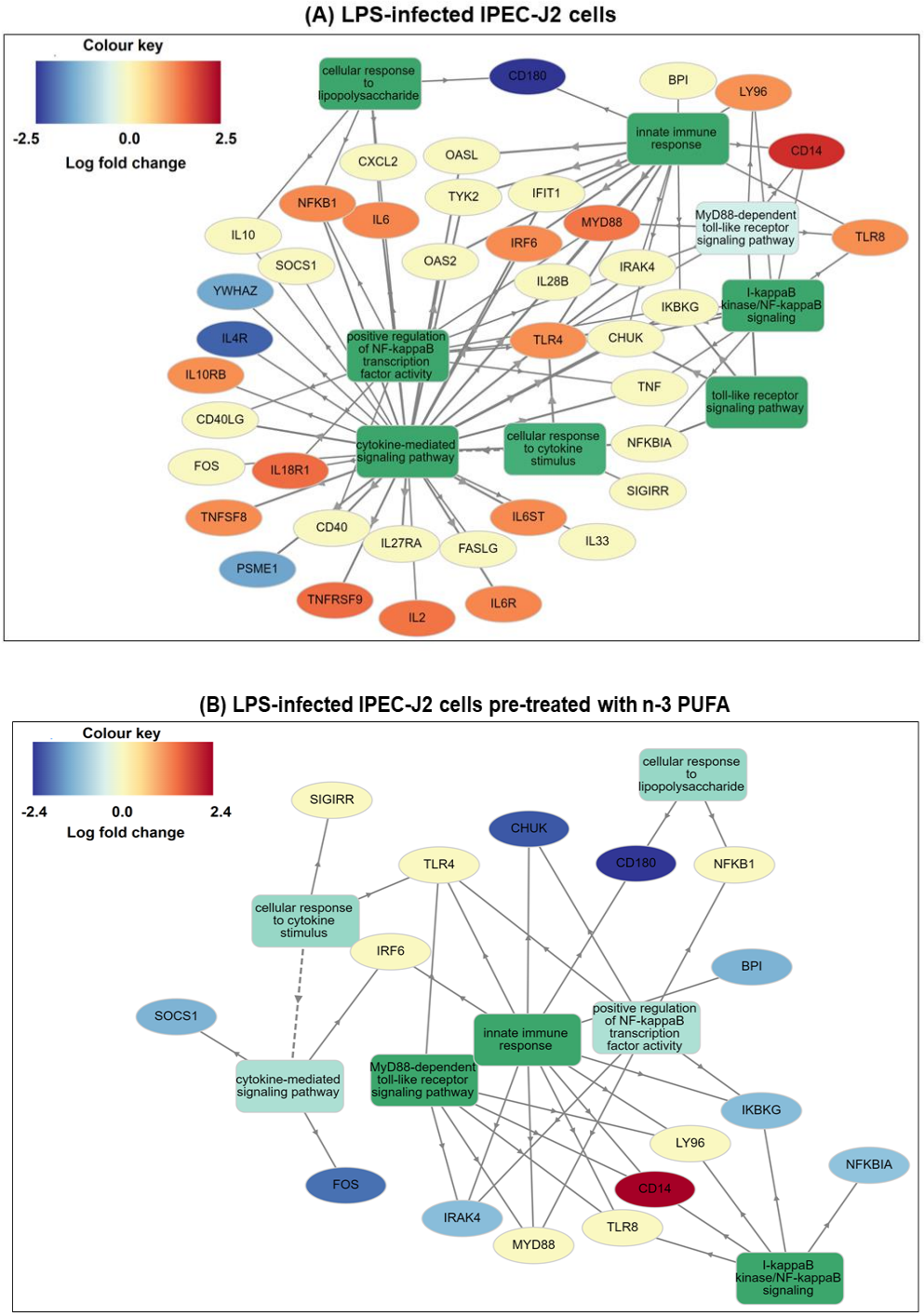

Schematic representation of the gene interaction network in TLR signaling pathway identified in the LPS-infected IPEC-J2 in the absence or presence or of n-3 PUFA pre-treatment. Scaling represents the range of log fold change (LogFC) values. Gene network generated using the GOnet application.

5.2.9 DEGs involved in cytokine signaling

Cytokines are multifunctional signaling proteins, secreted by immune cells to regulate the inflammatory process. In the present study, 38 genes (21 upregulated and 17 downregulated) were identified related to the cytokine signaling (Figure 20, Panel F). Particularly, LPS induced 16 genes in which the majority were upregulated (13 upregulated and 3 downregulated). Among the LPS activated genes, IL1B, IL1B2, IL2, IL6, and TNFSF8 were involved in encoding pro-inflammatory cytokines. Among these cytokines, the IL1B and IL6 are produced by macrophages in response to LPS-activated JAK/STAT3 signaling (SAMAVATI et al., 2009). Several cytokine receptor genes as the IL6R, IL6ST, IL10RB, IL18R1, IL1RL1 (IL33 receptor), and TNFRSF9 were also induced by LPS. Notably, n-3 PUFA was unable to stimulate any of these genes except the IL6ST. On the contrary, it inhibited the expression of all LPS-activated genes except the IL10RB, which was even amplified by 1.14-fold. Conversely, n-3 PUFA activated the pro-inflammatory cytokine, TNF in uninfected cells. Besides, the expression of ADAM17 was highly upregulated (logFC = 6.4) in the infected cells pre-treated with n-3 PUFA. ADAM17 is involved in the proteolytic release of various cell surface proteins including the TNF cytokine and IL6R cytokine receptor (SCHELLER et al., 2011). Cells treated with either only n-3 PUFA or LPS, did not express ADAM17.

IFNs are a family of cytokines, abundantly expressed on the barrier surfaces as the gastrointestinal epithelium during infections (ANDREAKOS et al., 2017). LPS challenge activated the IFNB1 (Interferon Beta 1) and IFNGR1 (Interferon Gamma Receptor 1), while n-3 PUFA activated the IFNGR1. In infected cells, n-3 PUFA moderately amplified the expression of LPS-induced IFNB1 (1.15-fold), and uniquely downregulated the IFNL3 (IL28B). IFNB1 and IFNL3 belongs to the type I and III of the IFN cytokine family (ANDREAKOS et al., 2017). Whereas, IFNGR1 is the member of type II IFN receptor family. IFNL3 is closely related to the IL10 cytokine family, therefore can act as a ligand for IL10RB (IL10 receptor beta) to mediate the JAK/STAT pathway in antiviral defense (ANDREAKOS et al., 2017). Both type I and III IFN recruits the JAK/STAT signaling via TYK2 (Tyrosine kinase 2) (MAJOROS et al., 2017). Earlier, enterocytes were shown to activated the JAK1-STAT3 signaling during LPS infection, which resulted in ameliorating the expressions of IL-1β and TNF-α cytokines.

Presently, TYK2 was downregulated in the LPS-infected cells pre-treated with n-3 PUFA. Notably, neither LPS nor n-3 PUFA were able to regulate the expression of TYK2 individually. Moreover two antiviral proteins, OAS2 (2'-5'-Oligoadenylate Synthetase 2) and OASL (2'-5'-Oligoadenylate Synthetase Like) that produced in IFN signaling (CHOI et al., 2015), was upregulated by n-3 PUFA in the uninfected cells. The expression of these genes was absent in the infected cells (with or without n-3 PUFA pre-treatment), suggesting the role of n-3 PUFA in establishing antimicrobial resistance against future pathogenic invasions. Also, in both normal and infected cells, n-3 PUFA downregulated the expression CXCL2 (C-X-C Motif Chemokine Ligand 2), while upregulated the CSF1 (Colony Stimulating Factor 1). LPS was unable to alter the expression of these genes in the IPEC-J2 cells. Notably, CXCL2 is a chemokine that facilitates monocyte and neutrophil infiltration (ROUAULT et al., 2013), whereas CSF1 controls the macrophage proliferation, differentiation and chemokine production (JONES et al., 2013). Recently, increased expression of CSF1 and IL10 was observed in the monocytes of inflammatory bowel disease (IBD) patients in remission, suggesting the possible beneficial effect of CSF1 in intestinal inflammation (NIETO et al., 2017).

5.3 Proteomic analysis of LPS-infected cells with or without n-3 PUFA pre-treatment

5.3.1 Differentially abundant proteins

Differential analysis was performed comparing two experimental groups at a time; in particular, (i) LPS *vs* control, (ii) n-3 PUFA *vs* control, and (iii) n-3 PUFA+LPS *vs* control. Each treatment group was composed of four biological replicates. The abundance ratio was log-transformed (log_2) and differential proteins were predicted using the t-test (background based) and adjusting the *p*-value (FDR) with the Benjamini-Hochberg method. In total, around 5000-5500 differential proteins were mapped for each of the treatment group. Only the proteins that had log_2 fold change (log_2FC) value less than or equal to -1.2 and greater than or equal to +1.2 ($log_2FC \geq 1.2$ or ≤ -1.2) with FDR < 0.05 cut-off were considered as statistically significant, differentially abundant proteins (DAPs). To visualize the distribution of DAPs between the three treatment groups, volcano plots were generated using Microsoft Excel. As shown in the volcano plot (Figure 22C), n-3 PUFA+LPS treatment induced the broadest proteomic changes in the IPEC-J2 cells followed by LPS (Figure 22A), whereas n-3 PUFA evoked the narrowest change (Figure 22B). This pattern is in accordance with the gene expression changes observed in the transcriptomic analysis of the present study (Figure 16).

After statistical filtering ($log_2FC \geq 1.2$ or ≤ -1.2, FDR ≤ 0.05), 33 DAPs (20 increased and 13 decreased) were identified in the IPEC-J2 cells post n-3 PUFA treatment (Figure 23B). In the LPS challenged cells, 85 DAPs (6 increased and 79 decreased) were detected (Figure 23B). Likewise, 88 DAPs (35 increased and 53 decreased) were detected in the LPS challenged cells pre-treated with n-3 PUFA (Figure 23B). Moreover n-3 PUFA uniquely regulated 25 DAPs in the IPEC-J2 cells, while shared 1 DAP with the LPS and 7 DAPs with the n-3 PUFA+LPS treatment groups. Likewise, LPS uniquely regulated 79 DAPs and shared 5 DAPs with the n-3 PUFA+LPS treatment. The n-3 PUFA+LPS treatment group uniquely regulated 76 DAPs. However, none of the proteins were in common between all of the three treatment groups (Figure 23A).

Figure 22 DAPs identified in the IPEC-J2 cells exposed to LPS, n-3 PUFA or n-3 PUFA+LPS

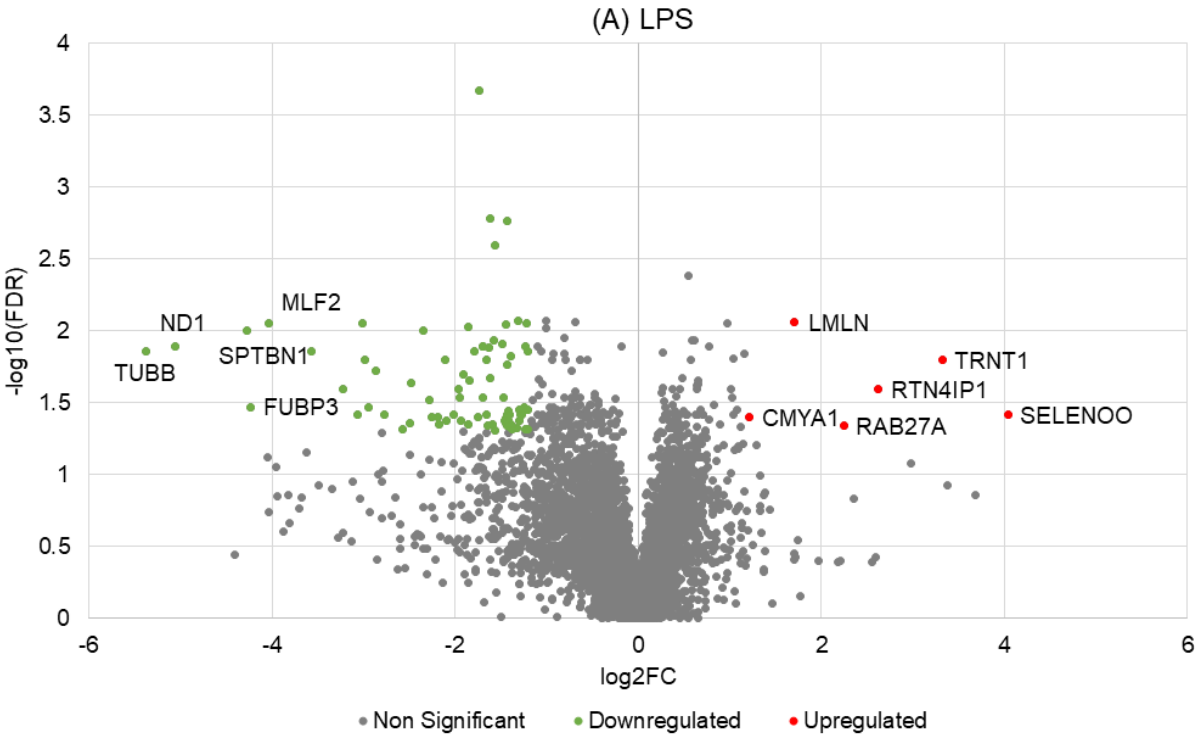

Volcano plot displaying the differentially abundant proteins (DAPs) identified in the porcine IPEC-J2 cells exposed to (A) LPS, (B) n-3 PUFA or (C) n-3 PUFA+LPS treatments. Red dots represent increased, green represents decreased and grey represents non-significant DAPs after statistical filtering ($log_2FC \geq 1.2$ or ≤ -1.2, adjusted p-value (FDR) ≤ 0.05).

Figure 23 Common and uniquely regulated DAPs between the treatment groups

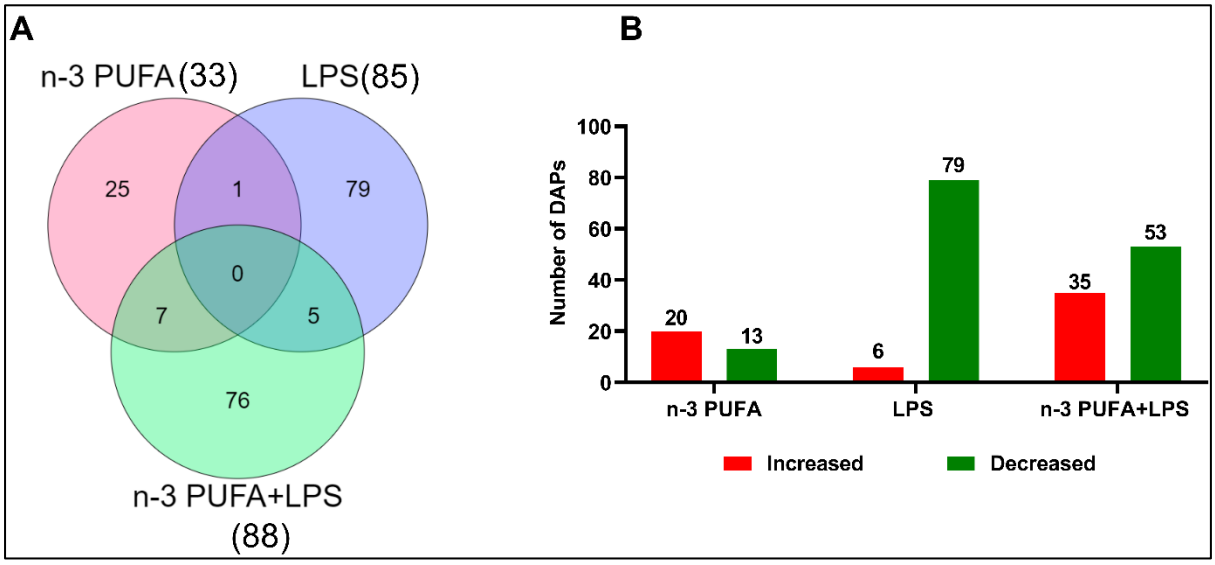

(A) Venn diagram shows the number of common and unique differentially abundant proteins (DAPs), and (B) bar chart shows the number of increased (red) and decreased (green) DAPs identified in the IPEC-J2 cells exposed to n-3 PUFA, LPS or n-3 PUFA+LPS treatments ($log_2FC \geq 1.2$ or ≤ -1.2, adjusted p-value (FDR) ≤ 0.05).

5.3.2 Gene Ontology annotation of biological process

After screening the differentially abundant proteins, the protein accession IDs were converted into gene names using the 'Retrieve/ID mapping' option in the UniProt database (https://www.uniprot.org/). Some proteins were unidentified, which was then compared against other species mainly Homo sapiens and Bos taurus for similar protein sequence related to the unknowns using the 'BLAST' search option in UniProt. Only the protein sequence that mapped 95% and above were selected, gene names retrieved and further added to the list of known proteins. These proteins were then subjected to the Gene Ontology (GO) annotation analysis. GO analysis provides information on the biological process in which the DAPs participate. GO analysis was performed using the open source, Generic Gene Ontology (GO) term finder web application (GoTERMFINDER, https://go.princeton.edu/cgi-bin/GOTermFinder) by comparing against the human database (GOA-Homo sapiens). In the outcome of GO analysis, LPS and n-3 PUFA+LPS treatment groups were mapped in different biological process following the statistical filtering of *p*-value < 0.01 after Bonferroni correction (Figure 24A, C) whereas, the n-3 PUFA group was mapped only without the filtering (*p*-value > 0.01) (Figure 24B). The DAPs of the n-3 PUFA group were also checked using other databases as STRING

and Gene Ontology Resource, however it did not map significantly to a specific biological process. Possibly, the information on the human database on the biological process related to these DAPs were not updated. Since this might be a novel information and to have a general idea on the biological process regulated by n-3 PUFA, the DAPs mapped without the filtering criteria was included for further analysis.

The GO analysis revealed the participation of DAPs in several cellular process in the present study. Particularly, in the LPS challenged cells, DAPs were mainly enriched in many metabolic processes as, 'small molecule metabolic process', 'carbohydrate derivative metabolic process', 'organic acid metabolic process' and 'oxoacid metabolic process', among others (Figure 24A). Similarly, LPS regulated several metabolic processes as 'small molecule metabolic process', 'lipid metabolic process', 'cellular lipid metabolic process' and 'fatty acid metabolic process' in the cells pre-treated with n-3 PUFA (Figure 24C). On the other hand, in the n-3 PUFA treatment group, the proteins were mapped in the biological process as 'anatomical structure development', cell differentiation', 'signaling' and 'lipid metabolic process' (Figure 24B).

Figure 24 GO biological process of the DAPs identified in IPEC-J2 cells

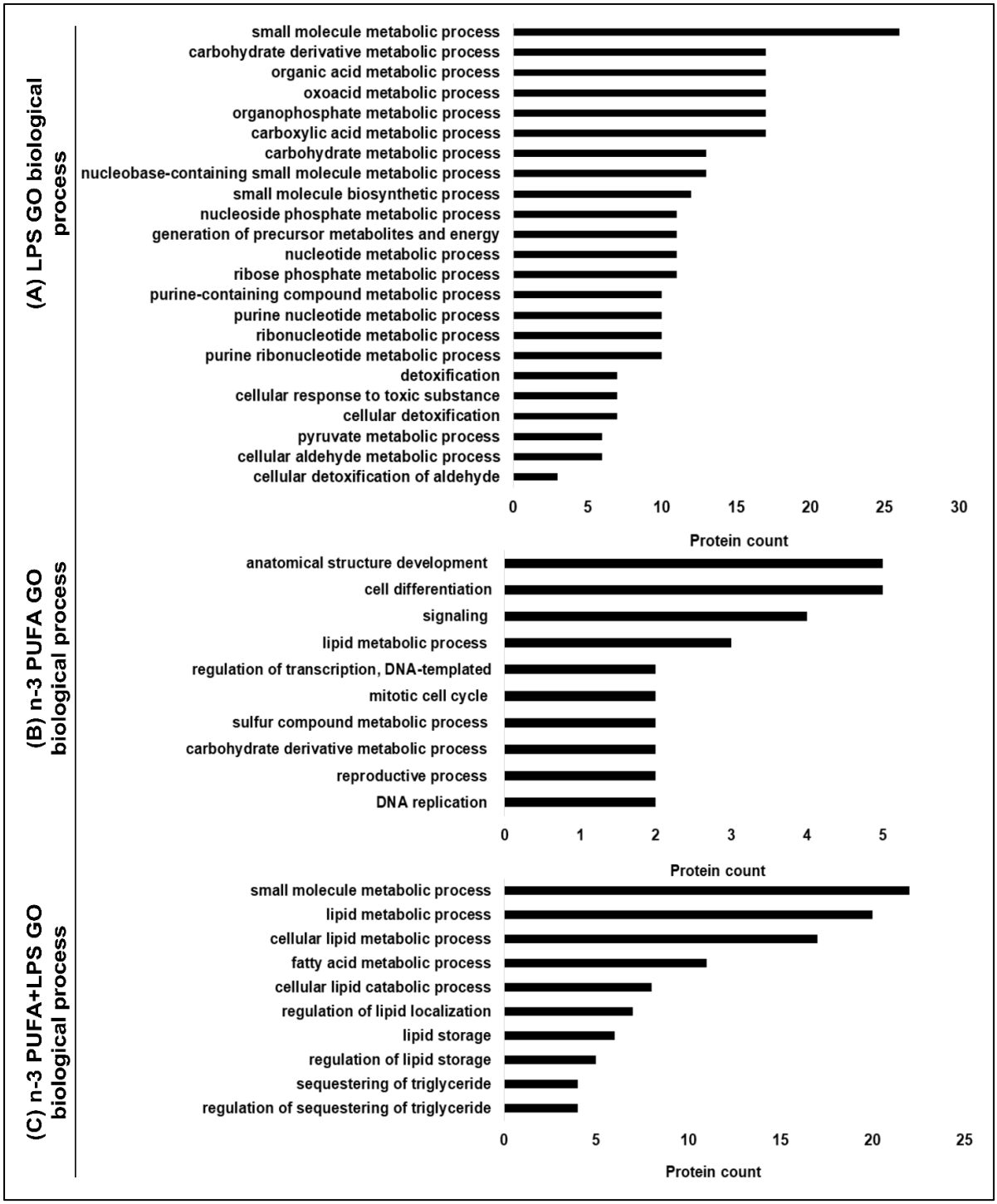

Gene Ontology (GO) of biological process identified in the porcine IPEC-J2 cells exposed to (A) LPS, (B) n-3 PUFA or (C) n-3 PUFA+LPS treatments. GO biological process was identified using the GoTERMFINDER application. Bonferroni corrected $p < 0.01$ for LPS and n-3 PUFA+LPS, $p > 0.01$ for n-3 PUFA.

5.3.3 Pathway enrichment analysis

The pathways modulated in the IPEC-J2 cells under different treatment conditions were evaluated using the open-source, Reactome pathway database. The outcome of the analysis revealed the enrichment of DAPs in several cellular pathways. For the analysis, only the pathways that satisfy the statistical filtering of $p < 0.05$ after correction with Benjamani-Hochberg method were considered. Further, the top ten highly regulated pathways in each treatment group were compared against every other treatment group (Figure 25A-C) to understand the dynamics of LPS infection in the presence and absence of n-3 PUFA pre-treatment. Notably, LPS challenge highly regulated the metabolic pathways of IPEC-J2 cells as 'Metabolism (R-HSA-1430729)', 'Metabolism of carbohydrates (R-HSA-71387)', 'Glucose metabolism (R-HSA-70326)'and 'Glycolysis (R-HSA-70171)' (Figure 25A). In the cells pre-treated with n-3 PUFA, the LPS regulated the metabolic pathways as, 'Metabolism of lipids (R-HSA-556833)', 'Cellular response to chemical stress (R-HSA-9711123)' and, 'Cytoprotection by HMOX1 (R-HSA-9707564)' (Figure 25C). On the other hand, in the cells treated with only n-3 PUFA, the pathways as, 'Transcriptional regulation by TP53 (R-HSA-3700989)', 'Regulation of cholesterol biosynthesis by SREBP (SREBF) (R-HSA-2426168)', and 'Activation of gene expression by SREBF (SREBP) (R-HAS-2426168)' were identified (Figure 25B).

Figure 25 Pathway enrichment analysis of the DAPs identified in the IPEC-J2 cells

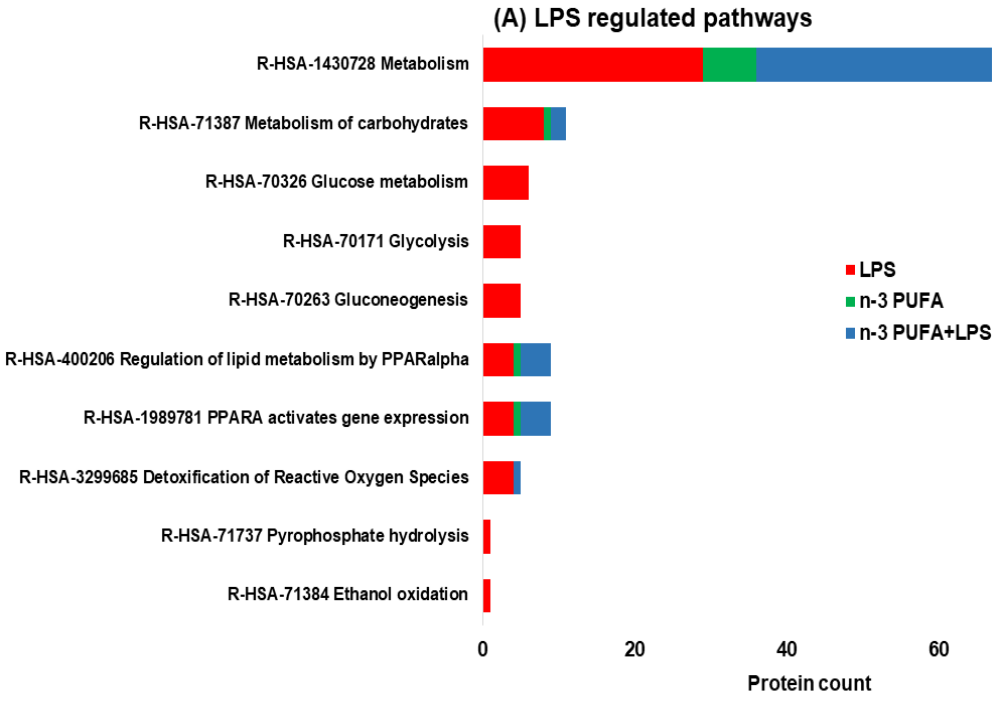

The top ten biological pathways regulated in the IPEC-J2 cells after treatment with (A) LPS, (B) n-3 PUFA or (C) n-3 PUFA+LPS. The pathways of each treatment group are compared with every other treatment group. All pathways filtered by $p < 0.05$ after Benjamani-Hochberg correction in the Reactome pathway database.

5.3.4 DAPs involved in the metabolic process

From the outcome of both the GO biological process and the Reactome pathway enrichment analysis, it can be seen that the metabolic process was highly regulated by LPS. Therefore, to understand and enumerate the role of n-3 PUFA in LPS infection, the DAPs involved in the 'Metabolism (R-HAS-1430729)' of Reactome pathway was evaluated. In total, 62 DAPs related to the metabolism was identified in which 12 were increased and 50 were decreased (Figure 26). Notably, in the LPS-induced cells, 30 DAPs were profoundly decreased. Pre-treatment of the cells with n-3 PUFA, prevented the LPS from reducing the abundance of all these proteins in the IPEC-J2 cells. Notably, the abundance (log_2FC) of ND1 (NADH ubiquinone oxidoreductase chain 1) in infected cells was -5.06, which raised to -2.31 when the cells were pre-treated with n-3 PUFA prior to the LPS challenge. Likewise, the abundance of DBI (Acyl-CoA-binding protein) in infected cells was -3.57, which was raised to -1.47 upon n-3 PUFA pre-treatment (Figure 26). The mitochondrial-encoded ND1 protein is a subunit of the NADH dehydrogenase enzyme, that participates in the mitochondrial respiratory chain to produce adenosine triphosphate (ATP) for energy (CARDOL et al., 2002). Whereas, the DBI is a multifunctional protein that involves in various process as fatty acid biosynthesis, regulation of intracellular level of acyl-CoA esters and provision of acyl-CoA for β-oxidation in the mitochondrial oxidative phosphorylation (OXPHOS) (BURTON et al., 2005). Recently, intravenous administration of DBI in mice, was reported to reduce the circulating glucose level, which in turn aggravated appetite in mice (PEDRO et al., 2019). In the cells treated with only n-3 PUFA, 8 DAPs were identified in which the abundance of PLIN2 (Perilipin 2) (log_2FC = 5.09) and EPHX1 (Epoxide hydrolase 1) (log_2FC = 2.81) were highly increased whereas, in a similar way the NUBPL (Nucleotide binding protein-like isoform A) (log_2FC = -4.23) and MVD (Diphosphomevalonate decarboxylase) (log_2FC = -2.69) enzymes were decreased (Figure 26). Among the n-3 PUFA regulated proteins, the MGLL (Monoglyceride Lipase), MVD and PLIN2 were also expressed in the infected cells when pre-treated with n-3 PUFA. Of note, n-3 PUFA profoundly increased the abundance of PLIN2 (log_2FC = 5.74) and MGLL (log_2FC = 1.43) proteins while, decreased the abundance of MVD (log_2FC = -2.6) protein in the infected cells.

Cells generally store excessive circulating triacylglycerols and cholesterol esters in lipid droplets for maintaining cellular lipid homeostasis and utilize it as energy source during starvations (AON et al., 2014). The protein PLIN2 belongs to the perilipin protein family, that

coats these intracellular lipid droplets (AON et al., 2014). Whereas, the MVD is a catalytic enzyme that supports the ATP-dependent decarboxylation of mevalonate 5-diphosphate in mevalonate pathway for cholesterol synthesis. Inhibition of the MVD enzyme was reported to reduce the cholesterol biosynthesis (VOYNOVA et al., 2008). The MGLL is a cytosolic serine hydrolase that converts the fatty acids into glycerol in the process of lipolysis (ZHANG et al., 2020).

Moreover, several DAPs were uniquely regulated (10 increased and 16 decreased) in the infected cells pre-treated with n-3 PUFA (Figure 26). Among these proteins, the HMOX1(Heme oxygenase 1) ($log_2FC = 3.24$) and ABHD5 (1-acylglycerol-3-phosphate O-acyltransferase) ($log_2FC = 2.14$) were significantly increased and in a similar way, the FADS4 (also known as SCD5) (Stearoyl-CoA Desaturase 5) ($log_2FC = -3.39$) and CAV1(Caveolin 1) ($log_2FC = -3.28$) proteins were decreased. Interestingly, the HMOX1 protein that involved in heme catabolism, is a key regulator of antioxidant/oxidant homeostasis (ARAUJO et al., 2012). Previously overexpression of HMOX1 was reported to exert cytoprotective properties as anti-inflammation, antioxidation and anti-apoptosis in vascular and ischemia reperfusion injuries (ARAUJO et al., 2012). On the other hand, the enzyme ABHD5 was reported to interact with the perilipins for regulating the lipolysis of triglycerides packed in lipid droplets (GRANNEMAN et al., 2009). Besides, the FADS4 (or SCD5) is a desaturase enzyme that mainly involved in cholesterol biosynthesis (IGAL et al., 2021) whereas, CAV1 is a plasma membrane protein that reported to participate in fatty acid and cholesterol trafficking in a lipoprotein chaperon complex (JASMIN et al., 2012).

Figure 26 DAPs related to the metabolism of IPEC-J2 cells

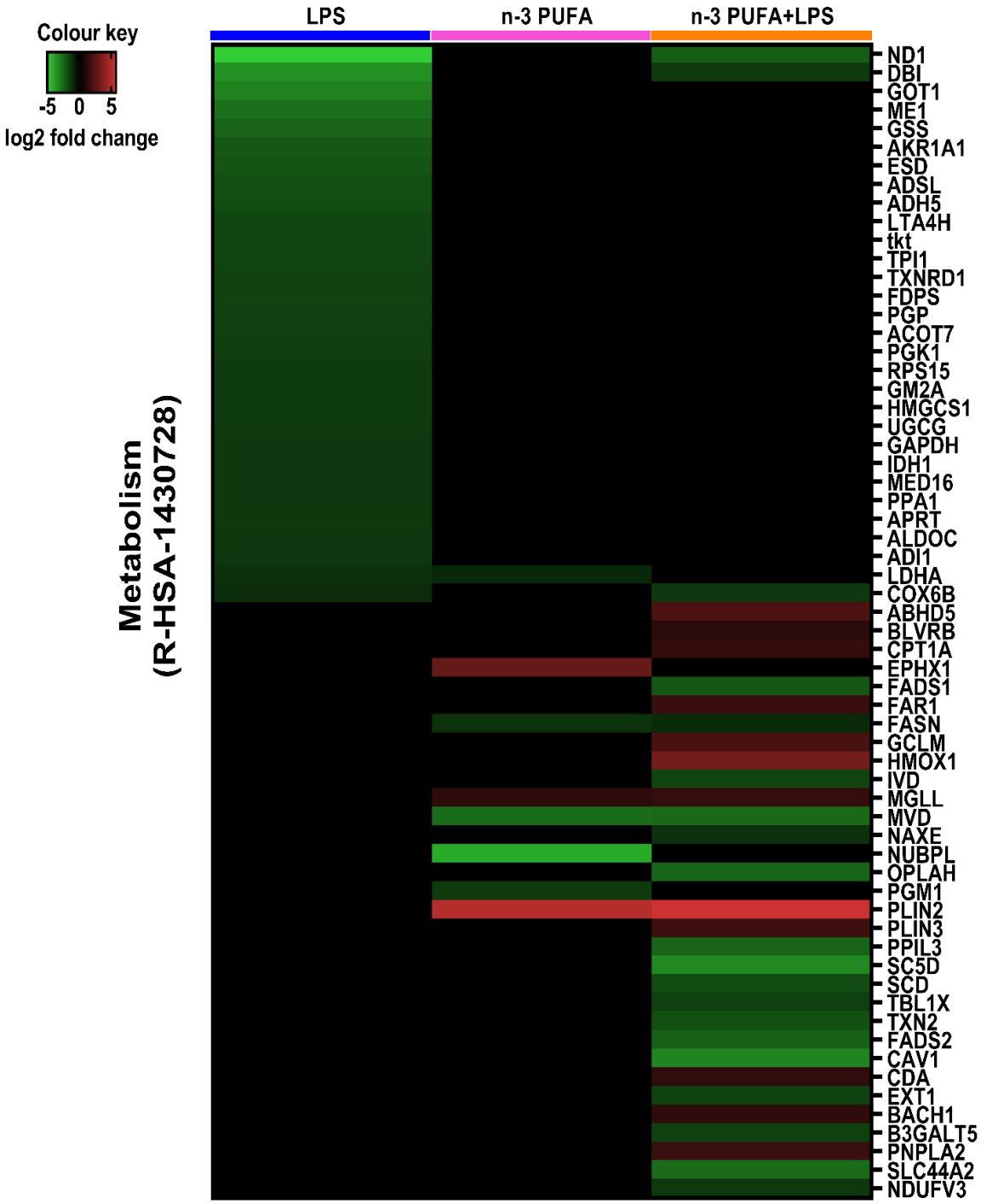

Heatmap displaying the differentially abundant proteins (DAPs) in the metabolic pathway of IPEC-J2 cells exposed to LPS, n-3 PUFA or n-3 PUFA+LPS treatments. Red denotes increased, green denotes decreased and black denotes no significant changes in the protein abundance. Scaling represents the range of log_2 fold change (log_2FC) values with $p < 0.05$ after Benjamani-Hochberg correction in the Reactome database.

5.3.5 Protein-protein interaction network of DAPs involved in the metabolic process

To understand the interaction between the proteins involved in metabolic pathway, the 62 DAPs identified related to the metabolism at different treatment conditions (LPS, n-3 PUFA and n-3 PUFA+LPS) were analysed using the STRING database (https://string-db.org/) (SZKLARCZYK et al., 2021). Study of protein-protein interaction (PPI) network will enable us to understand various events taking place inside the cells such as, the physical interaction between the proteins during the assembly of protein complexes, cell signaling and regulatory events, and cellular transportation at a given experimental condition (WESTERMARCK et al., 2013). The STRING database is a reservoir of information about the gene/gene products. It provides information about the physical interaction between the proteins in a PPI network and as well, tells its impact in the biological process (SZKLARCZYK et al., 2021). STRING also provides information by retrieving the data from other pathway databases as Kyoto Encyclopedia of Genes and Genomes (KEGG), Reactome, Gene Ontology Resources and Pfam. In the present study, the STRING analysis was performed with a high confidence score of 0.700 in order to investigate only the significantly regulated proteins. Confidence score represents the probability of identifying a PPI network related to a specific pathway. In the PPI network, proteins were represented as nodes whereas, the connecting links were represented as edges (lines). Only those proteins mapped in a network with p-value < 0.05 were considered while, the disconnected nodes were removed from the analysis.

Upon the analysis of 62 DAPs, 37 DAPs were significantly ($p < 0.05$) mapped in the PPI network for the set confidence (0.700) (Figure 27). Notably, all the LPS regulated DAPs, were closely mapped together in 9 pathways (Figure 27). In particular, 5 proteins that were decreased by LPS as the ALDOC (Fructose-bisphosphate aldolase C), TPI1 (Triosephosphate Isomerase 1), GADPH (Glyceraldehyde-3-phosphate dehydrogenase), PGK1 (Phosphoglycerate kinase 1), and LDHA (Lactate Dehydrogenase A) were mapped in the KEGG pathway, ‘Glycolysis/Gluconeogenesis (ssc00010)’ (Figure 27, 28). Glycolysis is the metabolic pathway of breaking down glucose into pyruvic acid to release energy, whereas gluconeogenesis is the process of glucose synthesis. Both these processes are interconvertably regulated according to cellular energy requirements (XIONG et al., 2011). Specifically, ALDOC participates in the initial steps of glycolysis, where it converts the fructose-1,6-biphosphate to dihydroxyacetone phosphate (DHAP). Then TPI1 converts the DHAP to glyceraldehyde 3-phosphate (G3P). Subsequently, GADPH catalyses the conversion of G3P

into 1,3-biphosphoglycerate which in turn, is converted to 3-phosphoglycerate by PGK1 (AKMAN et al., 2011; DANG, 2013). At the end of Glycolysis, pyruvate and ATP are produced. Pyruvate is further converted into LDHA in the cytoplasm or it enters into the mitochondria for oxidation via OXPHOS reaction (AKMAN et al., 2011; ZHENG, 2012). Presently, LPS decreased the abundance of LDHA in addition to the OXPHOS-related ND1 (NADH ubiquinone oxidoreductase chain 1), and COX6B (Cytochrome c oxidase) enzymes in the PPI network, 'Oxidative phosphorylation (ssc00190)'. Pre-treatment of the cells with n-3 PUFA, profoundly prevented the LPS from suppressing the ND1 abundance by 2.2-fold [ND1 log_2FC in LPS treatment group is -5.06, whereas in n-3 PUFA+LPS treatment group is -2.31]. Conversely, n-3 PUFA slightly enhanced the LPS-induced suppression on COX6B enzyme [COX6B log_2FC in LPS treatment group is -1.1, whereas in n-3 PUFA+LPS treatment group is -1.42]. In the same pathway, n-3 PUFA uniquely decreased the abundance of NDUFV3 (NADH ubiquinone oxidoreductase 9 kDa subunit) enzyme in the infected cells (Figure 27).

Generally, in the gluconeogenesis process, glucose is synthesized from the amino acids. Notably, the abundance of GAPDH, TKT (Transketolase), PGK1, TPI1, GOT1 (Aspartate aminotransferase), and IDH1 (Isocitrate dehydrogenase [NADP]) proteins that were mapped in the PPI network of 'Biosynthesis of amino acids (ssc01230)', was decreased by LPS (Figure 27). Notably, pre-treatment of the cells with n-3 PUFA, prevented the LPS from supressing the abundance of these proteins (Figure 27).

Further, 8 DAPs that were mapped in the Reactome pathway, 'Ribose phosphate metabolic process (GO:0019693)' as the GAPDH, ALDOC, TPI1, PGK1, TKT, ME1 (Malic Enzyme 1), ADSL (Adenylosuccinate lyase) and APRT (Adenine phosphoribosyltransferase), were decreased by LPS (Figure 27). Among these proteins, the TKT and ALDOC were also mapped in the 'Pentose phosphate pathway (ssc00030)'. Pentose phosphate pathway (PPP) is a parallel pathway to glycolysis, that produces nicotinamide adenine dinucleotide phosphate (NADPH) and precursors for nucleic acid and amino acid biosynthesis (CHO et al., 2018; GE et al., 2020). Intriguingly, n-3 PUFA pre-treatment prevented the LPS from decreasing the abundance all these proteins in the infected cells

Furthermore, the GSS (Glutathione synthetase), GCLM (Glutamate-cysteine ligase modifier subunit), and OPLAH (5-oxoprolinase, ATP hydrolysing) enzymes were identified in the PPI network of 'Glutathione metabolic process (GO:0006749)'. Glutathione (GSH) is an antioxidant that protects the cells from oxidative damage by scavenging excessive ROS

(KUEHNE et al., 2015). Challenge with LPS, significantly decreased the abundance of GSS enzyme in the IPEC-J2 cells (log_2FC = -1.93). Notably, pre-treatment with n-3 PUFA, prevented the reduction of GSS abundance in the infected cells. In addition, n-3 PUFA uniquely increased the abundance of GCLM while, decreased the OPLAH enzyme in infected cells. GCLM enzyme mainly catalyzes the synthesis of glutathione from L-cysteine and L-glutamate (CHEN et al., 2005) whereas, the OPLAH catalyzes the conversion of 5-oxo-L-proline to L-glutamate using ATP hydrolysis (WERF et al., 1971).

Moreover, in the n-3 PUFA+LPS treated cells, the abundance of 6 DAPs as the PLIN2, PLIN3 (Perilipin 3), PNPLA(Patatin Like Phospholipase Domain Containing)2, ABHD5, MGLL, and CPT1A (Carnitine O-palmitoyltransferase 1A) mapped in the 'Lipid metabolic process (GO:0006629), were enhanced (Figure 27, 29). Among these proteins, the PLIN2 abundance was also increased (log_2FC = 5.09) in the cells treated with only n-3 PUFA. As mentioned earlier, PLIN2 and PLIN3 are the perilipin proteins that encoats the intracellular lipid droplets (SZTALRYD et al., 2017). Whereas, PNPLA2 catalyzes the first step in triglyceride hydrolysis in adipocytes and as well that stored in lipid droplets (SZTALRYD and BRASAEMLE, 2017). PNPLA family of hydrolases acts a coactivator for ABDH5 in the hydrolysis process (SZTALRYD and BRASAEMLE, 2017). Of note, the protein ABHD2 was also increased in both n-3 PUFA and n-3 PUFA+LPS treatment groups, however it was unmapped in the PPI, nevertheless it exhibits similar hydrolase function as ABHD5. Further, the enzyme CPT1A facilitates the delivery of long chain fatty acids to mitochondria for β-oxidation (SEBASTIAN et al., 2009).

Further, the enzymes as FADS1 (Fatty Acid Desaturase 1), FADS2 (Fatty Acid Desaturase 2), FADS4 (or SCD5), and FADS5 (also known as SCD) (Stearoyl-CoA Desaturase) that were uniquely decreased in the n-3 PUFA+LPS treatment group, were also mapped in the PPI network of lipid metabolism (Figure 27,29). All these enzymes that belongs to the fatty acid desaturase (FADS) family, are involved in fatty acid synthesis. In particular, the FADS1 and FADS2 synthesizes highly unsaturated fatty acids (MATHIAS et al., 2014) whereas, the FADS4 and FADS5 synthesizes monounsaturated fatty acids (NTAMBI, 1995). None of these enzymes were regulated by LPS, however in the same pathway, it uniquely decreased the abundance of HMGCS1 (3-hydroxy-3-methylglutaryl coenzyme A synthase) and FDPS (Farnesyl pyrophosphate synthase) enzymes that involved in cholesterol biosynthesis.

Figure 27 Protein-protein interaction network of the DAPs identified in LPS-infected cells with or without n-3 PUFA pre-treatment

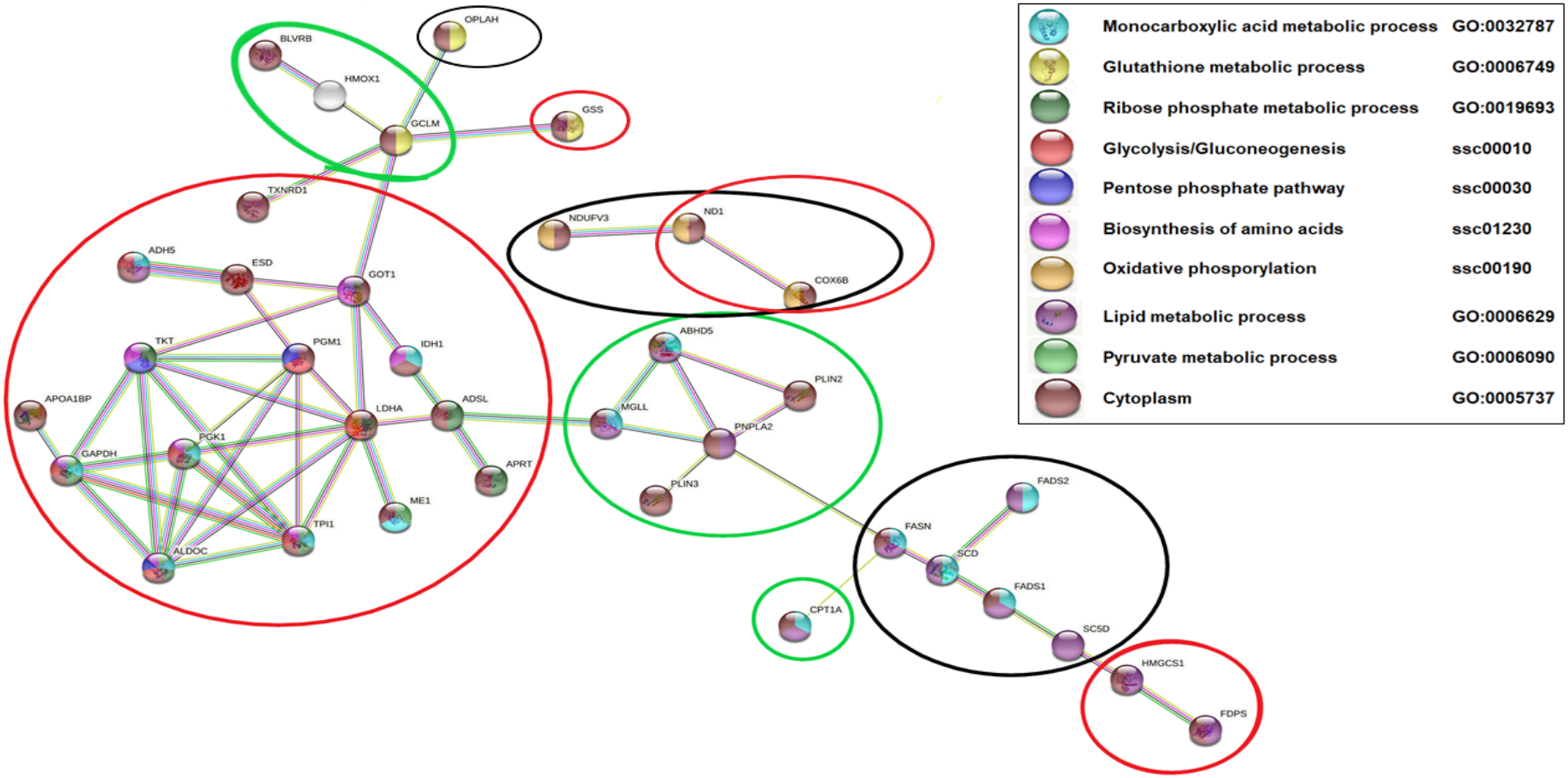

Differentially abundant proteins (DAPs) that were decreased in the LPS-infected cells were encircled in red. Green represents the increased, while black represents the decreased DAPs identified in the LPS-infected cells pre-treated with n-3 PUFA. Protein-protein network generated from STRING database.

Figure 28 KEGG analysis of Glycolysis/Gluconeogenesis pathway

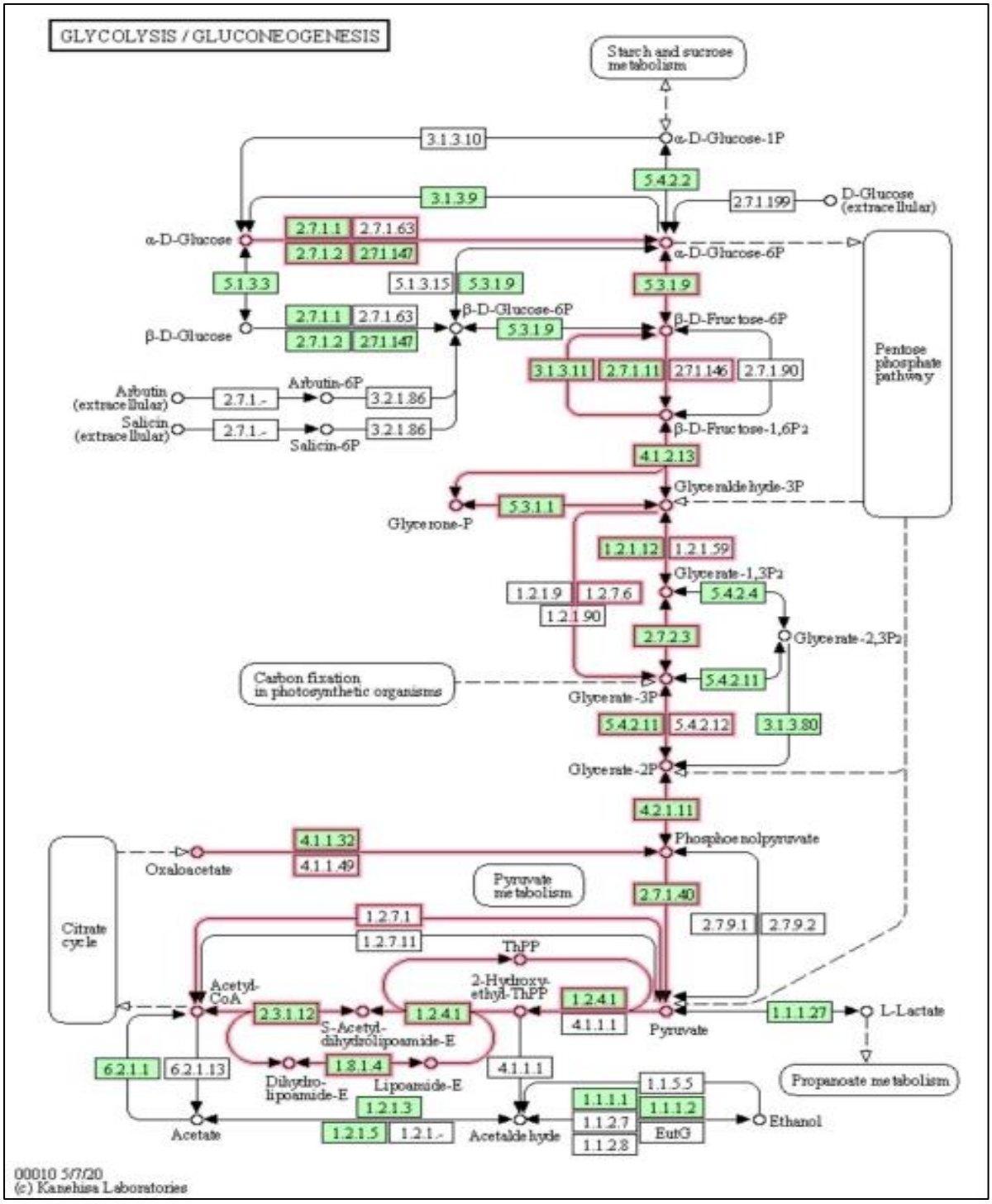

The lines highlighted in red within the glycolysis/gluconeogenesis pathway, were the LPS-inhibited regions in the IPEC-J2 cells.

Figure 29 KEGG analysis of Glycerolipid metabolic pathway

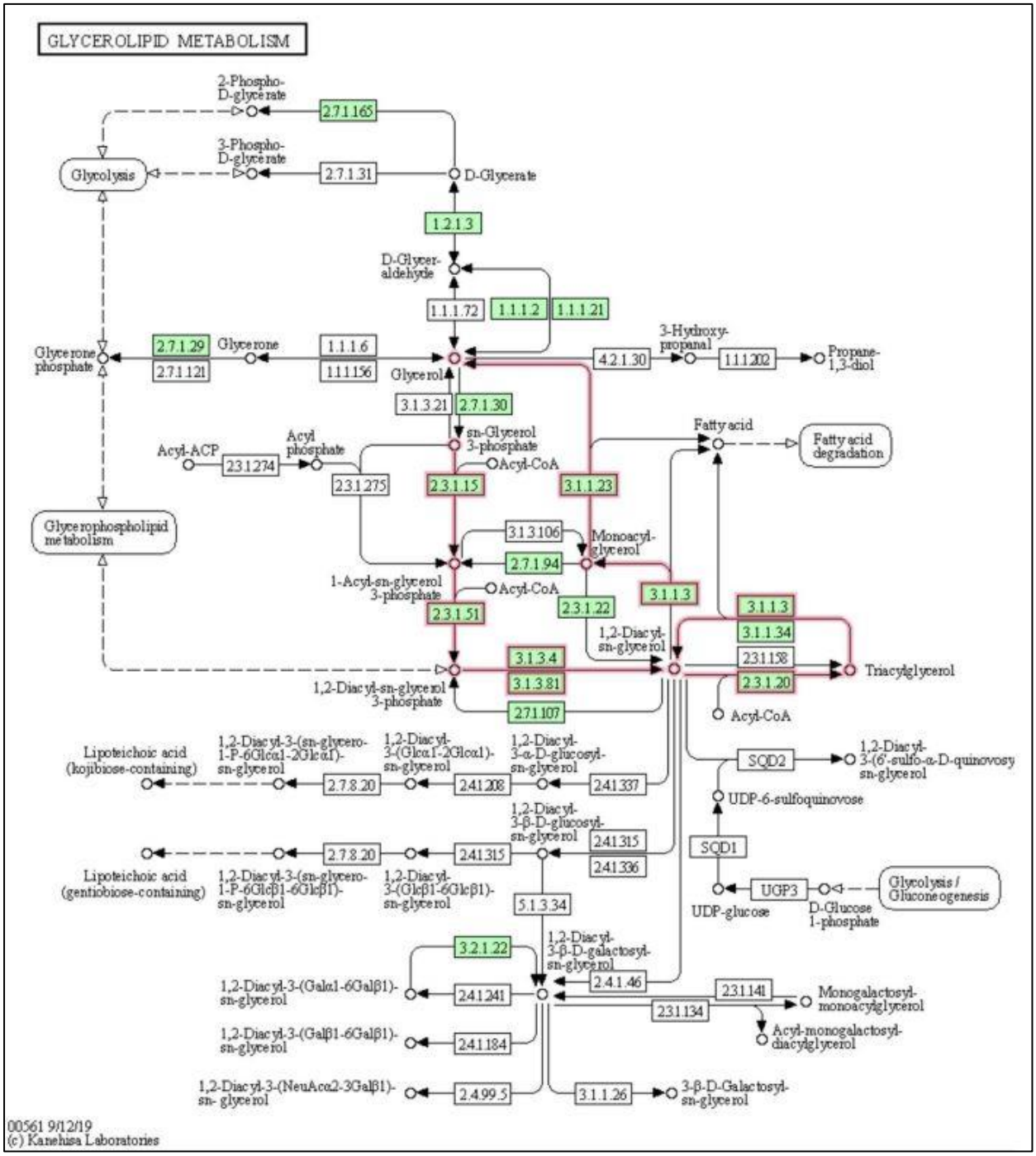

The lines highlighted in red within the glycerolipid metabolic pathway, were the uniquely activated regions in the LPS-infected cells when pre-treated with n-3 PUFA.

5.4 Preliminary results on establishment of chicken embryonic IEC culture

5.4.1 Characterization of the primary intestinal IECs in the mixed cell population

Microscopic image of the propagation of chicken embryonic intestinal cells isolated by mechanical tissue disruption method is shown in the figure 30. Among the mixed cells, some cells resembled the morphology of columnar-shaped intestinal epithelial cells (IECs) (yellow arrows) (Figure 30). The abundance of IECs in the mixed intestinal cell population was estimated by flow cytometry. As shown in the figure 31, cells stained with both E-cadherin (primary antibody) and Protein A-alexa 647 (secondary antibody) showed ~28% of the cells positive for IECs (Figure 31B, Q4-UR) compared to 1.7% in the control cells stained with only secondary antibody (Figure 31A, Q4-UR).

Figure 30 Morphological appearance of chicken embryonic IECs

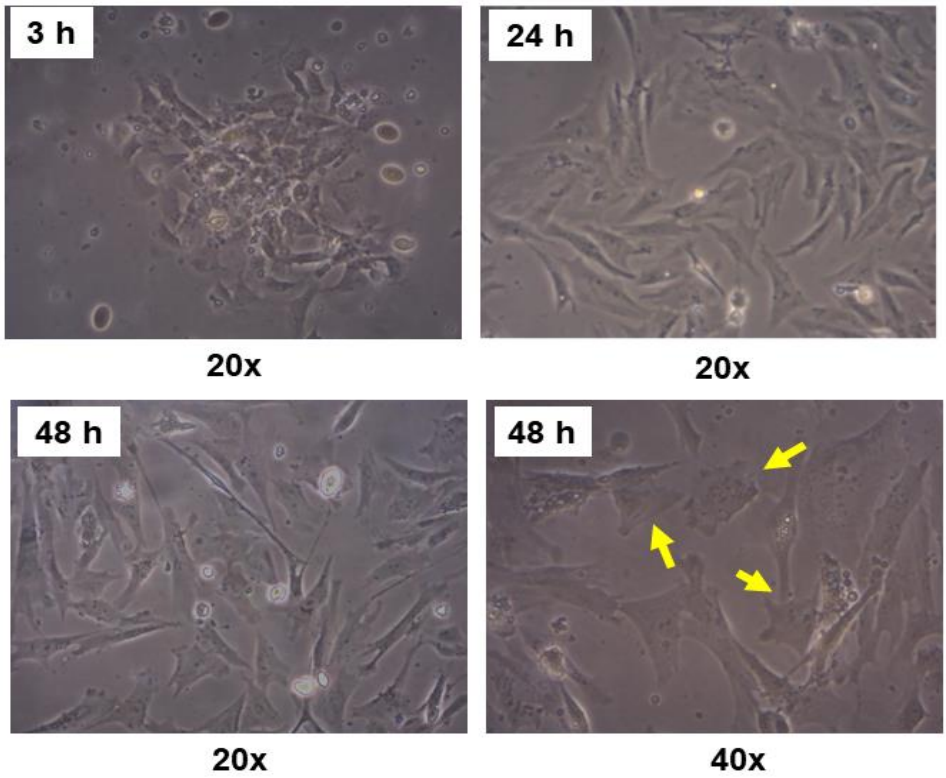

Chicken embryonic intestinal cells at different time points (3-48 h). The cells morphologically resembling the columnar-shaped intestinal epithelial cells are indicated in yellow arrows.

Figure 31 Flow cytometric analysis of chicken embryonic IECs

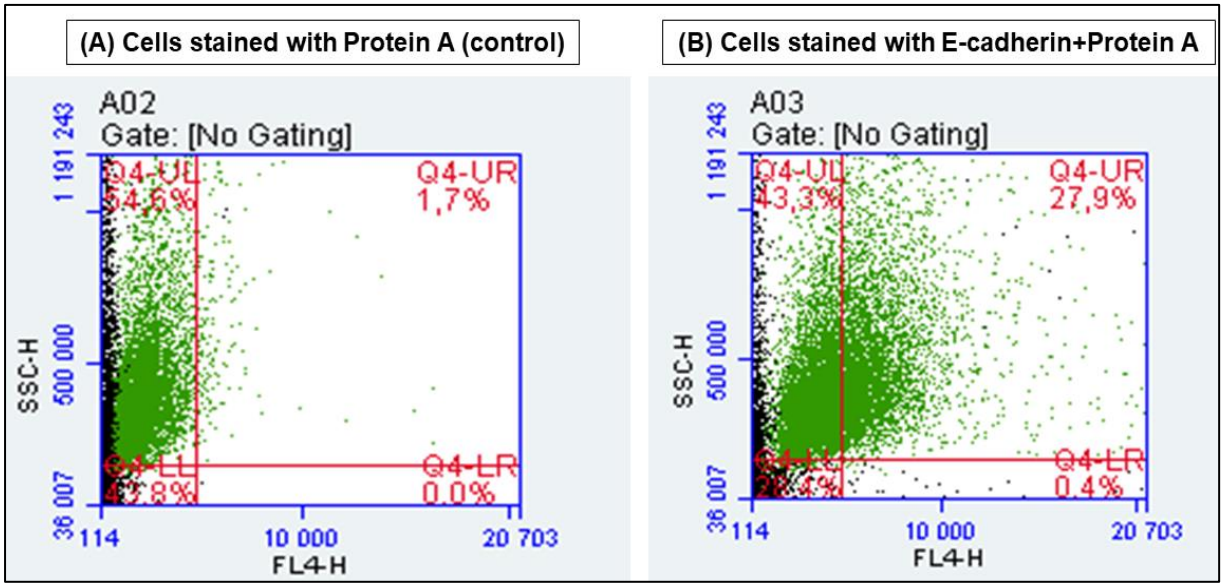

Characterization of intestinal epithelial cells (IECs) from the mixed intestinal cell population by flow cytometric analysis. (A) Cells stained with only Protein A-alexa 647 (control). (B) Cells stained with both primary E-cadherin antibody and secondary Protein A-alexa 647 antibody.

5.4.2 Dose-response effect of different test compounds on the IPEC-J2 cell viability

The dose-response curves of LPS in the chicken IECs and porcine IPEC-J2 cells are reported in the figure 32(A-B). 24 h exposure of LPS did not affect the chicken IEC viability until 12.5 µg/mL, but from 25-50 µg/mL it decreased in a dose-dependent manner (Figure 32A) compared to the control (0 µg/mL). On the other hand, the LPS concentration up to 25 µg/mL did not alter the viability of porcine IPEC-J2 cells, but from 50-100 µg/mL it decreased in a dose-dependent manner as before (Figure 32B). Subsequently, the LPS dose-response curves were used to estimate the IC_{50} values, which showed a value of 48.35 µg/mL for chicken IECs and 62.02 µg/mL for IPEC-J2 cells respectively. Based on these values, the LPS concentrations of 25 µg/mL for chicken IECs and 50 µg/mL for IPEC-J2 cells were chosen below the IC_{50} range for further nutrient assessment. As shown in the figure 32C, the concentrations of citrus pectin (CPn) from 0.2-1.3 mg/mL did not affect the viability of chicken IECs after 24 h of treatment. However, between 2.5-5 mg/mL, significantly (**p=0.0016, ****p < 0.0001) enhanced the cell viability (Figure 32C) compared to the control (0 mg/mL). On the contrary, CPn concentration between 0.2-5 mg/mL tested on IPEC-J2 cells for 24 h, did not show any significant impact on the viability compared to the control cells (Figure 32D). As a starting

point, a concentration range of 0-2.5 mg/mL CPn was chosen to study its cytoprotective effects against LPS challenge in both the cell model.

Figure 32 Dose-response of LPS and CPn in the chicken IECs and porcine IPEC-J2 cells

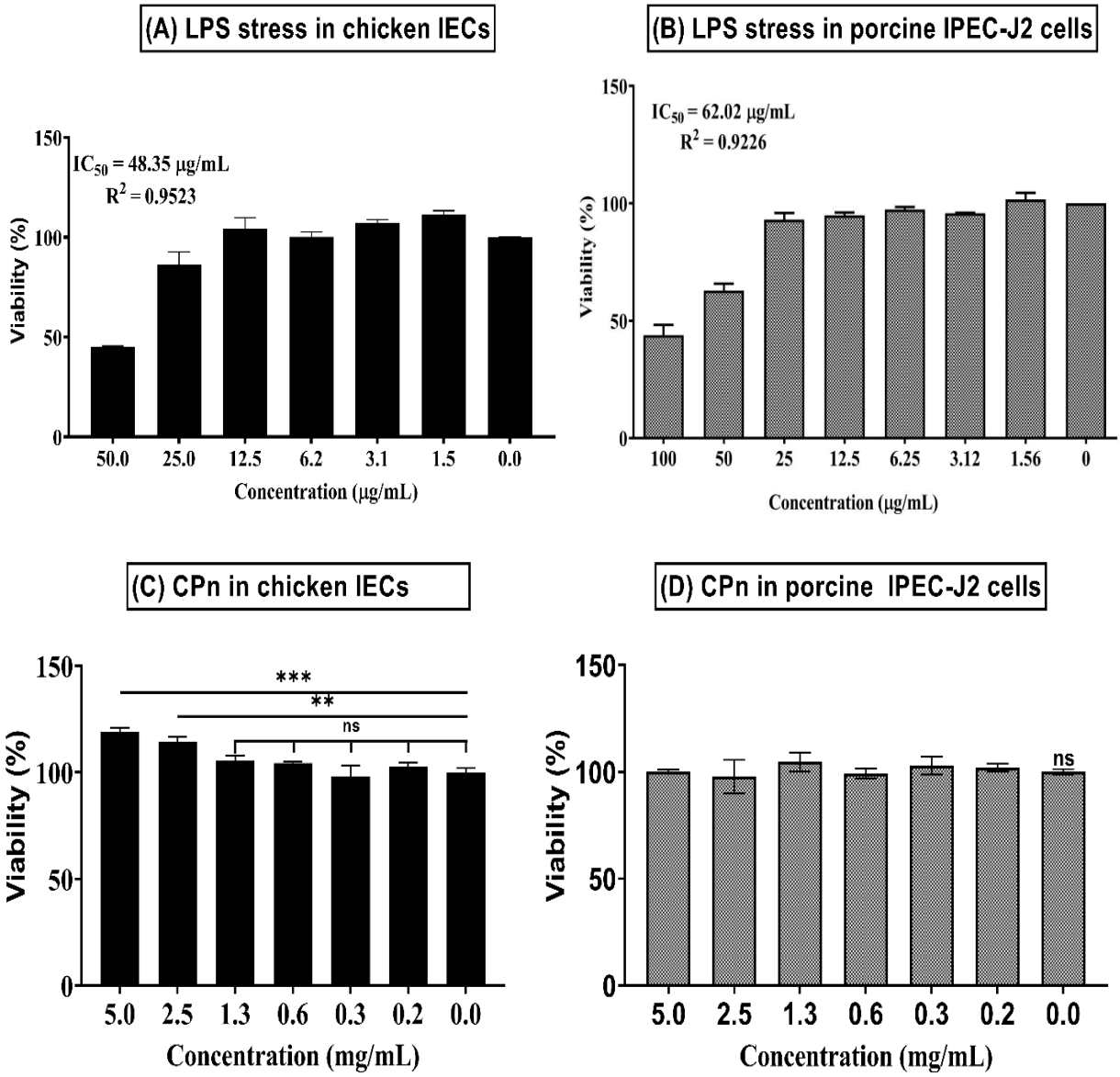

*Dose response study. LPS (0-50 or 100 µg/mL) in chicken intestinal epithelial cells (IECs) (A), and porcine IPEC-J2 cells (B) for 24 h. CPn (0-5 mg/mL) in chicken IECs (C), and IPEC-J2 cells (D) for 24 h. Data are presented as mean ± SEM. Each treatment compared with the control (0) for CPn treatments (n=3, one-way ANOVA with Dunnett's correction, **p=0.0016, ****p < 0.0001, ns=non-significant). For LPS challenge study, the 50% inhibitory concentrations (IC_{50}) were calculated by non-linear regression analysis, where R^2 represents the goodness of fit. LPS: Lipopolysaccharides; CPn: Citrus pectin.*

5.4.3 Viability effects of CPn on chicken IECs and porcine IPEC-J2 cells against LPS

Viability assay determines the mitochondrial activity of the cells based on its capability to reduce the tetrazolium salt in the assay buffer into colored formazan end-product. Pre-treatment of the IPEC-J2 cells with CPn, substantially increased the mitochondrial activity that damaged by the LPS. In particular, cells pre-treated with CPn (2.5, 0.6 or 0.15 mg/mL) exhibited similar viability as control after LPS stress compared to the LPS only treated cells (Figure 32F). Conversely, in the chicken IECs, none of the treatments significantly altered the viability compared to the control. However, visually a slight cytoprotective effect of CPn with increasing concentration was observed upon LPS challenge even though the data fell below significance (Figure 32E).

Figure 33 CPn impact on the viability of chicken IECs and porcine IPEC-J2 cells under LPS stress

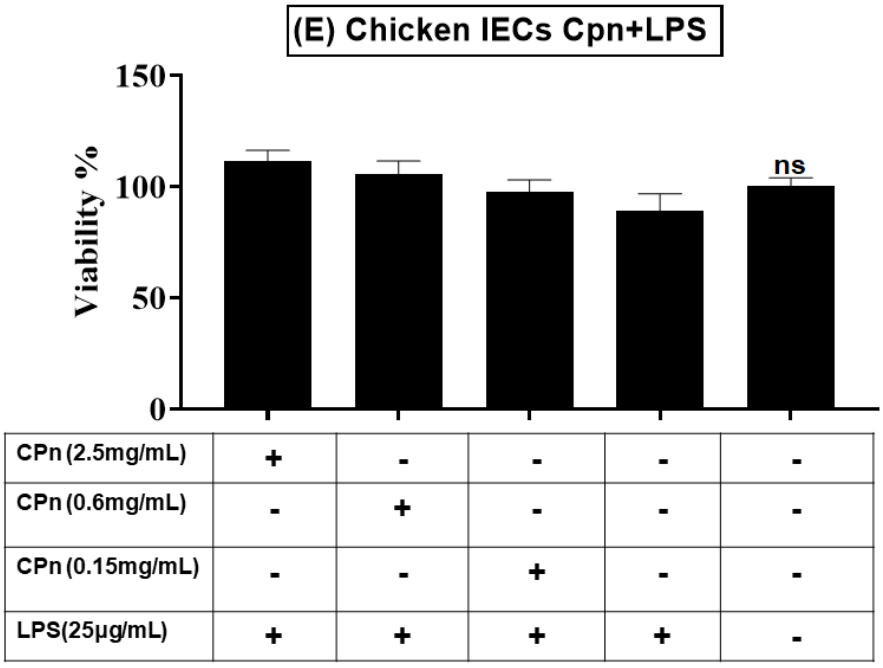

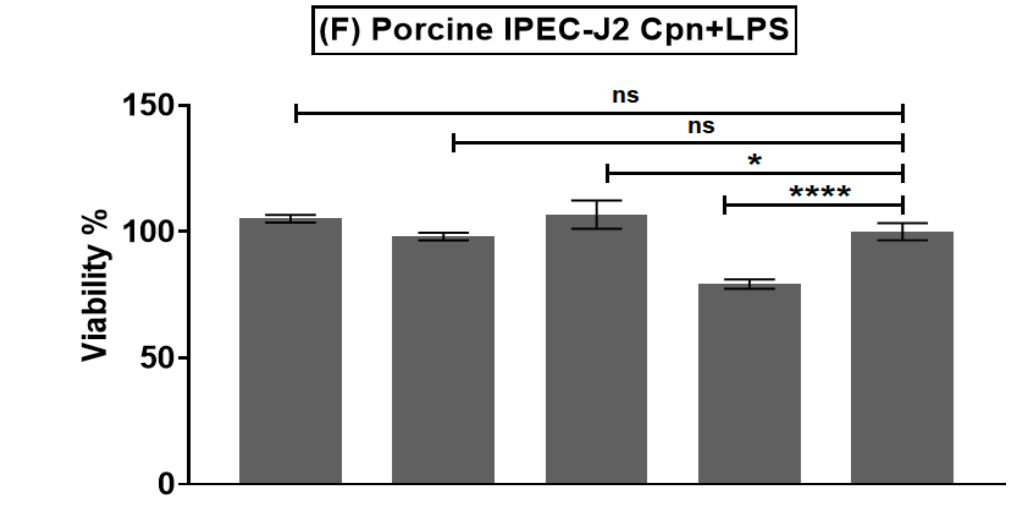

CPn (2.5mg/mL)	+	-	-	-	-
CPn (0.6mg/mL)	-	+	-	-	-
CPn (0.15mg/mL)	-	-	+	-	-
LPS(50µg/mL)	+	+	+	+	-

*Effects of citrus pectin (CPn) (2.5, 0.6 or 0.15 mg/mL) pre-treatment (24 h) on the viability of chicken IECs (E), and porcine IPEC-J2 cells (F) challenged by LPS (25 or 50 µg/mL) for 24 h. Each treatment compared against the control (0). Data are presented as mean ± SEM (n=3, one-way ANOVA with Dunnett's correction, *p <0.0101, **p=0.0066, ***p < 0.0008, ****p < 0.0001, ns=non-significant)*

6 Discussion

6.1 Establishment of IPEC-J2 cells as an *in vitro* inflammatory model of pig small intestinal barrier for assessment of n-3 PUFA effects

Supplementation of n-3 PUFAs in human and animal diet have been reported to combat a wide range of inflammatory diseases (AGAZZI et al., 2004; CALDER, 2010; MEYDANI et al., 1991; SAVOINI et al., 2016). Besides, n-3 PUFA was shown to improve reproductive performance in farm animals (MATEO et al., 2009; ROOKE et al., 2001; ROSSI et al., 2010). Till date, its molecular mechanism of action at the level of intestinal epithelial layer (IEL) under inflammatory and oxidative stress remains uncertain. Previously, the significance of cell models and different cell-based techniques available for nutrient evaluation has been described (CHELI and BALDI, 2011). In particular, the intestinal cells models are widely used for validation of bioactive nutrients in food/feed analysis (GIROMINI et al., 2015; GIROMINI et al., 2019a; GIROMINI et al., 2019c; LANGERHOLC et al., 2011). The anti-inflammatory properties of n-3 PUFA was earlier evaluated in colon cancer enterocyte model (KAIA MOBRATEN, 2013; YAN et al., 2017b). However, cancer cells exhibit altered signal transduction and metabolic pathways, which not a representative of normal cellular functions (HAKOMORI, 1996; LANGERHOLC et al., 2011; S.A. BROOKS et al., 2008). Here, we demonstrated the cytoprotective properties of n-3 PUFAs (EPA, DHA, and DHA:EPA) in the porcine IPEC-J2 enterocyte model using different cell-based assays and high-throughput bioinformatic analysis as transcriptomics and proteomics.

Firstly, the events of bacterial infection and oxidative stress are stimulated in IPEC-J2 cells by challenge against different stressors as LPS, H_2O_2 and DSS. LPS is a component of gram-negative bacterial cell wall, widely applied in IPEC-J2 and other cancer cell models to induce pro-inflammatory response by activating cell surface TLR2/4 receptors (DZIARSKI et al., 2001). H_2O_2 triggers inflammation mediated through oxidative stress by altering the subcellular DNA, proteins and lipids (BRIEGER et al., 2012). Besides, H_2O_2 is a commonly used chemical in IPEC-J2 cells for the characterization of dietary antioxidants (CHEN et al., 2018; VERGAUWEN et al., 2016; VERGAUWEN et al., 2015). While, the DSS is mainly used in animal models to induce leaky epithelial barrier for stimulation of inflammatory bowel disease (CHEN et al., 2019). This is the first report of DSS application in IPEC-J2 cells as previously it has been mainly used in cancer cells (ZHANG et al., 2018).

It is essential to choose an optimal concentration of the stressor that renders mild toxicity without completely killing or causing irrecoverable cell damage. To estimate this mild range, a dose-response study was performed by exposing the cells to increasing concentration of each stressor. Then, their corresponding IC_{50} values were calculated from the viability assay. Further, the concentrations for the evaluation of the nutrients under stress conditions were chosen below the IC_{50} range. We observed an LPS concentration of 50-100 µg/mL is required to decrease the IPEC-J2 cell viability after 24 h exposure. It was reported that, a high concentration of LPS between 100-300 µg/mL is required to decrease the viability of non-transformed IEC-18 cells after 24 h (LEE et al., 2017). Also, LPS concentrations between 1-10 µg/mL did not affect the IPEC-J2 viability until 24 h while, 10 µg/mL activated the expression of pro-inflammatory IL6 and IL8 mRNA (CHEN et al., 2019). Likewise, in another study, 10 µg/mL of LPS did not cause any cytotoxic effects in IPEC-J2 until 24 h while, 8 h of exposure activated the pro-inflammatory genes (YAN et al., 2017a). From these observations, in addition to the outcome of our present dose-response study, it is evident that the LPS concentrations as low as 0.1-10 µg/mL (1-24 h) is sufficient to activate the pro-inflammatory genes in IPEC-J2 cells, while, a high concentration above 25 µg/mL (24 h) is required to induce cytotoxicity. Therefore, an LPS concentration of 50 µg/mL below the IC_{50} range was chosen to investigate the n-3 PUFA effects on biological damage. Likewise, a concentration of 1 mM H_2O_2 (1 h) and 2 % DSS (24 h) was chosen to evaluate the n-3 PUFA effects on chemical damage. Similar concentrations of H_2O_2 were previously reported to reduce IPEC-J2 viability (CHEN et al., 2018; DZIARSKI et al., 2001). Also, 2% DSS was used to induce inflammation in the cancer cell models (ZHANG et al., 2018).

From the dose-response study of EPA and DHA, we identified that a low to moderate concentrations between 6.25-50 µM significantly increased the viability. Conversely, the concentrations ≥ 100 µM was toxic for the IPEC-J2 cells. As reported previously, EPA and/or DHA exhibits anti-proliferative effects in human cancer enterocytes as HT-29, Caco2 and DLD-1 at concentrations between 150-200 µM (GIADA GELSOMINO et al., 2013; HOSSAIN et al., 2009; PETTERSEN et al., 2016). On the contrary, this concentration range is toxic for the non-cancer IPEC-J2 cells as observed in the present dose-response study. In another study, cancer cells were reported to exhibit differential n-3 PUFA uptake and membrane distribution due to decreased activity of n-3 PUFA synthesizing Δ^5/Δ^6-desaturase enzymes over normal cells (D'ELISEO et al., 2016; MATHERS et al., 1975; MORTONA et al., 1979). In addition,

excessive production of reactive oxygen species (ROS) by cancer cells was reported to accelerate n-3 PUFA-mediated lipid peroxidation, making it more vulnerable to n-3 PUFA than normal cells (D'ELISEO and VELOTTI, 2016). These factors could explain the differential outcome of n-3 PUFA activity in cancer and non-cancer enterocytes. Therefore, it is essential to choose appropriate concentrations of n-3 PUFA in order to avoid membrane damage due to lipid peroxidation.

Presently, a concentration of 10 µM EPA/DHA was chosen as a starting point to determine its lowest cytoprotective dose in the IPEC-J2 cells. Furthermore, 10 µM was the minimal concentration reported to significantly exhibit anti-inflammation in macrophages (ALLAM-NDOUL et al., 2016) and 12.5–25 µg/mL in IPEC-1 cells (XIAO et al., 2020). Additionally, 10 µM lies in the range of n-3 PUFA concentrations that exhibited cell proliferative effects in our dose–response study. Generally, the marine and plant sources of n-3 PUFAs as the fish and linseed oil, comprises a mixture of short and long chain fatty acids with major proportions of EPA and DHA in different ratios. In order to mimic this natural co-existence of EPA and DHA, we mainly focused on the effects of DHA:EPA combination in 1:2 ratio as chosen from previous *in vivo* trials (ARTEMIS P. SIMOPOULOS, 2002; DESIRE´ E CAMUESCO et al., 2005; KRALIK et al., 2008).

Our experimental set-up enabled us to demonstrate that, the pre-treatment of IPEC-J2 cells with individual EPA (6.7 µM) and the combination DHA:EPA (1:2, 10 µM) significantly recovered the mitochondrial activity and membrane integrity from LPS damage as observed from viability and LDH assay. However, the individual DHA (3.3 µM) did not show any impact. Probably its concentration was too low unlike the EPA or the combination to confer cytoprotection. Additionally, post-LPS challenge, a 2-fold remarkable decline in apoptotic caspase-3/7 was witnessed for cells with DHA:EPA (1:2, 10µM) pre-treatment than those without. Both individual DHA (3.3 µM), EPA (6.7 µM) and the DHA:EPA (1:2, 10 µM) combination significantly recovered the mitochondrial activity from the DSS and H_2O_2 damage. Likewise, it increased the membrane integrity from H_2O_2 damage, while it was unable to do so for DSS. The concentration of DSS tested in the current study is speculated to have disrupted the IPEC-J2 cell membrane beyond the recovery potential of nutrients. Further, DHA:EPA (1:2, 10 µM) combination significantly reduced the caspase-3/7 activity induced by DSS. On the contrary, no caspase-3/7 activity observed for H_2O_2. Perhaps, acute challenge of H_2O_2 activated necrosis instead of apoptosis, which requires further analysis.

Generally, cellular apoptosis is activated by different pathways such as DNA fragmentation, electrolyte imbalance created during cell membrane damage or through certain proteins released by mitochondria. Possibly, increased intracellular mitochondrial activity and membrane integrity by EPA/DHA play a crucial role in preventing apoptosis of enterocytes during inflammatory and oxidative damage.

6.2 Transcriptomic profiling of LPS-infected cells with or without n-3 PUFA pre-treatment

From the confirmation of n-3 PUFA's cytoprotective properties in cell-based assays, we further proceeded with the bioinformatic analysis to comprehensively map the biological pathways underlying n-3 PUFA's activity under LPS stress. To this goal, the transcriptional dynamics of IPEC-J2 cells under different treatment conditions (n-3 PUFA, LPS and n-3 PUFA+LPS) were assessed by RNA sequencing (RNA-seq) technology. RNA-seq enables us to explore the global transcriptional changes occurring within the cells in a high degree of sensitivity and accuracy. As n-3 PUFA exhibited cell proliferative and anti-apoptotic activities in our MTT viability and apoptosis assays, the expression of genes related to these processes were searched in the transcriptome. Accordingly in the Gene Ontology (GO) analysis, we found the biological process related to both positive and negative regulation of enterocyte proliferation. Many genes were mapped in these processes, in particular the LPS upregulated IRF6 (KWA et al., 2014) and downregulated DLL4 genes posed particular interest as they participate in the Notch signaling pathway that regulates cell proliferation and turnover (THOO et al., 2019; ZENGIN et al., 2015b). When the cells were pre-treated with n-3 PUFA and then challenged by LPS, the genes as EPCAM, PHB2, PDCD10, and PPP1CA were uniquely downregulated, resulting in impaired cell proliferation. In particular, loss of EPCAM is associated with reduced cell proliferation and delayed cell cycle progression (SCHNELL et al., 2013). The overexpression of PDCD10 promotes cell proliferation via protein phosphatase (PP) activity (SUN et al., 2021). Whereas, the PPP1CA gene encodes one of the three subunits of serine/threonine PP1. These observations suggest that, LPS could have stimulated stress-induced cell proliferation via Notch signaling, which was ameliorated by n-3 PUFA through the same pathway or by controlling the PP activity in enterocytes.

When we searched for apoptosis-related genes, we found that LPS regulated TNFRSF9, IL2 and CD28 genes, are involved in controlling the T cell survival and apoptosis through TCR/CD3 signaling. In particular, IL2 induces apoptosis in activated T cells via Fas/TCR/CD3

signaling in a process called activation-induced cell death. Remarkably, pre-treatment of the cells with n-3 PUFA, inhibited the expression TNFRSF9 and IL2 genes in addition to the cell death receptor gene, FasL. Additionally, n-3 PUFA also exhibited anti-caspase-3/7 activity in the apoptosis assay. These outcomes suggest that, n-3 PUFA might have evaded LPS-induced apoptosis via the Fas/caspase inhibition in our present study.

Further, it is well known that the bacterial infection results in host-cell infiltration by the disruption of cell junction proteins. Interestingly, in the present study, LPS highly enhanced the gene expressions of adherens junction (AJs) proteins (CDC42SE1 and PARD6B) that regulates the formation of apical cell-cell junction and apical-basal polarization (NOLAN et al., 2008). In addition, LPS upregulated the ITGAV gene that controls the cell-ECM interactions and the ARR3 gene that involved in disassembly of cell-ECM interactions (BUCKLEY et al., 2018). Interestingly, n-3 PUFA pre-treatment promoted the LPS-induced upregulation of ARR3, CDC42SE1 and PARD6B genes. Also, n-3 PUFA uniquely upregulated the expression of cell junction genes as ITGB3, CLDN1 (TJ protein) and CDH11 (AJ protein) while, downregulated the GNAI2, EPHA4 and PPP1CA genes in the infected cells. ITGAV and ITGB3 genes activated in infected cells are the subunits of Alpha-v beta-3 ($\alpha_V\beta_3$) integrin receptors, that mediates the cell-ECM interactions (DESGROSELLIER and CHERESH, 2010). Earlier, scratch test in astrocytes induced localized activation of integrins followed by 4-fold increase in Cdc42 expression. Cdc42 then recruited Par6 and facilitated repolarization of migrating astrocytes (HENRIQUE, 2003). Also, overexpression of Par6 was reported to induce epithelial proliferation without affecting the cell polarity (NOLAN et al., 2008). The experimental outcome of astrocytes, suggest that, the ITGAV, CDC42SE1 and PARD6B genes are cordially expressed under stress conditions as witnessed in the present study. Moreover, the n-3 PUFA downregulated GNAI2 gene was reported to interact with claudin-5 (TJ protein) and knockdown of which, reduced the TJ resealing after a hyperosmotic shock in the brain endothelial cells (LUISSINT et al., 2012). Under distinct physiological conditions, the LPS upregulated ITGAV was reported to release ROS by engaging with the EGFR for cell survival and proliferation (KOZAK and TATE, 1982). When the cells were pre-treated with n-3 PUFA prior to LPS challenge, the expression of ATOX1 antioxidant gene was highly enhanced. Possibly, n-3 PUFA activated ATOX1 gene to counterbalance the LPS-mediated oxidative damage stimulated via ITGAV-EGFR interactions.

Also, in a previous study, overexpression of cadherin protein CDH11 in the AJs, induced ECM remodelling in the heart valves of mice with calcific aortic valve disease (SUNG et al., 2016). ECM remodelling is essential for the morphogenesis, development and maintenance of intestinal barrier. Dysregulation of this process can result in the progression of inflammation associated diseases and even cancer (BONNANS et al., 2014). Generally, overexpression of E-cadherin in the AJs, stimulates the biological process as formation of cell-cell junction, prevention of cell migration, proliferation and differentiation (BEAMISH et al., 2018). Whereas, loss of E-cadherin represents the process as cell junction damage, ECM remodelling and cell death. In the present study, CDH11 that was upregulated in the n-3 PUFA+LPS treatment group, is closely related to E-cadherin, suggest its role in re-formation of cell junctions. Additionally, E-cadherin-deficiency in intestinal epithelium also displayed the loss of CLDN1 as observed presently (BUCKLEY and TURNER, 2018).

Interestingly, cell junction genes (EPHA4, ADAM10, and NCK1) that participates in the Eph/Ephrin signaling-mediated axonal guidance has been modulated by n-3 PUFA. Axon guidance represents the formation, breaking, and remodelling of cell junction organization for developmental and maintenance process (BEAMISH et al., 2018). Eph proteins are the largest subfamily of receptor tyrosine kinases, that mediates the cell-cell signaling upon activation by Ephrin ligands. Eph/Ephrin signaling also plays a crucial role in activating the innate and adaptive immune cells (DARLING et al., 2019). Notably, EphA and EphB are the two groups of Eph receptors that are localized at the intercellular junctions. EphB signaling was reported to recruit ADAM10 and induce E-cadherin shedding at the AJs, leading to the disruption of cell junctions (MARETZKY et al., 2005). Conversely, EphA recruits NCK1 to inhibit ARF6 (ADP-ribosylation factor 6), a negative regulator of E-cadherin based cell-cell connections (BEAMISH et al., 2018). Presently, n-3 PUFA downregulated the expression of EPHA4 in both uninfected and infected cells while, upregulated the ADAM10 and NCK1 expressions only in the uninfected cells.

Altogether, outcome on the analysis of cell junction genes implies that, LPS infection could have controlling the genes of cell-cell/ECM interactions to facilitate the disassembly of cell junctions enabling cell proliferation. On the other hand, n-3 PUFA exhibited distinct behaviour in the normal and infection cells. In the absence of LPS stress, n-3 PUFA facilitated enterocyte proliferation and morphogenesis by dysregulating the cell-cell/ECM contacts via Eph/Ephrin signaling in the developmental process as axon guidance. Conversely, in the

infected cells, n-3 PUFA prevented the stress-induced proliferation by repairing the cell-cell/ECM disassembly induced by LPS.

TLR signaling plays a crucial in the host-innate immune system by recognizing specific pathogen-associated molecular patterns (PAMPs) on various microbes (AIN et al., 2020). In the present study, LPS infection mainly activated the TLR and its downstream NF-κB and MAPK signaling pathways. Major regulatory genes (CD14, LY96, TLR4, TLR8, MyD88, IRF6, NKAP and NFKB1) in this pathway has been significantly upregulated by LPS in the IPEC-J2 cells. Intriguingly, pre-treatment with n-3 PUFA (24 h), inhibited these genes in the infected cells and instead uniquely downregulated the expression of several genes (IRAK4, CHUK, IKBKG, NFKBIA and NFKBIZ) that involved in NF-κB activation. Further, the LPS-induced TLR signaling lead to the activation of many pro-inflammatory genes (IL1B, IL1B2, IL2, IL6, TNFSF8, IL6ST, IL18R1, IL1RL1, and TNFRSF9) that involved in cytokine production in the IPEC-J2 cells. Remarkably, n-3 PUFA inhibited the expression of all these LPS-activated pro-inflammatory genes in the infected cells.

6.3 Proteomic profiling of LPS-infected cells with or without n-3 PUFA pre-treatment

Given that our transcriptomics study confirmed the anti-inflammatory properties of n-3 PUFA, as a next step, we investigated the changes in proteomic profiles under same experimental conditions. Interestingly, proteomic study showed the enrichment of DAPs in the central carbon metabolic process such as glycolysis/gluconeogenesis, oxidative phosphorylation (OXPHOS) and pentose-phosphate pathway (PPP). Specifically, LPS decreased the abundance of several key regulatory enzymes (ALDOC, TPI1, GADPH, PGK1, and LDHA) that controls the catalysis of glycolysis/gluconeogenesis pathway (AKMAN et al., 2011; DANG, 2013). Glucose is the major source of energy for most cellular biochemical process. Glycolysis is the process that converts the glucose into pyruvate to produce ATP for basal energy requirements (AKMAN et al., 2011; ZHENG, 2012). Conversely, gluconeogenesis is the reverse process of glycolysis, that synthesizes glucose from the pyruvate. Gluconeogenesis mainly occurs during high energy demands or under starvations (XIONG et al., 2011). Both the glycolysis and gluconeogenesis are closely and reciprocally regulated in the cytosol as per cellular energy demands; therefore, they shared several catalytic enzymes as observed in our present study (XIONG et al., 2011). Apart from pyruvate, the gluconeogenesis also utilizes amino acids for glucose synthesis. In the present study, many

DAPs related to the biosynthesis of amino acids (GAPDH, TKT, PGK1, TPI1, GOT1, and IDH1) were also reduced by the LPS, which could have reflected on the gluconeogenesis regulation.

In anaerobic conditions, the pyruvate generated from glycolysis is converted into lactate by the action of lactate dehydrogenase (LDH) to produce ATP in the cell cytosol. Whereas, under aerobic conditions, the pyruvate enters into the mitochondria where it acts as a precursor for OXPHOS reaction (ZHENG, 2012). In OXPHOS, the pyruvate is oxidized into acetyl-CoA, which combines with oxaloacetic acid and enters into the citric acid cycle to produce ATP. Notably, glycolysis produces only 2 ATPs whereas, OXPHOS produces 36 ATPs, therefore 70% of the cellular energy requirement is supplied by mitochondrial OXPHOS (ZHENG, 2012). Presently, challenge with LPS, reduced the abundance of important enzymes related to both anaerobic glycolysis (LDHA enzyme) and as well aerobic glycolysis leading to OXPHOS (ND1, DBI, COX6B).

Pentose phosphate pathway (PPP) is a metabolic process that branches out in the very first step of glycolysis from the glucose-6-phosphate (G6P). PPP primarily produce ribose 5-phosphate (R5P) and NADPH as energy for cellular functions (CHO et al., 2018). R5P acts as a percussor for synthesis of nucleic acids, whereas NADH assist in the synthesis of fatty acids, sterols, nucleotides and non-essential amino acids (GE et al., 2020). More importantly, NADPH is involved in the maintenance of redox homeostasis (CHO et al., 2018). GSH is an important antioxidant peptide that scavenges excessive ROS to protect the cells from oxidative damage (KUEHNE et al., 2015). Generally, GSH exist in both reduced and oxidized forms. The NADPH that generated from PPP, enhances the cellular antioxidant defense by supporting the glutathione reductase (GR) to reduce the oxidized glutathione (GANSEMER et al., 2020).

Presently, LPS reduced the abundance of many proteins that involved in both PPP pathway (GAPDH, ALDOC, TPI1, PGK1, TKT, ME1, ADSL and APRT) and GSH defense system (GSS enzyme). On the other hand, when the cells were pre-treated with n-3 PUFA, the LPS-induced inhibition on these metabolic pathways were profoundly abrogated. Moreover, n-3 PUFA counterbalanced the disruption of GSH synthesis by enhancing the GCLM enzyme. GCLM is the first-rate limiting enzyme of GSH synthesis, where it produces GSH from the L-cysteine and L-glutamate (CHEN et al., 2005). Conversely, n-3 PUFA highly reduced the abundance of OPLAH enzyme in these cells that involved in the synthesis of L-glutamate. Specifically, OPLAH catalyzes the cleavage of 5-oxo-L-proline to L-glutamate at the expense

of ATP (WERF et al., 1971). Possibly, for energy conservation, n-3 PUFA enabled the cells to convert the available L-glutamate into GSH via GCLM instead for synthesising new precursor for GSH synthesis via OPLAH.

Furthermore, in the infected cells, n-3 PUFA reduced the fatty acid synthesis and instead, enhanced the breakdown of fat stored in the lipid droplets. In particular, the abundance of 4 enzymes (FADS1, FADS2, FADS4 and FADS5) that primarily involves in the synthesis of unsaturated fatty acids (IGAL and SINNER, 2021; MATHIAS et al., 2014; NTAMBI, 1995), were significantly reduced by n-3 PUFA in the infected cells. Cells generally stores excessive circulating triacylglycerol and cholesterol esters in the form of lipid droplets for maintaining cellular lipid homeostasis (AON et al., 2014; SZTALRYD and BRASAEMLE, 2017). During high energy demands or under starvations, cells utilize the fats stored in these lipid droplets as energy source (AON et al., 2014; SZTALRYD and BRASAEMLE, 2017). The perilipin proteins (PLIN2 and/or PLIN3) that were highly enhanced by n-3 PUFA with or without LPS infection in the present study, encoats these intracellular lipid droplets (SZTALRYD and BRASAEMLE, 2017). Additionally, in the LPS-infected cells, n-3 PUFA increased the abundance of important hydrolases (PNPLA2, ABDH5 and ABDH2) that breaks down these lipid droplets into free fatty acids and glycerols (AON et al., 2014; GRANNEMAN et al., 2009). Furthermore, in the cells treated with only n-3 PUFA, the abundance of PLIN2 and ABDH2 proteins were increased while, the PNPLA2 and ABDH5 proteins were not regulated. The PNPLA family of hydrolases was reported to act as a co-activator for ABDH5 to facilitate the lipolysis by interact with the perilipins (AON et al., 2014). This implies that, n-3 PUFA could have facilitated lipid storage by controlling the abundance of perilipin proteins under normal conditions. Conversely, during LPS infection, n-3 PUFA enhanced the abundance of PNPLA2 protein possibly to facilitate the breakdown of lipid droplets to balance the cellular energy requirements. The fatty acids released from the lipid droplets can further enter into the OXPHOS for oxidation to produce ATP for energy. Likewise, the glycerols released from these lipid droplets can enter the glycolysis pathway to produce ATP.

Interestingly, similar to LPS, n-3 PUFA also moderately decreased the abundance of key regulatory enzymes (ND1, COX6B and NDUFV3) of mitochondrial OXPHOS only under the LPS infection. In uninfected cells, n-3 PUFA did not regulate any of these proteins. Possibly, n-3 PUFA enabled the cells to utilize the fat stored in lipid droplets as fuel to stabilize the glycolysis that disrupted by LPS infection. Even though glycolysis produces only 2 ATP unlike

OXPHOS that produces much higher energy of 36 ATP, the former process is much rapid (SOTO-HEREDERO et al., 2020; ZHENG, 2012). In normal cells, OXPHOS is the major source of energy, however cancer cells shift this to glycolysis for fast energy requirements to cope up with the rapid cell division (ESCOLL et al., 2018; LUO et al., 2020). This process is described as Warburg effect (ESCOLL and BUCHRIESER, 2018). Possibly, under stress conditions such as in LPS infection, n-3 PUFA shifted the cellular energy metabolism from OXPHOS to glycolysis following the Warburg effect in order to rescue the cells from undergoing starvation.

Furthermore, in the proteomic analysis, many DAPs corresponding to the pro-inflammatory TLR/MyD88 signaling cascade was identified in accordance with the transcriptomic analysis. However, all these proteins fell below the significance level. Possibly, these proteins could have undergone degradation during the post-translational modification or in general might have been expressed in low abundance, reducing its overall intracellular concentrations. Another possible reason could be that the cells may have entered the later stages of inflammation. Several studies have reported that the infected cells acutely enhance the metabolic process, mainly glycolysis (Warburg-like effect) to support the energy required for recruitment of immune cells to the site of inflammation (ESCOLL and BUCHRIESER, 2018; SOTO-HEREDERO et al., 2020; WANG et al., 2020). Besides, infected cells also enhance the synthesis of fatty acids to support the production of lipid-based signaling mediators as pro-inflammatory cytokines and chemokines. During the later stages of inflammation, the infected cells were reported to dampen the glycolysis process and enhance OXPHOS in order to facilitate cellular homeostasis (ESCOLL and BUCHRIESER, 2018; SOTO-HEREDERO et al., 2020). Presently, we observed dysregulation of both glycolysis and OXPHOS along with other important metabolic process as amino acid and lipid biosynthesis, which suggest that the infected cells might have undergone starvation leading to cell death at the later stage of inflammation. These factors could have reflected on the shift from inflammatory proteins to metabolic stress related proteins in the present study. Similar to the outcome of our proteomic study, recently in another study using transcriptomics and metabolomics, *Salmonella typhimurium (S. typhimurium)* was shown to abrogate the glycolysis process and its associated insulin-signaling to impair the macrophage defense system (GUTIERREZ et al., 2021). The LPS tested in the present study was extracted from *S. typhimurium,* possibly this also the reason why we witnessed similar such outcome on the metabolism of IPEC-J2 cell. Control of immune

cell metabolism to escape the host defense system could be intrinsic to Salmonella infection. As the enterocytes are part of the immune system, Salmonella could have controlled the metabolism of IPEC-J2 cells which is an enterocyte model similar to macrophages. These observations need to be further verified.

6.4 Establishment of chicken embryonic primary IEC culture for citrus pectin characterization

Unlike other species, there are no previously established intestinal epithelial cell (IEC) models for poultry. Lack of specific cell models mainly limits the *in vitro* assessment of nutrition-based studies in poultry. Presently, in the preliminary experiment we have demonstrated the establishment of an *in vitro* of setup chicken intestinal epithelial cell (IEC) culture for characterization citrus pectin (CPn). Generally, animal cell models are established by isolating cells from the tissues of specific organs and culturing in artificial medium with solid support or in suspension culture system. Cell isolation is performed by different methods as enzymatic digestion or mechanical disruption of the tissues.

As a first step, we utilized the mechanical tissue disruption method to establish the primary intestinal cell culture. Further, the abundance of IECs in the mixed intestinal cell population was estimated by characterizing the presence of IEC-specific tight junction protein, E-cadherin by flow cytometric analysis. About ~28% of the total cells were stained positive for E-cadherin. Confirming the presence of IECs, we further, proceeded with a preliminary viability experiment to determine the suitability of the cell model for characterizing immunomodulatory properties of CPn against LPS stress for application in poultry nutrition. Presently, the porcine IPEC-J2 cells was utilized as a reference model for the nutrient assessment. In the dose-response study with both CPn and LPS, the chicken primary IECs were observed to respond in accordance with the IPEC-J2 cells. Moreover, CPn exhibited proliferative effects in the chicken IECs between 2.5-5 mg/mL concentrations on comparison against the control. The concentration below this range did not alter the cell viability. Conversely, CPn concentration tested (0.2-5 mg/mL) in the IPEC-J2 cells, exhibited similar viability as the control, possibly the CPn did not have any cytotoxic effect in the intestinal cells.

In the LPS dose-response study, the chicken IECs exhibited low IC_{50} value (48.35 μg/mL) compared to IPEC-J2 cells (62.02 μg/mL), suggesting its higher sensitivity towards inflammatory stimulus. Further, we chose an LPS concentration below the IC_{50} range of each

cell model (25 μg/mL for chicken IECs and 50 μg/mL for IPEC-J2 cells) and tested the cytoprotective effects of CPn against LPS stress (24 h). We observed that IPEC-J2 cells pre-treated with CPn (0.6-2.5 mg/mL, 24 h), were able to escape the damage induced by LPS compared to the cells without nutrient pre-treatment, confirming its cytoprotective effects. On the other hand, none of the treatments tested showed statistically significant effect in the chicken IEC viability, although a slight cytoprotective effect of CPn was observed visually, which needs to be verified with real-time PCR to notice small changes at gene level. The experiments need to be repeated in order to confirm the effects of CPn in enterocytes.

7 Conclusion

Omega-3 polyunsaturated fatty acids (n-3 PUFA) have been an important source of energy in mammalian diet since time immemorial. Moderate consumption of n-3 PUFA is vital for normal physiological functions, moreover at a specific level, it exhibits therapeutic benefits. Overwhelming studies have demonstrated their anti-inflammatory and antioxidative effects in different experimental models. Notably, intestinal epithelial layer (IEL) is the primary site of fatty acid absorption. However, till date, a comprehensive picture on the biological processes modulated by n-3 PUFA in intestinal barrier especially during infection remains elusive.

Presently, we tested the hypothesis that eicosapentaenoic acid (EPA), docosahexaenoic acid (DHA) and its 1:2 combination could counteract the inflammatory and oxidative damage induced by various stress factors such as lipopolysaccharides (LPS), dextran sodium sulphate (DSS) and hydrogen peroxide (H_2O_2) in an *in vitro* set-up using the non-transformed, porcine IPEC-J2 enterocyte model. Our study confirmed the proliferative effect of n-3 PUFA (EPA, DHA) in the enterocytes after 24 h of treatment, at low to moderate concentrations (6.25–50 μM). Additionally, we also confirmed that n-3 PUFA (24 h) pre-treatment was able to counteract the cell damage induced by LPS, DSS and H_2O_2 in the colorimetric/fluorimetric cell-based viability, lactate dehydrogenase (LDH) and apoptosis assays.

Further, the changes induced by n-3 PUFA (DHA:EPA, 1:2 ratio, 10 μM, 24 h) in the transcriptomic and proteomic profiles of IPEC-J2 cells under LPS stress conditions was explored. The outcome of the present bioinformatic analysis, have enabled us to shed important insights onto n-3 PUFA's mechanism of action (with or without LPS) in enterocytes.

Using transcriptomics analysis, we revealed that n-3 PUFA was able to promote anti-bacterial and anti-viral defense response in IPEC-J2 cells even in the absence of LPS challenge. This property of n-3 PUFA would be highly beneficial for the enterocytes to protect from future pathogenic challenges in the gut environment. Additionally, we showed that n-3 PUFA was able to stimulate enterocyte proliferation and morphogenesis by controlling the cell-signaling events of axon guidance in the normal cells. The biological process of axon guidance is fundamental for the cell developmental process as differentiation and organogenesis especially in highly regenerating intestinal epithelium. Disruption of this biological process could stimulate pathological conditions as chronic inflammation and even cancer.

Further, we showed that, n-3 PUFA pre-treatment was able to ameliorate the LPS-induced TLR/MyD88 signaling cascade and its downstream production of pro-inflammatory cytokines. Moreover, the property of n-3 PUFA in counteracting the LPS stress-induced proliferation via cell-junction disassembly and apoptosis via Fas/caspase signaling was demonstrated.

Unlike the outcome of transcriptomics study, interestingly, our proteomic analysis showed an increased metabolic damage, while decreased inflammation after LPS challenge. Early stages of inflammation exhibit active metabolism to support inflammatory cell infiltration and cytokine production. Whereas, at the later stages of inflammatory process, metabolism is dampened to either resolve the inflammatory process or to further stimulate cell starvation and death.

Presently, we showed the stimulation of cell starvation related to later stages of LPS inflammation in the proteomic analysis. This was confirmed based on the literature study and by observing the trend of metabolic stress related proteins to inflammatory proteins in the proteomic profile of infected cells. In particular, we showed the LPS-mediated dysregulation of central carbon metabolic process such as the glycolysis/gluconeogenesis, pentose phosphate pathway and mitochondrial oxidative phosphorylation. Moreover, glutathione antioxidant defense system and amino acid biosynthesis process were also shown to be disrupted by LPS.

We have demonstrated that pre-treatment of the cells with n-3 PUFA, was able to abolish the metabolic dysregulation stimulated by LPS. Additionally, n-3 PUFA was shown to re-establish the dysregulated metabolism, by utilizing the fat stored in lipid droplets to produce energy at faster rate via glycolysis/gluconeogenesis. Even though, oxidative phosphorylation produces much higher energy, it is a slow process, hence cells avoid this pathway during the recovery from starvation.

To conclude, our experimental model using the porcine IPEC-J2 cells, enabled us to decipher the distinct behaviour of n-3 PUFA in the normal and LPS-infected cells. In the normal enterocytes, n-3 PUFA enhanced proliferation, antimicrobial defense response and fatty acid storage in lipid droplets enabling lipid homeostasis. Conversely, in the enterocytes under LPS infection, n-3 PUFA abrogated stress-induced cell proliferation, apoptosis, cell-junction disassembly, inflammatory response, cytokine production and metabolic dysregulation. To the best of our knowledge, this is the first study to comprehensively report the biological pathways

regulated by n-3 PUFA in the normal intestinal barrier and under its infection, utilizing the state-of-the-art cell-based and omics technologies. Our present outcome could contribute to better understanding the molecular properties of n-3 PUFA in intestinal barrier for efficiently planning n-3 PUFA-based nutritional or therapeutic strategies in farm animal diets.

Additionally, in our preliminary study of establishing chicken *in vitro* intestinal epithelial cell (IEC) model, we have demonstrated a simple method to setup primary intestinal cell culture from chicken embryos. Besides, we have verified the response of chicken IECs to be in accordance with the reference porcine IPEC-J2 cell model with a dose-response study utilizing LPS and citrus pectin. Unlike the cost-intensive and complex enzymatic tissue digestion method of cell isolation, the straightforward mechanical method shown in the present study, can be utilized as a starting point to further purify and setup single cell population for omics studies underpinning poultry nutrition.

Figure 34 The graphical conclusion of the study

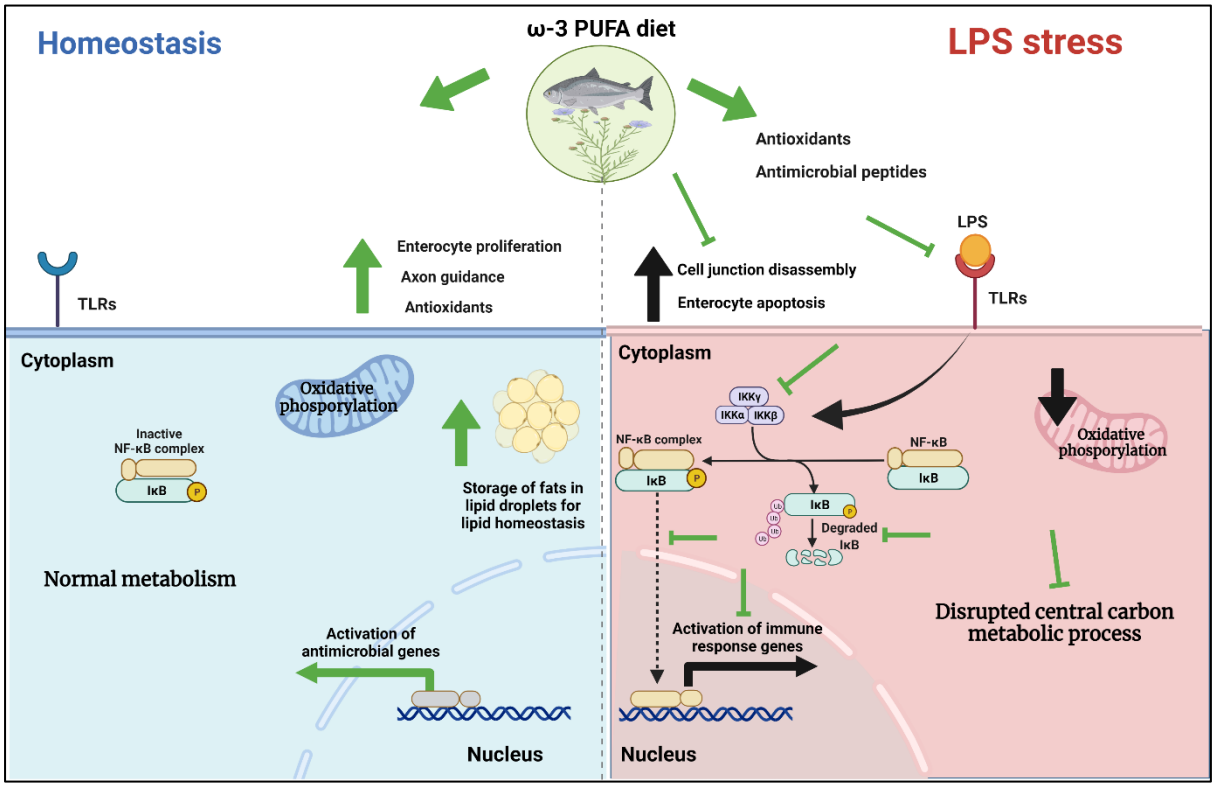

Black lines denote LPS regulated, while green denotes n-3 PUFA regulated molecular events

8 References

1. ABE, H., ISHIOKA, M., FUJITA, Y., et al. Yuzu (Citrus junos Tanaka) Peel Attenuates Dextran Sulfate Sodium-induced Murine Experimental Colitis. J Oleo Sci. 2018, 3, 67, 335-344.

2. AGAZZI, A., CATTANEO, D., DELL'ORTO, V., et al. Effect of administration of fish oil on aspects of cell-mediated immune response in periparturient dairy goats. Small Ruminant Research. 09214488, 2004, 1-3, 55, 77-83.

3. AIN, Q.U., BATOOL, M., CHOI, S. TLR4-Targeting Therapeutics: Structural Basis and Computer-Aided Drug Discovery Approaches. Molecules. 1420-3049, 2020, 3, 25.

4. AKISÜ, M., BAKA, M., COKER, I., et al. Effect of dietary n-3 fatty acids on hypoxia-induced necrotizing enterocolitis in young mice. n-3 fatty acids alter platelet-activating factor and leukotriene B4 production in the intestine. Biol Neonate. 1998, 1, 74, 31-38.

5. AKMAN, H.O., RAGHAVAN, A., CRAIGEN, W.J. Animal models of glycogen storage disorders. Prog Mol Biol Transl Sci. 2011, 100, 369-388.

6. ALLAIRE, J.M., CROWLEY, S.M., LAW, H.T., et al. The Intestinal Epithelium: Central Coordinator of Mucosal Immunity. Trends Immunol. 1471-4981, 2018, 9, 39, 677-696.

7. ALLAM-NDOUL, B., GUENARD, F., BARBIER, O., et al. Effect of n-3 fatty acids on the expression of inflammatory genes in THP-1 macrophages. Lipids Health Dis. 2016, 15, 69.

8. ALMALLAH, Y.Z., RICHARDSON, S., O'HANRAHAN, T., et al. Distal procto-colitis, natural cytotoxicity, and essential fatty acids. Am J Gastroenterol. 1998, 5, 93, 804-809.

9. ANADÓN, A., ARES, I., MARTÍNEZ-LARRAÑAGA, M.R., et al., 2019, Nutraceuticals Used as Antibacterial Alternatives in Animal Health and Disease, In: Nutraceuticals in Veterinary Medicine. pp. 315-343.

10. ANDREAKOS, E., SALAGIANNI, M., GALANI, I.E., et al. Interferon-lambdas: Front-Line Guardians of Immunity and Homeostasis in the Respiratory Tract. Front Immunol. 1664-3224, 2017, 8, 1232.

11. AON, M.A., BHATT, N., CORTASSA, S.C. Mitochondrial and cellular mechanisms for managing lipid excess. Front Physiol. 2014, 5, 282.

12. ARAUJO, J.A., ZHANG, M., YIN, F. Heme oxygenase-1, oxidation, inflammation, and atherosclerosis. Front Pharmacol. 1663-9812, 2012, 3, 119.

13. ARITA, M., YOSHIDA, M., HONG, S., et al. Resolvin E1, an endogenous lipid mediator derived from omega-3 eicosapentaenoic acid, protects against 2,4,6-trinitrobenzene sulfonic acid-induced colitis. Proc Natl Acad Sci U S A. 2005, 21, 102, 7671-7676.

14. ARTEMIS P. SIMOPOULOS, M., FACN. Omega-3 Fatty Acids in Inflammation and Autoimmune Diseases. Journal of the American College of Nutrition. 2002, 21, No. 6, 495–505.

15. AZAM, S., JAKARIA, M., KIM, I.S., et al. Regulation of Toll-Like Receptor (TLR) Signaling Pathway by Polyphenols in the Treatment of Age-Linked Neurodegenerative Diseases: Focus on TLR4 Signaling. Front Immunol. 2019, 10, 1000.

16. BALS, R. Epithelial antimicrobial peptides in host defense against infection. Respir Res. 2000, 3, 1, 141-150.
17. BARBOSA, D.S., CECCHINI, R., EL KADRI, M.Z., et al. Decreased oxidative stress in patients with ulcerative colitis supplemented with fish oil ω-3 fatty acids. Nutrition. 2003, 10, 19, 837-842.
18. BARONDES, S.H., COOPER, D.N., GITT, M.A., et al. Galectins. Structure and function of a large family of animal lectins. Journal of Biological Chemistry. 1994, 33, 269, 20807-20810.
19. BASSAGANYA-RIERA, J., HONTECILLAS, R. CLA and n-3 PUFA differentially modulate clinical activity and colonic PPAR-responsive gene expression in a pig model of experimental IBD. Clin Nutr. 2006, 3, 25, 454-465.
20. BEAMISH, I.V., HINCK, L., KENNEDY, T.E. Making Connections: Guidance Cues and Receptors at Nonneural Cell-Cell Junctions. Cold Spring Harb Perspect Biol. 2018, 11, 10.
21. BEUKEMA, M., FAAS, M.M., DE VOS, P. The effects of different dietary fiber pectin structures on the gastrointestinal immune barrier: impact via gut microbiota and direct effects on immune cells. Exp Mol Med. 2020, 9, 52, 1364-1376.
22. BEUKEMA, M., ISHISONO, K., DE WAARD, J., et al. Pectin limits epithelial barrier disruption by Citrobacter rodentium through anti-microbial effects. Food Funct. 2021, 2, 12, 881-891.
23. BIRD, J.K., CALDER, P.C., EGGERSDORFER, M. The Role of n-3 Long Chain Polyunsaturated Fatty Acids in Cardiovascular Disease Prevention, and Interactions with Statins. Nutrients. 2018, 6, 10.
24. BONNANS, C., CHOU, J., WERB, Z. Remodelling the extracellular matrix in development and disease. Nat Rev Mol Cell Biol. 014, 12, 15, 786-801.
25. BOUDRY, G., DOUARD, V., MOUROT, J., et al. Linseed oil in the maternal diet during gestation and lactation modifies fatty acid composition, mucosal architecture, and mast cell regulation of the ileal barrier in piglets. J Nutr. 2009, 6, 139, 1110-1117.
26. BRAHMBHATT, V., OLIVEIRA, M., BRIAND, M., et al. Protective effects of dietary EPA and DHA on ischemia-reperfusion-induced intestinal stress. J Nutr Biochem. 2013, 1, 24, 104-111.
27. BRIEGER, K., SCHIAVONE, S., MILLER, F.J., JR., et al. Reactive oxygen species: from health to disease. Swiss Med Wkly. 2012, 142, w13659.
28. BUCKLEY, A., TURNER, J.R. Cell Biology of Tight Junction Barrier Regulation and Mucosal Disease. Cold Spring Harb Perspect Biol. 2018, 1, 10.
29. BURTON, M., ROSE, T.M., FAERGEMAN, N.J., et al. Evolution of the acyl-CoA binding protein (ACBP). Biochem J. 2005, Pt 2, 392, 299-307.
30. CALDER, C.P. Immunoregulatory and anti-inflammatory effects of n-3 polyunsaturated fatty acids. Braz J Med Biol Res. 1998, 4, 31, 467-490.
31. CALDER, P.C. Polyunsaturated fatty acids and inflammatory processes: New twists in an old tale. Biochimie. 2009, 6, 91, 791-795.
32. CALDER, P.C. Omega-3 fatty acids and inflammatory processes. Nutrients. 2010, 3, 2, 355-374.
33. CALDER, P.C. Long-chain fatty acids and inflammation. Proc Nutr Soc. 2012, 2, 71, 284-289.
34. CALDER, P.C. Omega-3 polyunsaturated fatty acids and inflammatory processes: nutrition or pharmacology? Br J Clin Pharmacol. 2013, 3, 75, 645-662.
35. CALDER, P.C., GRIMBLE, R.F. Polyunsaturated fatty acids, inflammation and immunity. European Journal of Clinical Nutrition. 2002, 56, S12-S19.

36. CAMPBELL, J.M., FAHEY JR, G.C., LICHTENSTEIGER, C.A., et al. An enteral formula containing fish oil, indigestible oligosaccharides, gum arabic and antioxidants affects plasma and colonic phospholipid fatty acid and prostaglandin profiles in pigs. J Nutr. 1997, 1, 127, 137-145.
37. CAMPOS, F.G., WAITZBERG, D.L., HABR-GAMA, A., et al. Impact of parenteral n-3 fatty acids on experimental acute colitis. Br J Nutr. 2002, 87 Suppl 1, S83-88.
38. CAMUESCO, D., GALVEZ, J., NIETO, A., et al. Dietary olive oil supplemented with fish oil, rich in EPA and DHA (n-3) polyunsaturated fatty acids, attenuates colonic inflammation in rats with DSS-induced colitis. J Nutr. 2005, 4, 135, 687-694.
39. CAO, W., WANG, C., CHIN, Y., et al. DHA-phospholipids (DHA-PL) and EPA-phospholipids (EPA-PL) prevent intestinal dysfunction induced by chronic stress. Food Funct. 2019, 1, 10, 277-288.
40. CAPLAN, M.S., RUSSELL, T., XIAO, Y., et al. Effect of polyunsaturated fatty acid (PUFA) supplementation on intestinal inflammation and necrotizing enterocolitis (NEC) in a neonatal rat model. Pediatr Res. 2001, 5, 49, 647-652.
41. CARDOL, P., MATAGNE, R.F., REMACLE, C. Impact of Mutations Affecting ND Mitochondria-encoded Subunits on the Activity and Assembly of Complex I in Chlamydomonas. Implication for the Structural Organization of the Enzyme. Journal of Molecular Biology. 2002, 5, 319, 1211-1221.
42. CENCIC, A., CHINGWARU, W. The role of functional foods, nutraceuticals, and food supplements in intestinal health. Nutrients. 2010, 6, 2, 611-625.
43. CHASSAING, B., KUMAR, M., BAKER, M.T., et al. Mammalian gut immunity. Biomed J. 2014, 5, 37, 246-258.
44. CHELI, F., BALDI, A. Nutrition-based health: cell-based bioassays for food antioxidant activity evaluation. J Food Sci. 2011, 9, 76, R197-205.
45. CHEN, C.H., SHEU, M.T., CHEN, T.F., et al. Suppression of endotoxin-induced proinflammatory responses by citrus pectin through blocking LPS signaling pathways. Biochem Pharmacol. 2006, 8, 72, 1001-1009.
46. CHEN, Y., SHERTZER, H.G., SCHNEIDER, S.N., et al. Glutamate cysteine ligase catalysis: dependence on ATP and modifier subunit for regulation of tissue glutathione levels. J Biol Chem. 2005, 40, 280, 33766-33774.
47. CHEN, Z.-G., XU, G.-R., YUAN, Q.-L., et al. Quercetin inhibits porcine intestinal inflammation in vitro. Tropical Journal of Pharmaceutical Research. 2019, 10, 17.
48. CHEN, Z., YUAN, Q., XU, G., et al. Effects of Quercetin on Proliferation and H(2)O(2)-Induced Apoptosis of Intestinal Porcine Enterocyte Cells. Molecules. 2018, 8, 23.
49. CHO, E.S., CHA, Y.H., KIM, H.S., et al. The Pentose Phosphate Pathway as a Potential Target for Cancer Therapy. Biomol Ther (Seoul). 2018, 1, 26, 29-38.
50. CHOI, U.Y., KANG, J.S., HWANG, Y.S., et al. Oligoadenylate synthase-like (OASL) proteins: dual functions and associations with diseases. Exp Mol Med. 2015, 47, e144.
51. COURTS, F.L. Profiling of modified citrus pectin oligosaccharide transport across Caco-2 cell monolayers. PharmaNutrition. 2013, 1, 1, 22-31.
52. D'ELISEO, D., VELOTTI, F. Omega-3 Fatty Acids and Cancer Cell Cytotoxicity: Implications for Multi-Targeted Cancer Therapy. J Clin Med. 2016, 2, 5.
53. DANG, C.V. Role of aerobic glycolysis in genetically engineered mouse models of cancer. BMC Biology. 2013, 1, 11, 3.
54. DARLING, T.K., LAMB, T.J. Emerging Roles for Eph Receptors and Ephrin Ligands in Immunity. Front Immunol. 2019, 10, 1473.

55. DAS, U.N. Essential fatty acids: biochemistry, physiology and pathology. Biotechnol J. 2006, 4, 1, 420-439.
56. DATLER C, P.E., MAHUL-MELLIER AL, CHAISAKLERT W, HWANG MS, OSBORNE F, GRIMM S. CKMT1 regulates the mitochondrial permeability transition pore in a process that provides evidence for alternative forms of the complex. J Cell Sci. 2014, 8, 127, 1816-1828.
57. DE BOER, R.A., VAN DER VELDE, A.R., MUELLER, C., et al. Galectin-3: a modifiable risk factor in heart failure. Cardiovasc Drugs Ther. 2014, 3, 28, 237-246.
58. DE PAULA MENEZES BARBOSA, P., ROGGIA RUVIARO, A., MATEUS MARTINS, I., et al. Effect of enzymatic treatment of citrus by-products on bacterial growth, adhesion and cytokine production by Caco-2 cells. Food Funct. 2020, 10, 11, 8996-9009.
59. DEPOIL, D., FLEIRE, S., TREANOR, B.L., et al. CD19 is essential for B cell activation by promoting B cell receptor-antigen microcluster formation in response to membrane-bound ligand. Nat Immunol. 2008, 1, 9, 63-72.
60. DESALDELEER, C., FERRET-BERNARD, S., DE QUELEN, F., et al. Maternal 18:3n-3 favors piglet intestinal passage of LPS and promotes intestinal anti-inflammatory response to this bacterial ligand. J Nutr Biochem. 2014, 10, 25, 1090-1098.
61. DESGROSELLIER, J.S., CHERESH, D.A. Integrins in cancer: biological implications and therapeutic opportunities. Nat Rev Cancer. 2010, 1, 10, 9-22.
62. DESIRE´ E CAMUESCO, JULIO GA´ LVEZ, ANA NIETO, et al. Dietary Olive Oil Supplemented with Fish Oil, Rich in EPA and DHA (n-3) Polyunsaturated Fatty Acids, Attenuates Colonic Inflammation in Rats with DSS-Induced Colitis. American Society for Nutritional Sciences. 2005.
63. DIAZ-ALVAREZ, L., ORTEGA, E. The Many Roles of Galectin-3, a Multifaceted Molecule, in Innate Immune Responses against Pathogens. Mediators Inflamm. 2017, 2017, 9247574.
64. DICHI, I., FRENHANE, P., DICHI, J.B., et al. Comparison of omega-3 fatty acids and sulfasalazine in ulcerative colitis. Nutrition. 2000, 2, 16, 87-90.
65. DO PRADO, S.B.R., CASTRO-ALVES, V.C., FERREIRA, G.F., et al. Ingestion of Non-digestible Carbohydrates From Plant-Source Foods and Decreased Risk of Colorectal Cancer: A Review on the Biological Effects and the Mechanisms of Action. Front Nutr. 2019, 6, 72.
66. DRZYMAŁA-CZYŻ, S., BANASIEWICZ, T., TUBACKA, M., et al. Discrepancy between clinical and histological effects of DHA supplementation in a rat model of pouchitis. Folia Histochem Cytobiol. 2012, 1, 50, 125-129.
67. DZIARSKI, R., WANG, Q., MIYAKE, K., et al. MD-2 enables Toll-like receptor 2 (TLR2)-mediated responses to lipopolysaccharide and enhances TLR2-mediated responses to Gram-positive and Gram-negative bacteria and their cell wall components. J Immunol. 2001, 3, 166, 1938-1944.
68. EKÇI, B., KARABICAK, I., ATUKEREN, P., et al. The effect of omega-3 fatty acid and ascorbic acid on healing of ischemic colon anastomoses. Ann Ital Chir. 2011, 6, 82, 475-479.
69. ELIAZ, I., RAZ, A. Pleiotropic Effects of Modified Citrus Pectin. Nutrients. 2019, 11, 11.
70. EMPEY, L.R., JEWELL, L.D., GARG, M.L., et al. Fish oil-enriched diet is mucosal protective against acetic acid-induced colitis in rats. Canadian Journal of Physiology and Pharmacology. 1991, 4, 69, 480-487.

71. ESCOLL, P., BUCHRIESER, C. Metabolic reprogramming of host cells upon bacterial infection: Why shift to a Warburg-like metabolism? FEBS J. 2018, 12, 285, 2146-2160.
72. ESSER MT, D.R., KRISHNAMURTHY B, GULLO CA, GRAHAM MB, BRACIALE VL. IL-2 induces Fas ligand/Fas (CD95L/CD95) cytotoxicity in CD8+ and CD4+ T lymphocyte clones. J Immunol. 1997, 12, 158, 5612-5618.
73. FALGARONE, G., CHIOCCHIA, G., 2009, Chapter 8 Clusterin, In, pp. 139-170.
74. FAN, F., PODAR, K. The Role of AP-1 Transcription Factors in Plasma Cell Biology and Multiple Myeloma Pathophysiology. Cancers (Basel). 2021, 10, 13.
75. FAN, L., ZUO, S., TAN, H., et al. Preventive effects of pectin with various degrees of esterification on ulcerative colitis in mice. Food Funct. 2020, 4, 11, 2886-2897.
76. FUKUNAGA, T., SASAKI, M., ARAKI, Y., et al. Effects of the soluble fibre pectin on intestinal cell proliferation, fecal short chain fatty acid production and microbial population. Digestion. 2003, 1-2, 67, 42-49.
77. GALLEY, J.D., BESNER, G.E. The Therapeutic Potential of Breast Milk-Derived Extracellular Vesicles. Nutrients. 2020, 3, 12.
78. GANSEMER, E.R., MCCOMMIS, K.S., MARTINO, M., et al. NADPH and Glutathione Redox Link TCA Cycle Activity to Endoplasmic Reticulum Homeostasis. iScience. 2020, 5, 23, 101116.
79. GAO, H.N., REN, F.Z., WEN, P.C., et al. Yak milk-derived exosomal microRNAs regulate intestinal epithelial cells on proliferation in hypoxic environment. J Dairy Sci. 2021, 2, 104, 1291-1303.
80. GARCIA, A., CAYLA, X., GUERGNON, J., et al. Serine/threonine protein phosphatases PP1 and PP2A are key players in apoptosis. Biochimie. 2003, 8, 85, 721-726.
81. GAWISH, S.A.A., NOSSEIR, D.A., OMAR, N.M., et al. Protective Effect of Omega-3 Fatty Acids on 5-fluorouracil-induced Small Intestinal Damage in Rats: Histological and Histomorphometric Study. Trends in Medical Research. 2013, 2, 8, 36-62.
82. GE, T., YANG, J., ZHOU, S., et al. The Role of the Pentose Phosphate Pathway in Diabetes and Cancer. Front Endocrinol (Lausanne). 2020, 11, 365.
83. GENEROSO SDE, V., RODRIGUES, N.M., TRINDADE, L.M., et al. Dietary supplementation with omega-3 fatty acid attenuates 5-fluorouracil induced mucositis in mice. Lipids Health Dis. 2015, 14, 54.
84. GIADA GELSOMINO, PAOLA A CORSETTO, IVANA CAMPIA, et al. Omega 3 fatty acids chemosensitize multidrug resistant colon cancer cells by down-regulating cholesterol synthesis and altering detergent resistant membranes composition. Molecular Cancer. 2013, 12:137.
85. GIANNONI, E., BURICCHI, F., GRIMALDI, G., et al. Redox regulation of anoikis: reactive oxygen species as essential mediators of cell survival. Cell Death Differ. 2008, 5, 15, 867-878.
86. GIROMINI, C., BALDI, A., FUSI, E., et al. Effect of growth factors, estradiol 17-beta, and short chain fatty acids on the intestinal HT29-MTX cells : Growth factors and SCFAs effects on intestinal E12 cells. Cell Biol Toxicol. 2015, 4-5, 31, 199-209.
87. GIROMINI, C., CHELI, F., REBUCCI, R., et al. Invited review: Dairy proteins and bioactive peptides: Modeling digestion and the intestinal barrier. J Dairy Sci. 2019a, 2, 102, 929-942.
88. GIROMINI, C., CHELI, F., REBUCCI, R., et al. Invited review: Dairy proteins and bioactive peptides: Modeling digestion and the intestinal barrier. Journal of Dairy Science. 2019b, 2, 102, 929-942.

89. GIROMINI, C., LOVEGROVE, J.A., GIVENS, D.I., et al. In vitro-digested milk proteins: Evaluation of angiotensin-1-converting enzyme inhibitory and antioxidant activities, peptidomic profile, and mucin gene expression in HT29-MTX cells. J Dairy Sci. 2019c, 12, 102, 10760-10771.
90. GLOVER, L.E., LEE, J.S., COLGAN, S.P. Oxygen metabolism and barrier regulation in the intestinal mucosa. J Clin Invest. 2016, 10, 126, 3680-3688.
91. GONZALEZ, M.J., MIRANDA-MASSARI, J.R., DUCONGE, J., et al. Nutrigenomics, Metabolic Correction and Disease: The Restoration of Metabolism as a Regenerative Medicine Perspective. Journal of Restorative Medicine. 2015, 1, 4, 74-82.
92. GRANNEMAN, J.G., MOORE, H.P., KRISHNAMOORTHY, R., et al. Perilipin controls lipolysis by regulating the interactions of AB-hydrolase containing 5 (Abhd5) and adipose triglyceride lipase (Atgl). J Biol Chem. 2009, 50, 284, 34538-34544.
93. GRAW, S., CHAPPELL, K., WASHAM, C.L., et al. Multi-omics data integration considerations and study design for biological systems and disease. Mol Omics. 2021, 2, 17, 170-185.
94. GREENFIELD, S.M., GREEN, A.T., TEARE, J.P., et al. A randomized controlled study of evening primrose oil and fish oil in ulcerative colitis. Aliment Pharmacol Ther. 1993, 2, 7, 159-166.
95. GRIMSTAD, T., BERGE, R.K., BOHOV, P., et al. Salmon diet in patients with active ulcerative colitis reduced the simple clinical colitis activity index and increased the anti-inflammatory fatty acid index--a pilot study. Scand J Clin Lab Invest. 2011, 1, 71, 68-73.
96. GUO, W., KONG, E., MEYDANI, M. Dietary polyphenols, inflammation, and cancer. Nutr Cancer. 2009, 6, 61, 807-810.
97. GUSTAFSON, R.H., BOWEN, R.E. Antibiotic use in animal agriculture. Journal of Applied Microbiology. 1997, 531-541, 83.
98. GUTIERREZ, S., FISCHER, J., GANESAN, R., et al. Salmonella Typhimurium impairs glycolysis-mediated acidification of phagosomes to evade macrophage defense. PLoS Pathog. 2021, 9, 17, e1009943.
99. HAKOMORI, S.-I. Tumor Malignancy Defined by Aberrant Glycosylation and Sphingo(glyco)lipid Metabolism. Perspectives in Cancer Research. 1996, CANCER RESEARCH 56, 5309-5318.
100. HARA, A., NIWA, M., NOGUCHI, K., et al. Galectin-3 as a Next-Generation Biomarker for Detecting Early Stage of Various Diseases. Biomolecules. 2020, 3, 10.
101. HEKMATDOOST, A., WU, X., MORAMPUDI, V., et al. Dietary oils modify the host immune response and colonic tissue damage following Citrobacter rodentium infection in mice. Am J Physiol Gastrointest Liver Physiol. 2013, 10, 304, G917-928.
102. HENRIQUE, D. Cell polarity: the ups and downs of the Par6/aPKC complex. Current Opinion in Genetics & Development. 2003, 4, 13, 341-350.
103. HILLIER, K., JEWELL, R., DORRELL, L., et al. Incorporation of fatty acids from fish oil and olive oil into colonic mucosal lipids and effects upon eicosanoid synthesis in inflammatory bowel disease. Gut. 1991, 10, 32, 1151-1155.
104. HORBER, S., HILDEBRAND, D.G., LIEB, W.S., et al. The Atypical Inhibitor of NF-kappaB, IkappaBzeta, Controls Macrophage Interleukin-10 Expression. J Biol Chem. 2016, 24, 291, 12851-12861.
105. HOSSAIN, Z., HOSOKAWA, M., TAKAHASHI, K. Growth inhibition and induction of apoptosis of colon cancer cell lines by applying marine phospholipid. Nutr Cancer. 2009, 1, 61, 123-130.

106. HSU, Y.L., SHI, S.F., WU, W.L., et al. Protective roles of interferon-induced protein with tetratricopeptide repeats 3 (IFIT3) in dengue virus infection of human lung epithelial cells. PLoS One. 2013, 11, 8, e79518.
107. IBRAHIM, A., AZIZ, M., HASSAN, A., et al. Dietary alpha-linolenic acid-rich formula reduces adhesion molecules in rats with experimental colitis. Nutrition. 2012, 7-8, 28, 799-802.
108. IGAL, R.A., SINNER, D.I. Stearoyl-CoA desaturase 5 (SCD5), a Delta-9 fatty acyl desaturase in search of a function. Biochim Biophys Acta Mol Cell Biol Lipids. 2021, 1, 1866, 158840.
109. INAGAKI-OHARA, K., KONDO, T., ITO, M., et al. SOCS, inflammation, and cancer. JAKSTAT. 2013, 3, 2, e24053.
110. IRTA, I.D.R.I.T.A. Review of immune stimulator substances/agents that are susceptible of being used as feed additives: mode of action and identification of end-points for efficacy assessment. EFSA Supporting Publications. 2015, 12, 12, 905E.
111. JACOBI, S.K., MOESER, A.J., CORL, B.A., et al. Dietary long-chain PUFA enhance acute repair of ischemia-injured intestine of suckling pigs. J Nutr. 2012, 7, 142, 1266-1271.
112. JASMIN, J.F., FRANK, P.G., LISANTI, M.P., 2012, Caveolins and Caveolae, Roles in Signaling and Disease Mechanisms, Vol 729. AEMB.
113. JIMENEZ-MUNGUIA, I., TOMECKOVA, Z., MOCHNACOVA, E., et al. Transcriptomic analysis of human brain microvascular endothelial cells exposed to laminin binding protein (adhesion lipoprotein) and Streptococcus pneumoniae. Sci Rep. 2021, 1, 11, 7970.
114. JOHN, S.P., SUN, J., CARLSON, R.J., et al. IFIT1 Exerts Opposing Regulatory Effects on the Inflammatory and Interferon Gene Programs in LPS-Activated Human Macrophages. Cell Rep. 2018, 1, 25, 95-106 e106.
115. JONES, C.V., RICARDO, S.D. Macrophages and CSF-1: implications for development and beyond. Organogenesis. 2013, 4, 9, 249-260.
116. KAIA MOBRATEN, T.M.H., CHARLOTTE R KLEIVELAND, TOR LEA. Omega-3 and omega-6 PUFAs induce the same GPR120-mediated signalling events, but with different kinetics and intensity in Caco-2 cells. Lipids in Health and Disease. 2013, 12, 101.
117. KAKU, H., ROTHSTEIN, T.L. Fas apoptosis inhibitory molecule enhances CD40 signaling in B cells and augments the plasma cell compartment. J Immunol. 2009, 3, 183, 1667-1674.
118. KAWABATA, A., VAN HUNG, T., NAGATA, Y., et al. Citrus kawachiensis Peel Powder Reduces Intestinal Barrier Defects and Inflammation in Colitic Mice. J Agric Food Chem. 2018, 42, 66, 10991-10999.
119. KAWASAKI, T., KAWAI, T. Toll-like receptor signaling pathways. Front Immunol. 2014, 5, 461.
120. KIM, D.W., SHIN, M.J., CHOI, Y.J., et al. Tat-ATOX1 inhibits inflammatory responses via regulation of MAPK and NF-κB pathways. BMB Reports. 2018, 12, 51, 654-659.
121. KIM, H.S., BERSTAD, A. Experimental colitis in animal models. Scand J Gastroenterol. 1992, 7, 27, 529-537.
122. KLIEWER, A., REINSCHEID, R.K., SCHULZ, S. Emerging Paradigms of G Protein-Coupled Receptor Dephosphorylation. Trends Pharmacol Sci. 2017, 7, 38, 621-636.

123. KOLEV, M.V., TEDIOSE, T., SIVASANKAR, B., et al. Upregulating CD59: a new strategy for protection of neurons from complement-mediated degeneration. Pharmacogenomics J. 2010, 1, 10, 12-19.
124. KOZAK, E.M., TATE, S.S. Glutathione-degrading enzymes of microvillus membranes. Journal of Biological Chemistry. 1982, 11, 257, 6322-6327.
125. KRALIK, G., ŠKRTIĆ, Z., SUCHÝ, P., et al. Feeding Fish Oil and Linseed Oil to Laying Hens to Increase the n-3 PUFA in Egg Yolk. Acta Veterinaria Brno. 2008, 4, 77, 561-568.
126. KUEHNE, A., EMMERT, H., SOEHLE, J., et al. Acute Activation of Oxidative Pentose Phosphate Pathway as First-Line Response to Oxidative Stress in Human Skin Cells. Mol Cell. 2015, 3, 59, 359-371.
127. KURASHIMA, Y., GOTO, Y., KIYONO, H. Mucosal innate immune cells regulate both gut homeostasis and intestinal inflammation. Eur J Immunol. 2013, 12, 43, 3108-3115.
128. KWA, M.Q., NGUYEN, T., HUYNH, J., et al. Interferon regulatory factor 6 differentially regulates Toll-like receptor 2-dependent chemokine gene expression in epithelial cells. J Biol Chem. 2014, 28, 289, 19758-19768.
129. LANGERHOLC, T., MARAGKOUDAKIS, P.A., WOLLGAST, J., et al. Novel and established intestinal cell line models – An indispensable tool in food science and nutrition. Trends in Food Science & Technology. 2011, 22, S11-S20.
130. LARA-ESPINOZA, C., CARVAJAL-MILLAN, E., BALANDRAN-QUINTANA, R., et al. Pectin and Pectin-Based Composite Materials: Beyond Food Texture. Molecules. 2018, 4, 23.
131. LECLERE, L., CUTSEM, P.V., MICHIELS, C. Anti-cancer activities of pH- or heat-modified pectin. Front Pharmacol. 2013, 4, 128.
132. LEE, B.O., MOYRON-QUIROZ, J., RANGEL-MORENO, J., et al. CD40, but not CD154, expression on B cells is necessary for optimal primary B cell responses. J Immunol. 2003, 11, 171, 5707-5717.
133. LEE, C., MINICH, A., LI, B., et al. Influence of stress factors on intestinal epithelial injury and regeneration. Pediatric Surgery International. 2017, 2, 34, 155-160.
134. LETELLIER, R.M., BUTLER, M., DÉCHELOTTE, P., et al. Comparison of cytokine modulation by natural peroxisome proliferator-activated receptor gamma ligands with synthetic ligands in intestinal-like Caco-2 cells and human dendritic cells--potential for dietary modulation of peroxisome proliferator-activated receptor gamma in intestinal inflammation. 2008, 4, 87, 939-948.
135. LEVY, B.D., CLISH, C.B., SCHMIDT, B., et al. Lipid mediator class switching during acute inflammation: signals in resolution. Nat Immunol. 2001, 7, 2, 612-619.
136. LIU, D., LIU, M., WANG, W., et al. Overexpression of apoptosis-inducing factor mitochondrion-associated 1 (AIFM1) induces apoptosis by promoting the transcription of caspase3 and DRAM in hepatoma cells. Biochem Biophys Res Commun. 2018a, 3, 498, 453-457.
137. LIU, H., PENG, J., ZHAO, M., et al. Downregulation of DLL4 predicts poor survival in nonsmall cell lung cancer patients due to promotion of lymph node metastasis. Oncol Rep. 2018b, 5, 40, 2988-2996.
138. LIU, L., FISHMAN, M.L., HICKS, K.B., et al. Interaction of various pectin formulations with porcine colonic tissues. Biomaterials. 2005, 29, 26, 5907-5916.
139. LIU, Y., CHEN, F., ODLE, J., et al. Fish oil enhances intestinal integrity and inhibits TLR4 and NOD2 signaling pathways in weaned pigs after LPS challenge. J Nutr. 2012, 11, 142, 2017-2024.

140. LIU, Y.H., LI, X.Y., CHEN, C.Y., et al. Omega-3 fatty acid intervention suppresses lipopolysaccharide-induced inflammation and weight loss in mice. Mar Drugs. 2015, 2, 13, 1026-1036.
141. LOESCHKE, K., UEBERSCHAER, B., PIETSCH, A., et al. n-3 fatty acids only delay early relapse of ulcerative colitis in remission. Dig Dis Sci. 1996, 10, 41, 2087-2094.
142. LONE, A.M., TASKEN, K. Proinflammatory and immunoregulatory roles of eicosanoids in T cells. Front Immunol. 2013, 4, 130.
143. LORENZ, R., WEBER, P.C., SZIMNAU, P., et al. Supplementation with n-3 fatty acids from fish oil in chronic inflammatory bowel disease--a randomized, placebo-controlled, double-blind cross-over trial. J Intern Med Suppl. 1989, 731, 225-232.
144. LOTTENBERG, A.M., AFONSO MDA, S., LAVRADOR, M.S., et al. The role of dietary fatty acids in the pathology of metabolic syndrome. J Nutr Biochem. 2012, 9, 23, 1027-1040.
145. LU, J., JILLING, T., LI, D., et al. Polyunsaturated fatty acid supplementation alters proinflammatory gene expression and reduces the incidence of necrotizing enterocolitis in a neonatal rat model. Pediatr Res. 2007, 4, 61, 427-432.
146. LUISSINT, A.C., FEDERICI, C., GUILLONNEAU, F., et al. Guanine nucleotide-binding protein Galphai2: a new partner of claudin-5 that regulates tight junction integrity in human brain endothelial cells. J Cereb Blood Flow Metab. 2012, 5, 32, 860-873.
147. LUO, J.C., SHIN, V.Y., YANG, Y.H., et al. Tumor necrosis factor-alpha stimulates gastric epithelial cell proliferation. Am J Physiol Gastrointest Liver Physiol. 2005, 1, 288, G32-38.
148. LUO, Y., MEDINA BENGTSSON, L., WANG, X., et al. UQCRH downregulation promotes Warburg effect in renal cell carcinoma cells. Sci Rep. 2020, 1, 10, 15021.
149. MAJOROS, A., PLATANITIS, E., KERNBAUER-HOLZL, E., et al. Canonical and Non-Canonical Aspects of JAK-STAT Signaling: Lessons from Interferons for Cytokine Responses. Front Immunol. 2017, 8, 29.
150. MANI, V., HOLLIS, J.H., GABLER, N.K. Dietary oil composition differentially modulates intestinal endotoxin transport and postprandial endotoxemia. Nutr Metab (Lond). 2013, 1, 10, 6.
151. MAO, Y., KASRAVI, B., NOBAEK, S., et al. Pectin-supplemented enteral diet reduces the severity of methotrexate induced enterocolitis in rats. Scand J Gastroenterol. 1996, 6, 31, 558-567.
152. MARCON, R., BENTO, A.F., DUTRA, R.C., et al. Maresin 1, a proresolving lipid mediator derived from omega-3 polyunsaturated fatty acids, exerts protective actions in murine models of colitis. J Immunol. 2013, 8, 191, 4288-4298.
153. MARETZKY, T., REISS, K., LUDWIG, A., et al. ADAM10 mediates E-cadherin shedding and regulates epithelial cell-cell adhesion, migration, and β-catenin translocation. Proc Natl Acad Sci U S A. 2005, 26, 102, 9182–9187.
154. MARKOV, P.A., POPOV, S.V., NIKITINA, I.R., et al. Anti-inflammatory activity of pectins and their galacturonan backbone. Russian Journal of Bioorganic Chemistry. 2011, 37, 817–821.
155. MARTINI, E., KRUG, S.M., SIEGMUND, B., et al. Mend Your Fences: The Epithelial Barrier and its Relationship With Mucosal Immunity in Inflammatory Bowel Disease. Cell Mol Gastroenterol Hepatol. 2017, 1, 4, 33-46.
156. MATEO, R.D., CARROLL, J.A., HYUN, Y., et al. Effect of dietary supplementation of n-3 fatty acids and elevated concentrations of dietary protein on the performance of sows. J Anim Sci. 2009, 3, 87, 948-959.

157. MATHERS, L., BAILEY, M.J. Enzyme deletions and essential fatty acid metabolism in cultured cells. Journal of Biological Chemistry. 1975, 3, 250, 1152-1153.
158. MATHIAS, R.A., PANI, V., CHILTON, F.H. Genetic Variants in the FADS Gene: Implications for Dietary Recommendations for Fatty Acid Intake. Curr Nutr Rep. 2014, 2, 3, 139-148.
159. MATSON DZEBO, M., ARIOZ, C., WITTUNG-STAFSHEDE, P. Extended functional repertoire for human copper chaperones. Biomol Concepts. 2016, 1, 7, 29-39.
160. MAXWELL, E.G., BELSHAW, N.J., WALDRON, K.W., et al. Pectin – An emerging new bioactive food polysaccharide. Trends in Food Science & Technology. 2012, 2, 24, 64-73.
161. MBODJI, K., CHARPENTIER, C., GUERIN, C., et al. Adjunct therapy of n-3 fatty acids to 5-ASA ameliorates inflammatory score and decreases NF-kappaB in rats with TNBS-induced colitis. J Nutr Biochem. 2013, 4, 24, 700-705.
162. MCCALL TB, O.L.D., BLOOMFIELD J, O'MORÁIN CA. Therapeutic potential of fish oil in the treatment of ulcerative colitis. Aliment Pharmacol Ther. 1989, 5, 3, 415-424.
163. MEGE, R.M., ISHIYAMA, N. Integration of Cadherin Adhesion and Cytoskeleton at Adherens Junctions. Cold Spring Harb Perspect Biol. 2017, 5, 9.
164. MERKWIRTH, C., DARGAZANLI, S., TATSUTA, T., et al. Prohibitins control cell proliferation and apoptosis by regulating OPA1-dependent cristae morphogenesis in mitochondria. Genes Dev. 2008, 4, 22, 476-488.
165. MEYDANI, S.N., ENDRES, S., WOODS, M.M., et al. Oral (n-3) fatty acid supplementation suppresses cytokine production and lymphocyte proliferation: comparison between young and older women. J Nutr. 1991, 4, 121, 547-555.
166. MIDDLETON, S.J., NAYLOR, S., WOOLNER, J., et al. A double-blind, randomized, placebo-controlled trial of essential fatty acid supplementation in the maintenance of remission of ulcerative colitis. Aliment Pharmacol Ther. 2002, 6, 16, 1131-1135.
167. MITCHELL, J., KANNOURAKIS, G. Does CD1a Expression Influence T Cell Function in Patients With Langerhans Cell Histiocytosis? Front Immunol. 2021, 12, 773598.
168. MORANDI, E.M., VERSTAPPEN, R., ZWIERZINA, M.E., et al. ITGAV and ITGA5 diversely regulate proliferation and adipogenic differentiation of human adipose derived stem cells. Sci Rep. 2016, 6, 28889.
169. MORGAN, M.J., LIU, Z.G. Crosstalk of reactive oxygen species and NF-kappaB signaling. Cell Res. 2011, 1, 21, 103-115.
170. MORTONA, R., HARTZ, J., REITZ, R., et al. The acyl-CoA desaturases of microsomes from rat liver and the Morris 7777 hepatoma. Biochimica et Biophysica Acta (BBA) - Lipids and Lipid Metabolism. 1979, 2, 573, 321–331.
171. NANGIA-MAKKER, P., HOGAN, V., HONJO, Y., et al. Inhibition of Human Cancer Cell Growth and Metastasisin Nude Mice by Oral Intake of Modified Citrus Pectin. Journal of the National Cancer Institute. 2002, 24, 94, 1854-1862.
172. NIETO, J.C., ZAMORA, C., CANTO, E., et al. CSF-1 regulates the function of monocytes in Crohn's disease patients in remission. Sci Rep. 2017, 1, 7, 92.
173. NIETO, N., FERNANDEZ, M.I., TORRES, M.I., et al. Dietary monounsaturated n-3 and n-6 long-chain polyunsaturated fatty acids affect cellular antioxidant defense system in rats with experimental ulcerative colitis induced by trinitrobenzene sulfonic acid. Dig Dis Sci. 1998, 12, 43, 2676-2687.

174. NIETO, N., TORRES, M.I., RÍOS, A., et al. Dietary polyunsaturated fatty acids improve histological and biochemical alterations in rats with experimental ulcerative colitis. J Nutr. 2002, 1, 132, 11-19.
175. NOLAN, M.E., ARANDA, V., LEE, S., et al. The polarity protein Par6 induces cell proliferation and is overexpressed in breast cancer. Cancer Res. 2008, 20, 68, 8201-8209.
176. NTAMBI, J.M. The regulation of stearoyl-CoA desaturase (SCD. Progress in Lipid Research. 1995, 2, 34, 139-150.
177. OECKINGHAUS, A., GHOSH, S. The NF-kappaB family of transcription factors and its regulation. Cold Spring Harb Perspect Biol. 2009, 4, 1, a000034.
178. OHTSUKA, Y., OKADA, K., YAMAKAWA, Y., et al. omega-3 fatty acids attenuate mucosal inflammation in premature rat pups. J Pediatr Surg. 2011, 3, 46, 489-495.
179. OKUMURA, R., TAKEDA, K. Roles of intestinal epithelial cells in the maintenance of gut homeostasis. Exp Mol Med. 2017, 5, 49, e338.
180. OTANO, I., AZPILIKUETA, A., GLEZ-VAZ, J., et al. CD137 (4-1BB) costimulation of CD8(+) T cells is more potent when provided in cis than in trans with respect to CD3-TCR stimulation. Nat Commun. 2021, 1, 12, 7296.
181. PACHECO, M.T., VEZZA, T., DIEZ-ECHAVE, P., et al. Anti-inflammatory bowel effect of industrial orange by-products in DSS-treated mice. Food Funct. 2018, 9, 9, 4888-4896.
182. PAENSUWAN, P., NGOENKAM, J., WANGTEERAPRASERT, A., et al. Essential function of adaptor protein Nck1 in platelet-derived growth factor receptor signaling in human lens epithelial cells. Sci Rep. 2022, 1, 12, 1063.
183. PAOLI, P., GIANNONI, E., CHIARUGI, P. Anoikis molecular pathways and its role in cancer progression. Biochim Biophys Acta. 2013, 12, 1833, 3481-3498.
184. PARK, S.H., MIN, B., KIM, S.A., et al., 2019, Pectin as an Alternative Feed Additive and Effects on Microbiota, In: Safety and Practice for Organic Food. pp. 305-319.
185. PEDRO, J.M.B., SICA, V., MADEO, F., et al. Acyl-CoA-binding protein (ACBP): the elusive 'hunger factor' linking autophagy to food intake. Cell Stress. 2019, 10, 3, 312-318.
186. PENG, H.Y., LUCAVS, J., BALLARD, D., et al. Metabolic Reprogramming and Reactive Oxygen Species in T Cell Immunity. Front Immunol. 2021, 12, 652687.
187. PETERSON, L.W., ARTIS, D. Intestinal epithelial cells: regulators of barrier function and immune homeostasis. Nat Rev Immunol. 2014, 3, 14, 141-153.
188. PETTERSEN, K., MONSEN, V.T., HAKVAG PETTERSEN, C.H., et al. DHA-induced stress response in human colon cancer cells - Focus on oxidative stress and autophagy. Free Radic Biol Med. 2016, 90, 158-172.
189. PIENTA, K.J., NAIK, H., AKHTAR, A., et al. Inhibition of spontaneous metastasis in a rat prostate cancer model by oral administration of modified citrus pectin. J Natl Cancer Inst. 1995, 5, 87, 348-353.
190. PROSSOMARITI, A., SCAIOLI, E., PIAZZI, G., et al. Short-term treatment with eicosapentaenoic acid improves inflammation and affects colonic differentiation markers and microbiota in patients with ulcerative colitis. Sci Rep. 2017, 1, 7, 7458.
191. QIU, S., LI, P., ZHAO, H., et al. Maresin 1 alleviates dextran sulfate sodium-induced ulcerative colitis by regulating NRF2 and TLR4/NF-kB signaling pathway. Int Immunopharmacol. 2020, 78, 106018.
192. RAMACHANDRAN, C., WILK, B., MELNICK, S.J., et al. Synergistic Antioxidant and Anti-Inflammatory Effects between Modified Citrus Pectin and Honokiol. Evid Based Complement Alternat Med. 2017, 2017, 8379843.

193. REDDY, K.V.K., NAIDU, K.A. Oleic acid, hydroxytyrosol and n-3 fatty acids collectively modulate colitis through reduction of oxidative stress and IL-8 synthesis; in vitro and in vivo studies. Int Immunopharmacol. 2016, 35, 29-42.
194. REFAELI Y, V.P.L., LONDON CA, TSCHOPP J, ABBAS AK. Biochemical Mechanisms of IL-2–Regulated Fas-Mediated T Cell Apoptosis. Immunity. 1998, 8, 615-623.
195. REIFEN, R., KARLINSKY, A., STARK, A.H., et al. alpha-Linolenic acid (ALA) is an anti-inflammatory agent in inflammatory bowel disease. J Nutr Biochem. 2015a, 12, 26, 1632-1640.
196. REIFEN, R., KARLINSKY, A., STARK, A.H., et al. α-Linolenic acid (ALA) is an anti-inflammatory agent in inflammatory bowel disease. J Nutr Biochem. 2015b, 12, 26, 1632-1640.
197. ROOKE, J.A., SHAO, C.C., SPEAKE, B.K. Effects of feeding tuna oil on the lipid composition of pig spermatozoa and in vitro characteristics of semen. Reproduction. 2001, 2, 121, 315-322.
198. ROSELLA, O., SINCLAIR, A., GIBSON, P.G. Polyunsaturated fatty acids reduce non-receptor-mediated transcellular permeation of protein across a model of intestinal epithelium in vitro. Journal of Gastroenterology and Hepatology. 2000, 6, 15, 626-631.
199. ROSSI, R., PASTORELLI, G., CANNATA, S., et al. Recent advances in the use of fatty acids as supplements in pig diets: A review. Animal Feed Science and Technology. 2010, 1-2, 162, 1-11.
200. ROUAULT, C., PELLEGRINELLI, V., SCHILCH, R., et al. Roles of chemokine ligand-2 (CXCL2) and neutrophils in influencing endothelial cell function and inflammation of human adipose tissue. Endocrinology. 2013, 3, 154, 1069-1079.
201. RUSTAN, A.C., DREVON, C.A., 2005, Fatty Acids: Structures and Properties, In: Encyclopedia of Life Sciences.
202. RUTHIG, D.J., MECKLING-GILL, K.A. Both (n-3) and (n-6) fatty acids stimulate wound healing in the rat intestinal epithelial cell line, IEC-6. J Nutr. 1999, 10, 129, 1791-1798.
203. RUTHIG, D.J., MECKLING-GILL, K.A. N-3 and n-6 fatty acids stimulate restitution by independent mechanisms in the IEC-6 model of intestinal wound healing. J Nutr Biochem. 2002, 1, 13, 27-35.
204. S.A. BROOKS, T.M. CARTER, L. ROYLE, et al. Altered Glycosylation of Proteins in Cancer: What Is the Potential for New AntiTumour Strategies. Anti-Cancer Agents in Medicinal Chemistry. 2008, 8, 2-21.
205. SAHASRABUDHE, N.M., BEUKEMA, M., TIAN, L., et al. Dietary Fiber Pectin Directly Blocks Toll-Like Receptor 2-1 and Prevents Doxorubicin-Induced Ileitis. Front Immunol. 2018, 9, 383.
206. SALOMON, P., KORNBLUTH, A.A., JANOWITZ, H.D. Treatment of ulcerative colitis with fish oil n--3-omega-fatty acid: an open trial. J Clin Gastroenterol. 1990, 2, 12, 157-161.
207. SALVO, R.E., ALONSO, C.C., PARDO, C.C., et al. The intestinal barrier function and its involvement in digestive disease. Rev Esp Enferm Dig. 2015, 11, 107, 686-696.
208. SAMAVATI, L., RASTOGI, R., DU, W., et al. STAT3 tyrosine phosphorylation is critical for interleukin 1 beta and interleukin-6 production in response to lipopolysaccharide and live bacteria. Mol Immunol. 2009, 8-9, 46, 1867-1877.

209. SATOH, H., HARA, T., MURAKAWA, D., et al. Soluble Dietary Fiber Protects Against Nonsteroidal Anti-inflammatory Drug-Induced Damage to the Small Intestine in Cats. Digestive Diseases and Sciences. 2009, 5, 55, 1264-1271.
210. SAVOINI, G., FARINA, G., DELL'ORTO, V., et al. Through ruminant nutrition to human health: role of fatty acids. Advances in Animal Biosciences. 2016, 2, 7, 200-207.
211. SCAIOLI, E., SARTINI, A., BELLANOVA, M., et al. Eicosapentaenoic Acid Reduces Fecal Levels of Calprotectin and Prevents Relapse in Patients With Ulcerative Colitis. Clin Gastroenterol Hepatol. 2018, 8, 16, 1268-1275 e1262.
212. SCHELLER, J., CHALARIS, A., GARBERS, C., et al. ADAM17: a molecular switch to control inflammation and tissue regeneration. Trends Immunol. 2011, 8, 32, 380-387.
213. SCHEPP, W., PESKAR, B.M., TRAUTMANN, M., et al. Fish oil reduces ethanol-induced damage of the duodenal mucosa in humans. Eur J Clin Invest. 1991, 2, 21, 230-237.
214. SCHNELL, U., CIRULLI, V., GIEPMANS, B.N. EpCAM: structure and function in health and disease. Biochim Biophys Acta. 2013, 8, 1828, 1989-2001.
215. SCHWAB, J.M., SERHAN, C.N. Lipoxins and new lipid mediators in the resolution of inflammation. Curr Opin Pharmacol. 2006, 4, 6, 414-420.
216. SEBASTIAN, D., GUITART, M., GARCIA-MARTINEZ, C., et al. Novel role of FATP1 in mitochondrial fatty acid oxidation in skeletal muscle cells. J Lipid Res. 2009, 9, 50, 1789-1799.
217. SEIDNER, D.L., LASHNER, B.A., BRZEZINSKI, A., et al. An oral supplement enriched with fish oil, soluble fiber, and antioxidants for corticosteroid sparing in ulcerative colitis: a randomized, controlled trial. Clin Gastroenterol Hepatol. 2005, 4, 3, 358-369.
218. SERHAN, C.N., CHIANG, N., VAN DYKE, T.E. Resolving inflammation: dual anti-inflammatory and pro-resolution lipid mediators. Nat Rev Immunol. 2008, 5, 8, 349-361.
219. SERHAN, C.N., SAVILL, J. Resolution of inflammation: the beginning programs the end. Nat Immunol. 2005, 12, 6, 1191-1197.
220. SETH, A., SHETH, P., ELIAS, B.C., et al. Protein phosphatases 2A and 1 interact with occludin and negatively regulate the assembly of tight junctions in the CACO-2 cell monolayer. J Biol Chem. 2007, 15, 282, 11487-11498.
221. SHIMIZU, T., FUJII, T., SUZUKI, R., et al. Effects of Highly Purified Eicosapentaenoic Acid on Erythrocyte Fatty Acid Composition and Leukocyte and Colonic Mucosa Leukotriene B4 Production in Children With Ulcerative Colitis. J Pediatr Gastroenterol Nutr. 2003, 5, 37, 581-585.
222. SIMOPOULOS, A.P. The Mediterranean Diets in Health and Disease. The American Journal of Clinical Nutrition. 1991, 4, 54, 771.
223. SOTO-HEREDERO, G., GOMEZ DE LAS HERAS, M.M., GABANDE-RODRIGUEZ, E., et al. Glycolysis - a key player in the inflammatory response. FEBS J. 2020, 16, 287, 3350-3369.
224. SRIAMORNSAK, P., WATTANAKORN, N., TAKEUCHI, H. Study on the mucoadhesion mechanism of pectin by atomic force microscopy and mucin-particle method. Carbohydrate Polymers. 2010, 1, 79, 54-59.
225. SUGIHARA, K., MORHARDT, T.L., KAMADA, N. The Role of Dietary Nutrients in Inflammatory Bowel Disease. Front Immunol. 2018, 9, 3183.

226. SUN, B., ZHONG, F.J., XU, C., et al. Programmed cell death 10 promotes metastasis and epithelial-mesenchymal transition of hepatocellular carcinoma via PP2Ac-mediated YAP activation. Cell Death Dis. 2021, 9, 12, 849.
227. SUN, L., HULT, E.M., CORNELL, T.T., et al. Loss of myeloid-specific protein phosphatase 2A enhances lung injury and fibrosis and results in IL-10-dependent sensitization of epithelial cell apoptosis. Am J Physiol Lung Cell Mol Physiol. 2019, 6, 316, L1035-L1048.
228. SUN, L., SUN, M., MA, K., et al. Let-7d-5p suppresses inflammatory response in neonatal rats with necrotizing enterocolitis via LGALS3-mediated TLR4/NF-kappaB signaling pathway. Am J Physiol Cell Physiol. 2020, 6, 319, C967-C979.
229. SUNDARAM, T.S., GIROMINI, C., REBUCCI, R., et al. Omega-3 Polyunsaturated Fatty Acids Counteract Inflammatory and Oxidative Damage of Non-Transformed Porcine Enterocytes. Animals (Basel). 2020, 6, 10.
230. SUNG, D.C., BOWEN, C.J., VAIDYA, K.A., et al. Cadherin-11 Overexpression Induces Extracellular Matrix Remodeling and Calcification in Mature Aortic Valves. Arterioscler Thromb Vasc Biol. 2016, 8, 36, 1627-1637.
231. SUTHAHAR, N., MEIJERS, W.C., SILLJE, H.H.W., et al. Galectin-3 Activation and Inhibition in Heart Failure and Cardiovascular Disease: An Update. Theranostics. 2018, 3, 8, 593-609.
232. SZKLARCZYK, D., GABLE, A.L., NASTOU, K.C., et al. The STRING database in 2021: customizable protein-protein networks, and functional characterization of user-uploaded gene/measurement sets. Nucleic Acids Res. 2021, D1, 49, D605-D612.
233. SZTALRYD, C., BRASAEMLE, D.L. The perilipin family of lipid droplet proteins: Gatekeepers of intracellular lipolysis. Biochim Biophys Acta Mol Cell Biol Lipids. 2017, 10 Pt B, 1862, 1221-1232.
234. THANABALAN, A., KIARIE, E.G. Influence of Feeding Omega-3 Polyunsaturated Fatty Acids to Broiler Breeders on Indices of Immunocompetence, Gastrointestinal, and Skeletal Development in Broiler Chickens. Front Vet Sci. 2021, 8, 653152.
235. THOO, L., NOTI, M., KREBS, P. Keep calm: the intestinal barrier at the interface of peace and war. Cell Death Dis. 2019, 11, 10, 849.
236. TILLEY, S.L., COFFMAN, T.M., KOLLER, B.H. Mixed messages: modulation of inflammation and immune responses by prostaglandins and thromboxanes. Journal of Clinical Investigation. 2001, 1, 108, 15-23.
237. TINH, N.T.T., SITOLO, G.C., YAMAMOTO, Y., et al. Citrus limon Peel Powder Reduces Intestinal Barrier Defects and Inflammation in a Colitic Murine Experimental Model. Foods. 2021, 2, 10.
238. TKACIKOVA, L., MOCHNACOVA, E., TYAGI, P., et al. Comprehensive mapping of the cell response to E. coli infection in porcine intestinal epithelial cells pretreated with exopolysaccharide derived from Lactobacillus reuteri. Vet Res. 2020, 1, 51, 49.
239. TURNER, M.D., NEDJAI, B., HURST, T., et al. Cytokines and chemokines: At the crossroads of cell signalling and inflammatory disease. Biochim Biophys Acta. 2014, 11, 1843, 2563-2582.
240. TYAGI, P., BHIDE, M. Development of a bioinformatics platform for analysis of quantitative transcriptomics and proteomics data: the OMnalysis. PeerJ. 2021, 9, e12415.
241. UERLINGS, J., SCHROYEN, M., BAUTIL, A., et al. In vitro prebiotic potential of agricultural by-products on intestinal fermentation, gut barrier and inflammatory status of piglets. Br J Nutr. 2020, 3, 123, 293-307.

242. USAMI, M., MURAKI, K., IWAMOTO, M., et al. Effect of eicosapentaenoic acid (EPA) on tight junction permeability in intestinal monolayer cells. Clin Nutr. 2001, 4, 20, 351-359.
243. VERGAUWEN, H., PRIMS, S., DEGROOTE, J., et al. In Vitro Investigation of Six Antioxidants for Pig Diets. Antioxidants (Basel). 2016, 4, 5.
244. VERGAUWEN, H., TAMBUYZER, B., JENNES, K., et al. Trolox and ascorbic acid reduce direct and indirect oxidative stress in the IPEC-J2 cells, an in vitro model for the porcine gastrointestinal tract. PLoS One. 2015, 3, 10, e0120485.
245. VOGT, L.M., SAHASRABUDHE, N.M., RAMASAMY, U., et al. The impact of lemon pectin characteristics on TLR activation and T84 intestinal epithelial cell barrier function. Journal of Functional Foods. 2016, 22, 398-407.
246. VOYNOVA, N.E., FU, Z., BATTAILE, K.P., et al. Human mevalonate diphosphate decarboxylase: characterization, investigation of the mevalonate diphosphate binding site, and crystal structure. Arch Biochem Biophys. 2008, 1, 480, 58-67.
247. WALKER LS, M.J., BOULOUGOURIS G, PATEL YI, HALL ND, SANSOM DM. Down-regulation of CD28 via Fas (CD95): influence of CD28 on T-cell apoptosis. Immunology. 1998, 1, 94, 41-47.
248. WALLACE, S.W., DURGAN, J., JIN, D., et al. Cdc42 regulates apical junction formation in human bronchial epithelial cells through PAK4 and Par6B. Mol Biol Cell. 2010, 17, 21, 2996-3006.
249. WANG, X., YAN, X., ZHANG, L., et al. Identification and Peptidomic Profiling of Exosomes in Preterm Human Milk: Insights Into Necrotizing Enterocolitis Prevention. Mol Nutr Food Res. 2019, e1801247.
250. WANG, Z., GUAN, D., WANG, S., et al. Glycolysis and Oxidative Phosphorylation Play Critical Roles in Natural Killer Cell Receptor-Mediated Natural Killer Cell Functions. Front Immunol. 2020, 11, 202.
251. WEBER, T.E., ZIEMER, C.J., KERR, B.J. Effects of adding fibrous feedstuffs to the diet of young pigs on growth performance, intestinal cytokines, and circulating acute-phase proteins. J Anim Sci. 2008, 4, 86, 871-881.
252. WERF, P.V.D., ORLOWSKI, M., MEISTER, A. Enzymatic Conversion of 5-Oxo-L-Proline (L-Pyrrolidone Carboxylate) to L-Glutamate Coupled with Cleavage of Adenosine Triphosphate to Adenosine Diphosphate, a Reaction in the γ-Glutamyl Cycle. Proc Natl Acad Sci U S A. 1971, 12, 68, 2982–2985.
253. WESTERMARCK, J., IVASKA, J., CORTHALS, G.L. Identification of protein interactions involved in cellular signaling. Mol Cell Proteomics. 2013, 7, 12, 1752-1763.
254. WIJENDRAN, V., BRENNA, J.T., WANG, D.H., et al. Long-chain polyunsaturated fatty acids attenuate the IL-1beta-induced proinflammatory response in human fetal intestinal epithelial cells. Pediatr Res. 2015, 6, 78, 626-633.
255. WILLEMSEN, L.E., KOETSIER, M.A., BALVERS, M., et al. Polyunsaturated fatty acids support epithelial barrier integrity and reduce IL-4 mediated permeability in vitro. Eur J Nutr. 2008, 4, 47, 183-191.
256. WILS-PLOTZ, E.L., JENKINS, M.C., DILGER, R.N. Modulation of the intestinal environment, innate immune response, and barrier function by dietary threonine and purified fiber during a coccidiosis challenge in broiler chicks. Poult Sci. 2013, 3, 92, 735-745.
257. WINDISCH, W., SCHEDLE, K., PLITZNER, C., et al. Use of phytogenic products as feed additives for swine and poultry. J Anim Sci. 2008, 14 Suppl, 86, E140-148.

258. XIAO, G., TANG, L., YUAN, F., et al. Eicosapentaenoic acid enhances heat stress-impaired intestinal epithelial barrier function in Caco-2 cells. PLoS One. 2013, 9, 8, e73571.
259. XIAO, K., LIU, C., QIN, Q., et al. EPA and DHA attenuate deoxynivalenol-induced intestinal porcine epithelial cell injury and protect barrier function integrity by inhibiting necroptosis signaling pathway. FASEB J. 2020, 2, 34, 2483-2496.
260. XIONG, Y., LEI, Q.Y., ZHAO, S., et al. Regulation of glycolysis and gluconeogenesis by acetylation of PKM and PEPCK. Cold Spring Harb Symp Quant Biol. 2011, 76, 285-289.
261. YAN, H., AJUWON, K.M. Butyrate modifies intestinal barrier function in IPEC-J2 cells through a selective upregulation of tight junction proteins and activation of the Akt signaling pathway. PLoS One. 2017a, 6, 12, e0179586.
262. YAN, Y., WANG, Z., GREENWALD, J., et al. BCFA suppresses LPS induced IL-8 mRNA expression in human intestinal epithelial cells. Prostaglandins Leukot Essent Fatty Acids. 2017b, 116, 27-31.
263. YEDGAR, S., KRIMSKY, M., COHEN, Y., et al. Treatment of inflammatory diseases by selective eicosanoid inhibition: a double-edged sword? Trends Pharmacol Sci. 2007, 9, 28, 459-464.
264. YEO, J.C., WALL, A.A., LUO, L., et al. Distinct Roles for APPL1 and APPL2 in Regulating Toll-like Receptor 4 Signaling in Macrophages. Traffic. 2016, 9, 17, 1014-1026.
265. YOU, C., SANDALCIOGLU, I.E., DAMMANN, P., et al. Loss of CCM3 impairs DLL4-Notch signalling: implication in endothelial angiogenesis and in inherited cerebral cavernous malformations. J Cell Mol Med. 2013, 3, 17, 407-418.
266. YUCEYAR, H., OZUTEMIZ, O., HUSEYINOV, A., et al. Is administration of n-3 fatty acids by mucosal enema protective against trinitrobenzene-induced colitis in rats? Prostaglandins Leukot Essent Fatty Acids. 1999, 6, 61, 339-345.
267. YUNIATI, L., SCHEIJEN, B., VAN DER MEER, L.T., et al. Tumor suppressors BTG1 and BTG2: Beyond growth control. J Cell Physiol. 2019, 5, 234, 5379-5389.
268. ZEMPLENI, J., AGUILAR-LOZANO, A., SADRI, M., et al. Biological Activities of Extracellular Vesicles and Their Cargos from Bovine and Human Milk in Humans and Implications for Infants. J Nutr. 2017, 1, 147, 3-10.
269. ZENGIN, T., EKINCI, B., KUCUKKOSE, C., et al. IRF6 Is Involved in the Regulation of Cell Proliferation and Transformation in MCF10A Cells Downstream of Notch Signaling. PLoS One. 2015a, 7, 10.
270. ZENGIN, T., EKINCI, B., KUCUKKOSE, C., et al. IRF6 Is Involved in the Regulation of Cell Proliferation and Transformation in MCF10A Cells Downstream of Notch Signaling. PLoS One. 2015b, 7, 10, e0132757.
271. ZHANG, H., GUO, W., ZHANG, F., et al. Monoacylglycerol Lipase Knockdown Inhibits Cell Proliferation and Metastasis in Lung Adenocarcinoma. Front Oncol. 2020, 10, 559568.
272. ZHANG, J., LIAN, B., SHANG, Y., et al. miR-135a Protects Dextran Sodium Sulfate-Induced Inflammation in Human Colorectal Cell Lines by Activating STAT3 Signal. Cell Physiol Biochem. 2018, 3, 51, 1001-1012.
273. ZHENG, J. Energy metabolism of cancer: Glycolysis versus oxidative phosphorylation (Review). Oncol Lett. 2012, 6, 4, 1151-1157.